THE CYCLOTRON PRODUCTION OF SELECTED RADIONUCLIDES USING MEDIUM ENERGY PROTONS

N. P. van der Meulen

Thesis presented in fulfillment of the requirements for the degree of Doctor of Philosophy at the University of Stellenbosch.

Supervisor: Prof. T. N. van der Walt
Faculty of Applied Sciences
Cape Peninsula University of Technology

Co-supervisors: Prof. H. G. Raubenheimer
Dept. of Chemistry
University of Stellenbosch

Dr. G. F. Steyn
Radionuclide Production
iThemba LABS

March 2008

DECLARATION

I, the undersigned, hereby declare that the work contained in this thesis is my own original work and that I have not previously in its entirety or in part submitted it at any university for a degree.

Signature: ……

Date: ……

ABSTRACT

Radiochemical research involving ion exchange chromatography is of paramount importance to the future of radionuclide production at the Radionuclide Production Group (RPG) of iThemba LABS. It is required for the production of high-activity yields of radionuclides to effectively remove impurities and for the safety of the operators performing such productions. The radiochemical separations of some new products from their target material, as well as experiments to determine whether production is viable, are described.

^{67}Ga is currently being produced at the RPG and makes use of zinc targets. With the production of ultra-pure ^{67}Ga, it was necessary to remove any Fe(III) impurities from the final product, such that it may be possible to label peptides with this product. The use of Amberchrom CG161M for this purpose was found to be satisfactory.

Interest was shown in ^{88}Y by an overseas company for the manufacture of sources. While a method involving extraction of the radionuclide and the ion exchange thereof using Chelex 100 chelating resin had been published, problems with the production persisted. Three methods, using ion exchange chromatography, were devised to produce the radionuclide, with two of them being adopted for production purposes. Thick-target nuclear data have also recently been accumulated in collaboration with colleagues from ATOMKI, Debrecen, Hungary.

There is a large demand for ^{82}Sr for the manufacture of ^{82}Sr/^{82}Rb generators for medical use. A method was developed to manufacture this radionuclide with thicker (32 g) target material, bombarded in the Vertical Beam Target Station (VBTS), and to separate ^{82}Sr from its target material with the use of Purolite S950 chelating resin.

^{68}Ge/^{68}Ga generators are becoming increasingly important in the world of radiopharmaceuticals. A project to develop a local generator was funded by the Innovation Fund and research was performed to produce ^{68}Ge, such that the generator could be manufactured. This involved bombarding thicker Ga targets in the VBTS and performing the chemical separation using AG MP-1 anion exchange resin. The

final product was loaded onto generators, although tests performed on different materials to the ones being marketed are also reported in this work.

A project was initiated to study the cluster radioactive decay of ^{223}Ac via ^{14}C and ^{15}N emission. To produce ^{223}Ac for these observations, a Th target was bombarded. The ^{227}Pa was separated from the target material using AG MP-1 macroporous anion exchange resin and used as a source, which decayed to ^{223}Ac. The chemical separation and the drying of the final product onto a source plate were completed within approximately 70 minutes from the end of bombardment. The work was performed in collaboration with JINR, Russia, and University of Milan and INFN, Italy.

^{133}Ba has a half-life of over 10 years and is an expensive radionuclide to produce. It has been used in medical and biological studies and there still appears to be a demand for it. A method was devised, utilizing AG50W-X4 cation exchange resin, to separate ^{133}Ba from its CsCl target material.

Agricultural specialists in the past have shown an interest in ^{28}Mg, to determine the uptake of the element in fruit. It has long been regarded by some of the local researchers as an interesting project to investigate. It has been determined that the product can be produced in reasonable quantities using LiCl target material, with ten targets being bombarded in series using a 200 MeV proton beam delivered by the Separated Sector Cyclotron. A method, involving the use of Purolite S950 chelating resin, was devised to separate ^{28}Mg from its target material.

OPSOMMING

Radiochemiese navorsing, wat ioonuitruiling chromatografie behels, is van uiterste belang vir die toekoms van die produksie van radionukliede by die Radionukliedproduksiegroep (RPG) van iThemba LABS. Dit is nodig vir die hoë aktiwiteit opbrengs van radionuklied produkte om onsuiwerhede te verwyder en vir die veiligheid van die operateurs wat die produksies moet uitvoer. Die skeiding van nuwe produkte van hulle skyfmateriaal, sowel as eksperimente om vas te stel of ‘n produksie uitvoerbaar is, word in die werk beskryf.

^{67}Ga word tans by RPG vervaardig en maak gebruik van sink as skyfmateriaal. Vir die produksie van “ultra-suiwer” ^{67}Ga was dit belangrik om enige Fe(III) onsuiwerhede uit die finale produk te verwyder om sodoende peptiede merking te kan uitvoer. Die gebruik van Amberchrom CG161M hars was voldoende vir dié eksperiment.

‘n Oorsese maatskappy het belangstelling getoon in ^{88}Y vir die vervaardiging van bronne. Alhoewel ‘n metode wat die ekstraksie van die radionuklied en die ioon-uitruiling daarvan met die gebruik van Chelex 100 chelerende hars reeds gepubliseer was, het probleme met die produksie voortgeduur. Drie metodes is opgestel om ^{88}Y te produseer, waarvan twee van die metodes tans gebruik word vir produksie doeleindes. Dik-skyf kerndata is ook versamel in samewerking met kollegas van ATOMKI, Debrecen, Hongarye.

Daar is ‘n groot aanvraag vir ^{82}Sr vir die vervaardiging van ^{82}Sr/^{82}Rb generators vir mediese doeleindes. ‘n Metode is ontwikkel om die radionuklied te vervaardig van dikker skyfmateriaal (32 g), in die Vertikale Bundelstasie gebombardeer, en om ^{82}Sr van sy skyfmateriaal te skei met die gebruik van Purolite S950 chelerende hars.

^{68}Ge/^{68}Ga generators is besig om toenemend belangrik te word in die wêreld van radiofarmasie. iThemba LABS kry baie navrae om die produk te vervaardig. Die projek was ook deel van die voorlegging aan die “Innovation Fund” en ‘n manier is ondersoek om ^{68}Ge te vervaardig, wat benodig word om so ‘n generator te laai. Dik

Ga skyfmateriaal word in die Vertikale Bundelstasie gebombardeer en ‘n chemiese skeiding is uitgevoer deur gebruik te maak van AG MP-1 anioonuitruiling hars. Die finale produk is op die generators gelaai vir toetsdoeleindes. Toetse is ook op ‘n ander tipe generator uitgevoer en word in die werk beskryf.

‘n Projek is begin om “cluster” radioaktiewe verval van ^{223}Ac, via ^{14}C en ^{15}N emissie, te bestudeer. ‘n Th-skyf is met protone gebombardeer om die ^{223}Ac te produseer vir die eksperiment. ^{227}Pa is vervaardig en geskei van die skyfmateriaal. Dit is gedoen met die gebruik van AG MP-1 makroporeuse anioonuitruiling hars en drooggemaak op ‘n bronplaat, waar dit verval het na ^{223}Ac. Die chemiese skeiding en die droogmaak van die finale produk op ‘n bronplaat is uitgevoer binne 70 minute na Einde van Bombardering (EVB). Die werk is deel van ‘n samewerking met kollegas van JINR, Rusland, en die Universiteit van Milaan, sowel as INFN, Italië.

^{133}Ba het ‘n halveertyd van oor die tien jaar en is ‘n duur produk om te vervaardig. Dit is al gebruik in mediese en biologiese studies en daar is deesdae ‘n redelike aanvraag daarvoor. ‘n Metode is uitgewerk om ^{133}Ba te skei van die CsCl skyfmateriaal met die gebruik van AG50W-X4 katioonuitruiling hars.

Spesialiste in landboustudies het in die verlede belangstelling getoon in ^{28}Mg. Dit word gebruik om die absorpsie van dié element in vrugte te ondersoek. Die produk kan vervaardig word met die gebruik van LiCl skyfmateriaal: tot soveel as tien skywe (agter mekaar) word gebombardeer met ‘n 200 MeV protonbundel te iThemba LABS. ‘n Metode, wat Purolite S950 behels, is daargestel om ^{28}Mg van die skyfmateriaal te skei.

ACKNOWLEDGEMENTS

I wish to express my gratitude to the following people without whom this study would not have been possible:

- Marianne, my beautiful wife, for her support, sacrifices and love throughout.

- Ryan and Colin, my two monsters, for keeping me sane in times of insanity.

- Dr. Nico van der Walt, my promoter, for his encouragement, support and guidance towards this work, as well as throughout my career. I will be eternally grateful for the time he spent with me, attempting to develop the potential he saw in me.

- Prof. Helgard Raubenheimer, my co-promoter, for accepting me as a student at the University of Stellenbosch, for believing in me and the time spent guiding me.

- Dr. Deon Steyn, my co-promoter, for his guidance and provision of expertise in the targetry side of this work. Thanks, too, for the time and effort spent perusing this work, as well as his belief in me…especially for the projects he was involved in that required chemistry to complete it.

- Stuart Dolley, singled out for his friendship, support and assistance above and beyond the call of duty, through adversity, particularly with regard to the ^{68}Ge production. Without him, the odds of not finishing this part of the work timeously would have been greatly increased.

- Monique van Rhyn, Charisse Perrang, Etienne Vermeulen and David Saal for their friendship, support and assistance they have provided at some stage during this endeavour.

- My parents and my sister, Michelle, who have provided me with love and support and have always encouraged me in all I do.

- My colleagues from Milan, Italy and Moscow, Russia, for giving me their blessing to produce the Cluster Radioactivity Decay piece as part of this work.

- My colleagues from ATOMKI, Debrecen, Hungary, for their blessing to produce the nuclear data of $SrCl_2$ in this work.

- Selwyn de Windt, for his superb work and perfectionism in the manufacturing of the ^{68}Ge production panel, as well as the ^{88}Y production panel.

- Neels Rabe, for his years of friendship and the time and effort spent on tidying up this work.

- Friends, family and colleagues whom I have not mentioned, but who are in my heart.

- The Lord Jesus Christ, for giving me strength, perseverance and determination when I had none left to give.

This work is dedicated to all of my family, friends and loved ones who have stuck it out with me through all my adversity in recent years…you know who you are.

CONTENTS

LIST OF FIGURES

LIST OF TABLES

PUBLICATIONS RESULTING FROM THIS WORK

1. Steyn G. F., van der Meulen N. P., van der Walt T. N., Vermeulen C., 2007. Proceedings of the International Conference on Nuclear Data for Science and Technology (Nice, France). *In press.*
2. Van der Meulen N. P., van der Walt T. N., 2007. *Z. Naturforsch.*, **62b**, 483.
3. Van der Meulen N. P., Steyn G. F., van der Walt T. N., Shishkin S. V., Vermeulen C., Tretyakova S. P., Guglielmetti A., Bonetti R., Ogloblin A. A., McGee D., 2006. *Czech. J. Phys.*, **56**, D357.
4. Guglielmetti A., Faccio D., Bonetti R., Shishkin S. V., Tretyakova S. P., Dmitriev S. V., Ogloblin A. A., Pik-Pichak G. A., van der Meulen N. P., Steyn G. F., van der Walt T. N., Vermeulen C., McGee D., 2008. Proceedings of the 9th International Cluster Conference (Stratford-Upon-Avon, U.K.). *In press*.

CHAPTER 1 INTRODUCTION

iThemba LABS utilises a 66 MeV proton beam for the routine production of a number of radionuclides, for radiopharmaceutical purposes as well as for other applications. The choice of 66 MeV is dictated by the neutron therapy programme, with which the radionuclide production programme shares the beam in a semi-parasitic way. Bombarding the appropriate target material, which can be sintered, cut or pressed into a disc, produces the desired radionuclide (and usually also some co-produced ones) which can be thought of as the reaction remains (or residues) of particular nuclear reactions that take place within the target. The radionuclide of choice has to be chemically separated from the target material, purified from any contaminants and sterilised before it can be labelled and considered for use as a diagnostic medicine.

1.1 The Case for Ion-Exchange Chromatography

The chemical separation of the radionuclide from the target material is complicated by the fact that a very small quantity of radionuclide is formed (10^{-9} - 10^{-12} g) in comparison with the very large quantity of target material it has to be separated from (1 – 32 g). What complicates the matter even further is the fact that there may be other radionuclides present which have been co-produced by competing nuclear reactions during the bombardment, or daughter radionuclides that have been formed by the decay of their respective parent radionuclides, as well as the chemical impurities initially present in the target material. Many chemical techniques have been employed to separate the radionuclide of choice from the non-required elements, namely, solvent extraction, distillation, electro-deposition, precipitation, co-precipitation and ion exchange chromatography.

Ion exchange chromatography has been used in many disciplines in the past and is sometimes regarded as an obsolete application of chemistry for these disciplines, with chemists and engineers using other “more effective” forms of chemistry. Although column ion exchange chromatography is almost obsolete in analytical chemistry laboratories today, it is still regarded as being the cutting edge of technology in

radiochemistry. It is easy to use in a hot cell environment and the removal of impurities in the separation process, before eluting the radionuclide of interest, provides a much purer product than with most other methods. The other big advantage of using ion exchange chromatography in a hot cell environment is that this technique also minimises the radiation exposure to the technician, while reducing the volume of radioactive waste.

Some points have to be considered when planning an ion exchange separation. Due to the fact that the target material in a specific production is generally of a large quantity (gram quantities), while the radionuclide to be produced is found in much smaller quantities (< µg quantities), a large separation factor (α^{A}_{B}) is required to separate the radionuclide (A) from the target material (B). It is generally considered that the radionuclide (element) should have a high distribution coefficient ($K_d > 500$), while the target material should have a much lower distribution coefficient ($K_d < 10$). Initially, the separation factor should ideally be greater than 50. It is recommended that equilibrium be reached as quickly as possible, therefore, it is necessary to have a column with good kinetics such that a sharp separation is obtained, with very little "tailing". A relatively small resin column will always be preferred over a larger column, as smaller elution volumes are preferred to elute the sorbed elements. This would also lead to a short chemical separation process and can be an important factor in the final product whose yield is dependent on the half-life of a specific radionuclide. It would also minimise the quantities of waste solutions being generated (which are normally radioactive, should the separation involve radioactivity), which are monitored and, normally, have to be stored for a period of time before being released to waste storage dams on site.

Ion exchange resins are normally categorised into three types, namely, cation exchange resins (for example, Dowex 50 or Bio Rad AG50- and AG MP-50 resins), anion exchange resins (such as Dowex 1 or Bio Rad AG1- and AG MP-1 resins) and chelating ion exchange resins (like Chelex 100 or Purolite S930 and S950). There are other types of resins available, including those containing no ion exchange groups or functional groups (for example, Amberlite XAD-7), but these are not often used for radionuclide production purposes at iThemba LABS[1-3]. The only exception to this

statement is the use of Amberchrom CG71cd, which is used in the separation of ^{67}Ga from its zinc target material and other co-produced radionuclides.

The type of resin to be used in a chemical separation depends on the charge of the radionuclide and that of the target material (that is, neutral, positive or negative) and the oxidation number of the radionuclide. Should the radionuclide be cationic, or a cationic species is formed by complex formation, then a cation exchange resin is chosen as the resin column of use for the production. Should the target material, however, be anionic, or an anionic species is formed by complex formation, then an anion exchange resin would be chosen to retain the radionuclide. Media that will promote the sorption of the required radionuclide cation, while eluting the target material anion at the same time, has also to be determined.

The radionuclide and the target material are not usually of opposite charge: they are generally found to be of the same charge and a separation with a cation or anion exchange resin can be devised with the aid of distribution coefficients in a specific resin/solution system. In this case the size, charge and valencies of the element ions play a vital role. The element is more strongly sorbed to the resin with an increase in ionic charge, while the other factor playing an important role is that of the nature and type of eluting solution, be it the concentration of the solution, the availability of coordinating ligands therein, the acidity of the solution and whether the solution is a mixture or not.

1.2 Radionuclides: A Brief Overview

Accelerated charged particles from a cyclotron can be used to induce many different nuclear reactions, the heavy residues of which often include useful radionuclides for biomedical imaging, internal radiotherapy and various kinds of tracer studies. This process realises the ancient alchemist's dream – the ability to transform one element into another. Cyclotron-produced radionuclides are usually proton-rich.

Another way of creating radionuclides is by means of neutron-induced reactions in a nuclear reactor. Although the reactor-produced radionuclides are often comparatively cheaper than cyclotron-produced ones, they usually have a much lower specific activity than those produced using a cyclotron. Nevertheless, accelerator and reactor produced radionuclides are complementary, most neutron-induced reactions leading to radionuclides which are neutron-rich. Even though the two production methods create wholly different classes of radionuclides, both are important in biomedical applications. Cyclotron-produced radionuclides have become increasingly popular in the medical field (especially the PET radionuclides) and in the industrial field, as well as for research purposes.

Radionuclides produced at iThemba LABS are generally used to prepare radiopharmaceuticals for medical diagnostic purposes, such as the possible diagnosis of tumours in the human body. The radiopharmaceutical is either injected into the body or ingested by the patient. The radiopharmaceutical makes it possible for the doctor to identify any tumours, as they scan the body, providing high-quality images of the activity distribution in the patient's system.

The following requirements play a vital role in the routine production of radionuclides and radiopharmaceuticals:

- The production method, involving the bombardment as well as the chemical separation of the radionuclide, must be economically viable.

- The final product must have a high specific activity, with little or, preferably, no radionuclidic, radiochemical or chemical impurities.

- The chemical separation must be as simple as possible, making it easy to perform the production within a hot cell with the minimum radiation exposure to the technician.

- The radiopharmaceutical must comply with certain specifications and be registered with the South African Medicines Control Council.

A carrier-free radionuclide is one that is recognised as having a high specific activity, high radionuclidic purity (that is, free from other radionuclides), high radiochemical purity (that is, free from any chemical form other than the required chemical form of the radionuclide) and high chemical purity (that is, a low presence of non-radioactive material).

Whereas the chemical and radiochemical purity levels in a final product are determined solely by the efficiency of the chemical procedures, the radionuclidic purity of the product is determined by both chemical and physical means. Two types of radionuclidic impurities can be distinguished, namely, radionuclides present in the product other than that of the desired product, which can be reduced to acceptable levels by chemical means, and radionuclides of the same element as that of the product, *i.e.* chemically indistinguishable from the desired radionuclide.

Quality control is performed on the final product to determine whether it is carrier-free (also referred to as no-carrier added) and that it complies with the standards as prescribed by the South African Medicines Control Council. A high-resolution gamma ray spectrometer is used to determine the radionuclidic purity, while the radiochemical purity is determined using paper, gel or thin layer chromatography. The chemical purity is determined using induced coupled plasma emission spectrometry, electrothermal atomisation spectrometry, flame atomic absorption spectrometry or colorimetric spectrophotometry. It is the chemistry of a production, therefore, that is the most important discipline in the isolation and purification of the relevant radionuclide, as one has to ensure that a high quality product is despatched to the client.

1.3 A Short History of Cyclotron Facilities in South Africa

The first cyclotron to be built in South Africa was situated at Pretoria and put into service in 1956, under the ownership of the Council for Scientific and Industrial Research (CSIR). This cyclotron was designed to produce both internal and external beams of protons (5.8 – 15.3 MeV), deuterons (11.5 – 17.3 MeV), ^{3}He (18 – 38 MeV) and alpha particles (23 – 34.6 MeV), making it a versatile machine for radionuclide

production. A routine radionuclide production programme existed from 1965 until its closure in 1988.

The radionuclide production programme in Pretoria began by producing ^{67}Ga, ^{109}Cd and ^{123}I, albeit in relatively low quantities. The radiochemical separations of these radionuclides were performed in normal ("cold") laboratories, using fume cupboards and a few lead bricks for shielding purposes. The methods used to separate the radionuclides from their respective target materials were based on solvent extraction and co-precipitation, with the result that the staff members involved were directly exposed to high levels of radiation.

Operators tended to pick up a severe hand dose, as well as an unacceptable radiation dose to the head area (in terms of today's standards), when performing solvent extraction procedures. Contamination issues were also rife in those early days as a result of the grease on the glass tap at the bottom of the extraction flask dissolving in the organic solvent used in the solution, allowing radioactive solution to seep through the bottom of the flask. The situation was aggravated by the fact that the operator would have to shake the flask, thereby spraying the radioactivity over himself and contaminating the laboratory at the same time. It was as a result of these issues that T. N. van der Walt and others laboured to convert those production procedures to ones employing ion exchange methods[4]. They managed to do so successfully, paving the way for South African radiochemists to perform productions more efficiently, safely and produce a final product that was more radiochemically pure.

While there was a discussion to build a bigger cyclotron in the Transvaal area (now known as Gauteng), the government decreed that a new facility be built in the Western Cape and the National Accelerator Centre was established in the Faure area, near Somerset West, in 1977 under the control of the CSIR.

The new 200 MeV separate sector cyclotron at Faure produced its first extracted proton beam in 1987. The new facility was tasked to support three main areas: 1) experimental physics research using accelerated ion beams, 2) radiotherapy using both neutrons and protons, and 3) radionuclide production. The Radionuclide Production Group (then known as Isotope Production) produced its first routine radionuclides in

1988, namely ^{67}Ga, ^{81}Rb and ^{123}I. These three radionuclides have been in production at Faure ever since.

Various other radionuclides and radiopharmaceutical products have been added to the list in the years to follow, some of which have been discontinued later when market interest in them declined, while others have shown increasing demand. Some of the radionuclides which have once been produced regularly and later discontinued are ^{111}In[6,7] and ^{201}Tl. This was because the requirements of the local nuclear medicine community changed. At one stage, the Department of Energy (DOE) of the United States requested iThemba LABS to produce non-processed ^{68}Ge and ^{82}Sr, in the form of bombarded targets, on a regular basis. Both these radionuclides are still important export products for iThemba LABS. In recent times, the "bread and butter" radionuclides for the local community include ^{67}Ga, ^{81}Rb, ^{123}I, and ^{18}F (as ^{18}F[FDG]). Certain labelled compounds of ^{123}I are also routinely produced. Various other radionuclides have been investigated at one time or another and can be added to the routine list if the market (or important clients) demands. These include ^{52}Fe, ^{55}Fe, ^{64}Cu, ^{88}Y, ^{133}Ba, and ^{139}Ce.

Other longer-lived radionuclides brought into the facility's arsenal include ^{22}Na, obtained from a Mg target[8] and ^{103}Pd, obtained from the bombardment of a silver target[9,10]. ^{22}Na is exported, either as solutions or as dry positron sources, on a regular basis. Local demand for ^{103}Pd never really materialised but small quantities for experimental purposes have been delivered on a few occasions.

The National Accelerator Centre, a multidisciplinary scientific research laboratory, was renamed iThemba LABS in 2001. It is currently one of several National Facilities administered by the National Research Foundation (NRF) and it provides facilities for:

- The training of students and post-graduates in basic and applied research, using accelerated particle beams.
- Particle radiotherapy for the treatment of cancer.

- The supply of accelerator-produced radionuclides for research and diagnostic nuclear medicine.

The success of iThemba LABS lies in bringing people from all over the world from medical, biological and physical science backgrounds together by providing opportunities for research and postgraduate training in these separate disciplines, as well as stimulating mutual interest in the interdisciplinary areas.

Five accelerators are currently operated by iThemba LABS, four of them at the Faure facility, namely a 6 MV Van der Graaff accelerator for material science, an 8 MeV injector cyclotron providing light ions for the separated sector cyclotron (SSC), a second 8 MeV injector cyclotron providing heavy ions and polarized protons for the SSC and the SSC itself. The SSC is a variable-energy machine capable of accelerating protons to a maximum energy of 200 MeV. A tandem Van der Graaff accelerator is also operated in Johannesburg at the iThemba LABS (Gauteng) facility. A layout of the SSC facility and its experimental areas is shown in Fig. 1.1.

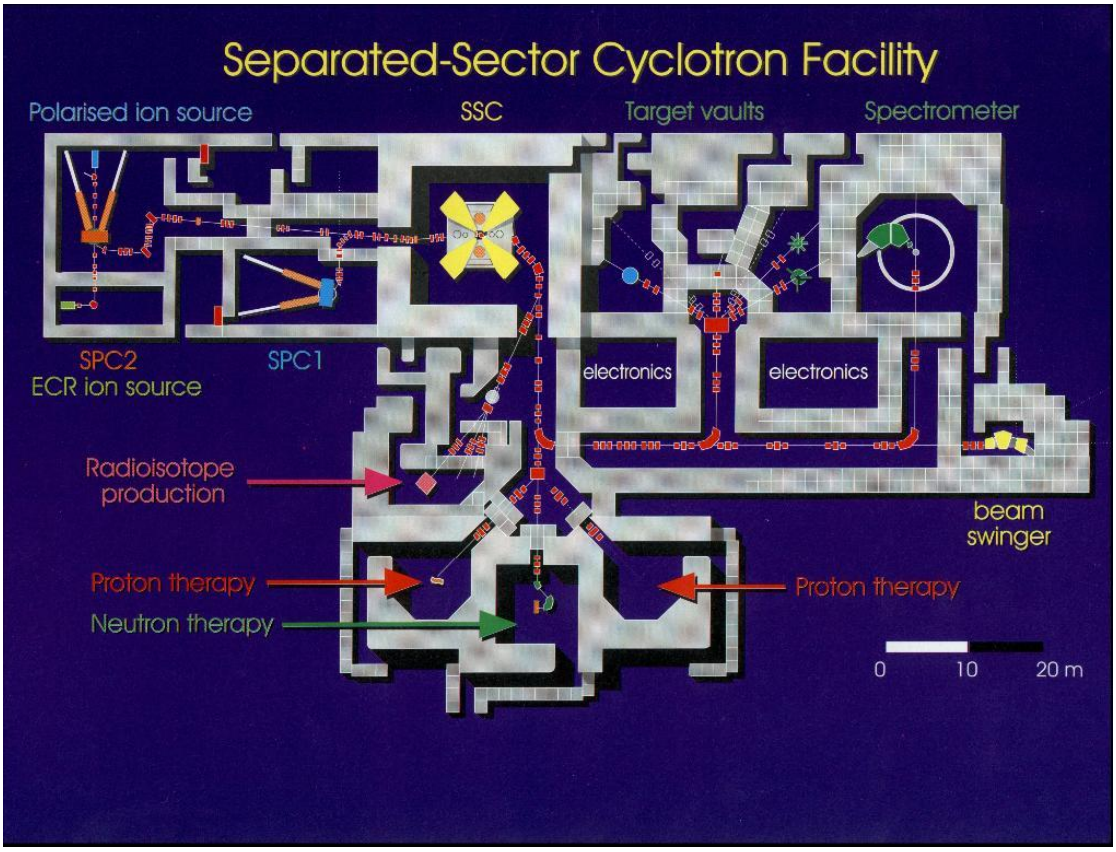

Fig. 1.1: The SSC facility layout at iThemba LABS

1.4 Radionuclide Production at iThemba LABS

The Radionuclide Production Group at iThemba LABS is heavily relied upon by nuclear medicine centres at local hospitals and clinics to produce various radiopharmaceuticals, using radionuclides to label specific organic or inorganic compounds. Some income is also generated for the laboratory by the sale of these products, as well as from exports of longer-lived radionuclides to other countries. As a result, the amount of radioactive material to be despatched has increased substantially, which requires certain facilities for personnel to be able to perform their duties safely. A brief explanation of the group's facilities follows below.

The schematic design of the layout of the Radionuclide Production complex was strongly influenced by safety considerations and, particularly, by the control over radioactive materials and the containment of radioactivity released accidentally. The complex is divided into three areas, namely, the so-called "red", "blue" and "white" areas. The "red" area is a high-risk environment from a radiation exposure point of view, where high levels of activity are handled, while only lower-risk or low-activity materials are handled in the "blue" area. The "white" area is, in principle, a clean area and this is where the staff offices and the like are situated.

Personnel moving from the "red" area to the "blue" area, or from the "blue" area to the "white" area, have to pass through a monitoring and decontamination station. In this way, the accidental spreading of radioactive contamination can be prevented. As the inhalation of radioactivity is a possible health hazard, negative pressures of 50 Pa (in the "blue" area) and 100 Pa (in the "red" area) with respect to ambient pressure are maintained by the air-conditioning system to ensure that any accidentally released radioactive dust, vapour or gases are contained (*i.e.* won't spread to an area of lower risk).

Support facilities, such as the target transport system, helium-cooling system for beam windows, cooling-water system (see Chapter 2), the hot cells and a radioactive waste management system are housed in the "red" area, which also includes two irradiation vaults. Other facilities required, such as those for target preparation, quality control,

dispensing and radiopharmaceutical labelling are situated in the “blue” area. It is only the area for the packing and despatch of the final product that is situated in the “white” area.

Radionuclide production targets become highly radioactive when irradiated and pose a potential health risk to personnel if not handled correctly. This problem is overcome to a large extent by transporting targets between the bombardment stations, hot-cell complex, target loading station and target storage using a remote controlled rail transport system.

Briefly, once the bombardment of a batch target has been completed, it is transported from the irradiation vault to one (of two) reception hot cells, where the target material is removed from the target holder. The radiochemical separation of the particular radionuclide is performed in one (of twelve) processing hot cells. Note that a designated hot cell is used for each of the routinely produced radionuclides in order to prevent any cross contamination of the final product. Once the chemical separation has been completed and the radiopharmaceutical prepared, it is transported to the dispensing laboratory, where the pharmacist performs the dispensing in aseptic conditions according to the orders received from clients. A sample of the final product will also be taken for quality control purposes (*e.g.* chemical purity, radionuclidic purity, etc.) to ensure that it meets the prescribed specifications as registered with the South African Medicines Control Council.

Once the dispensing is taken care of, the vials containing the radiopharmaceutical are sealed and packed into lead pots. The lead pots, in turn, are packed into tins and sealed, before placing them into their respective boxes. The boxes are despatched to the various hospitals or clinics which ordered the product. A schematic diagram of the layout of the Radionuclide Production facility is shown below[11].

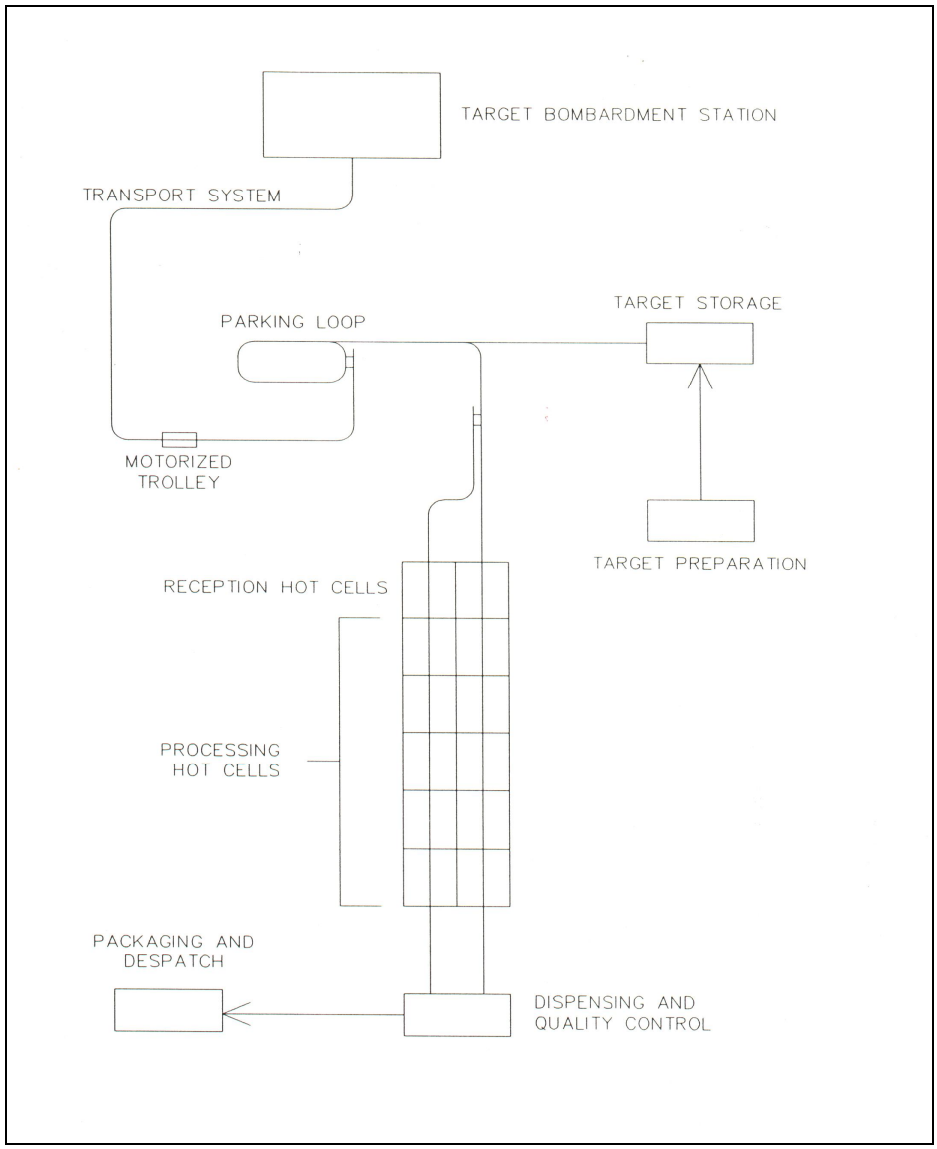

Fig. 1.2: Radionuclide Production facility layout

1.5 Project Motivation

There have been times in the recent past where it was thought that the Radionuclide Production Group should concentrate on product development and sales, on a commercial basis, forgoing research and development. Criticism has also been aimed at research in ion exchange chromatography, with the claim that this field has run dry. Similar criticism has also been aimed at the measurement of nuclear data using activation methods. The aim of this work is to prove that research and development is paramount to the future of Radionuclide Production at iThemba LABS, with the use

of ion exchange chromatography an essential component thereof, for the release of new products as well as in experiments of purely academic interest. Similarly, activation methods are crucial to this field of research.

To underline this aim, it was the author's objective to use activation methods, ion exchange chromatography and nuclear data to produce new products for iThemba LABS, namely:

- ^{88}Y from Sr metal-based target material;
- ^{82}Sr from Rb metal-based target material;
- ^{68}Ge from Ga metal-based target material;
- ^{133}Ba from Cs metal-based target material;
- The production of ultra-pure ^{67}Ga.

It was also the author's objective to perform chemical experiments, using ion exchange chromatography, to provide answers in research projects, namely:

- The separation of ^{28}Mg from LiCl target material;
- The separation of ^{227}Pa from Th target material in order to answer a long-standing question in cluster radioactive decay.

To be sure, other studies on these topics have been performed in the past, as evidenced by significant numbers of research papers in the literature. The question is whether these topics have been exhausted? The answer is clearly not. There are always new challenges, problems to solve and methods to improve. Of particular interest to iThemba LABS at the present time is that it has invested heavily to increase the beam intensity of the 66 MeV proton beam delivered by the SSC in order to increase the capacity of the radionuclide production programme. The SSC can now deliver external beams of 500 μA, which cannot be fully utilized by current targetry. Some targets had to be enlarged in order to create more surface from which they can be cooled. This increased the volume of target material to be processed, thus the chemical separation procedures had to be revisited. Another exciting development is that sometime in the near future, the proton beam will be split and provided to two

target stations simultaneously. A new beam splitter is in an advanced stage of construction and will be commissioned towards the end of 2008. These developments affect all aspects of the radionuclide production programme, since it will enable the RPG to use the two main bombardment stations simultaneously.

The above-mentioned topics will be addressed as independent case studies in the chapters to follow. Most of the work presented should be seen in the light of the expansion programme for radionuclide production at iThemba LABS. Towards this end, it is necessary to give some more detail on the production facilities, the topic of the next chapter.

1.6 References

1. Samuelson O., 1963. Ion Exchange in Analytical Chemistry, 3rd Ed. John Wiley and Sons Inc., New York.
2. Reiman W., Walton H. F., 1970. Ion Exchange in Analytical Chemistry, 1st Ed. Pergamon Press, New York.
3. Van der Walt T. N., 1993. *Ph.D. Thesis*, Randse Afrikaanse Universiteit, South Africa.
4. Van der Walt T. N., 2007. Personal conversation.
5. Naidoo C., 1998. *M.Sc. Thesis*, University of Cape Town, South Africa.
6. Van der Meulen N. P., 1997. *B. Tech. Thesis*, Cape Technikon, South Africa.
7. Van der Meulen N. P., van der Walt T. N., Dolley S. G., 2005. *Radiochim. Acta*, **93**, 575.
8. Van der Walt T. N., Haasbroek F. J., 1994. In: *Synthesis and Applications of Isotopically Labelled Compounds* (Ed: Allen J., Voges R.), John Wiley and Sons Ltd.
9. Faβbender M., Nortier F. M., Schroeder I. W., van der Walt T. N., 1999. *Radiochim. Acta*, **87**, 87.
10. Aardeneh K., 2002. *Ph. D. Thesis*, University of Stellenbosch, South Africa.
11. Stevens C. J., 1992. *M. Dip. Thesis*, Cape Technikon, South Africa.

CHAPTER 2 BOMBARDMENT FACILITIES FOR RADIONUCLIDE PRODUCTION AT iThemba LABS

There are four dedicated bombardment facilities for radionuclide production at iThemba LABS, three of which have been extensively used during the course of this work. There is also a fifth "open" high-energy beamline available for any temporary experimental set-ups required for research or testing purposes. Each of the bombardment facilities will be briefly discussed below.

2.1 The Horizontal Beam Target Stations

Two bombardment stations with horizontal beamlines are located in the same vault. This vault also accommodates the open experimental beamline.

2.1.1 Bombardment Station for Batch Targets

The first bombardment station to be designed and built at iThemba LABS was planned to be a multi-purpose facility in which many types of batch targets could be irradiated. It has been in routine use since 1988. A sceptical group of cyclotron operators named the station the "White Elephant" at that time but once it demonstrated its functionality, the "White" was dropped and the facility came to be known as "the Elephant" ever since.

An overall view of the Elephant is shown in Fig. 2.1. During bombardment, the target is located inside a local, cylindrical radiation shield[1] to protect sensitive components inside the vault against excessive radiation damage and to reduce neutron activation of the vault and its contents. The station accommodates a remotely-controlled, rotatable target magazine[2] which, in its present incarnation, can hold up to nine standardized target holders. A selected target holder can be rotated to the irradiation position or to a load/unload position under stepper motor control. A remotely-controlled pneumatic robot arm facilitates the transfer of a target holder between the

station and a target transporter, which moves on an electrified rail network. In this way, highly radioactive targets can be transferred and transported between the bombardment station and the hot-cell complex without any direct radiation exposure to staff. The station is remotely controlled and monitored by means of a computer-based system, located in the radionuclide production control room.

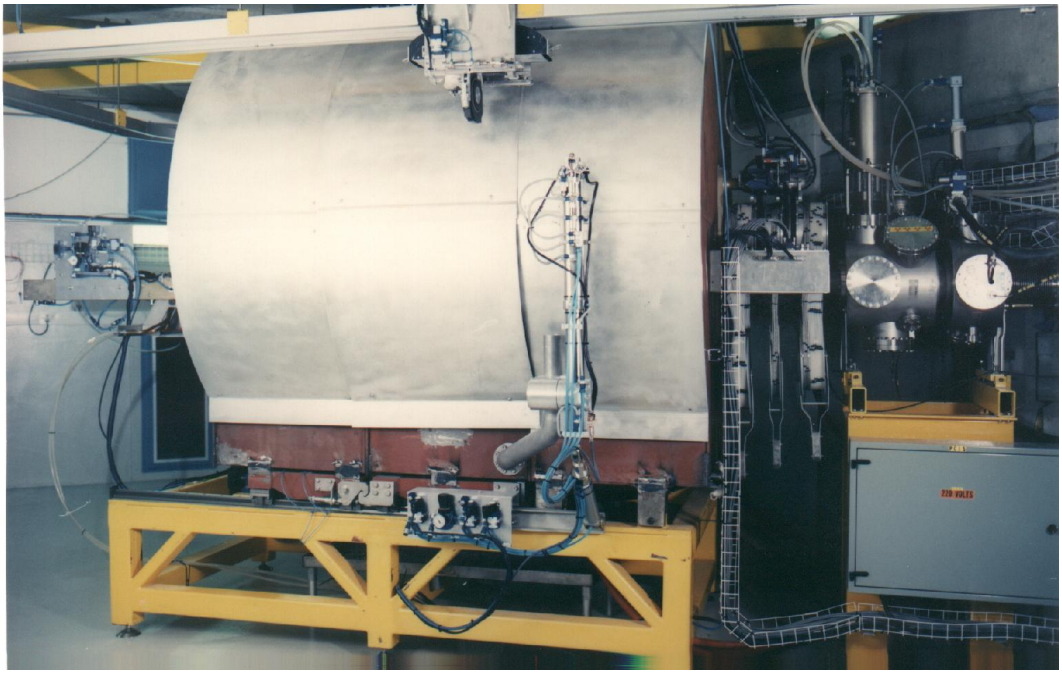

Fig. 2.1: An overall view of the Elephant[2], a bombardment station for batch targets utilizing a horizontal proton beam. The station is showed with the radiation attenuation shield closed and a target transport trolley, with target holder, is shown in the target transfer position (towards the top of the figure). Note the beam diagnostics chambers immediately upstream (to the right) of the target station. The pneumatic pusher arm to connect the cooling water lines to a target holder is visible on the left side of the station.

The targets are irradiated outside the beamline vacuum, from which they are isolated by a helium-cooled double-foil beam window. This is done to protect the high vacuum of the cyclotron against possible gaseous releases from targets during bombardment and to make rapid target exchanges possible, which is especially important for the production of short-lived radionuclides. Cooling water is supplied to the targets through a pneumatic pusher arm.

The design philosophy[2] of the station strives to reduce maintenance and repairs to radioactive components inside the shielding, as far as humanly possible. All pneumatic components, electric motors, service connections, valves, etc., are mounted

on the outside of the local radiation shield. Mainly metals are used on the inside, which are extremely radiation resistant. For many years, the Elephant was the only dedicated bombardment station for radionuclide production at iThemba LABS. In recent times, the Elephant is the work horse for the production of most of the shorter-lived radionuclides for the local radiomedical community (^{67}Ga, ^{81}Rb, ^{123}I). It is also extensively used for the production of ^{22}Na. Beams of 66 MeV protons and intensities up to 100 µA are routinely used in this facility.

2.1.2 Bombardment Station for Semi-Permanent Targets

A smaller bombardment station with similar characteristics to the Elephant was designed and built for semi-permanent targets[3] (see Fig. 2.2). The main difference is the absence of the robot arm for target exchanges (as the targets would be semi-permanently installed) and, consequently, there was also no need for the station to be serviced by the electric-rail target transport system. This station (which has been named Babe) was completed in 1999 and was initially used to produce small quantities of ^{18}F using an experimental ^{nat}Ne gas target. Currently, this bombardment station only houses one target, a commercial ^{18}O-water target for the large-scale production of ^{18}F, for which purpose it is used extensively.

2.2 The Vertical Beam Target Station

The Vertical Beam Target Station[4] (VBTS) is the latest edition to the dedicated bombardment facilities for routine production of radionuclides at iThemba LABS (see Fig. 2.3). Its construction was completed in 2005 and it has been in routine use ever since.

The design philosophy of the VBTS was exactly the same as for the Elephant. The main difference, other than the direction of the beam being vertical, is the omission of a target magazine. The main aim of the VBTS is to produce long-lived radionuclides with increased beam intensities, thus a target holder would normally stay in the station

for several weeks at a time. Consequently, there was no need for a target magazine. VBTS targets are physically larger than Elephant targets in order to have more surface area for cooling. This will be described in more detail later. Beam currents up to 250 µA are routinely used, mainly for the production of ^{82}Sr and ^{68}Ge.

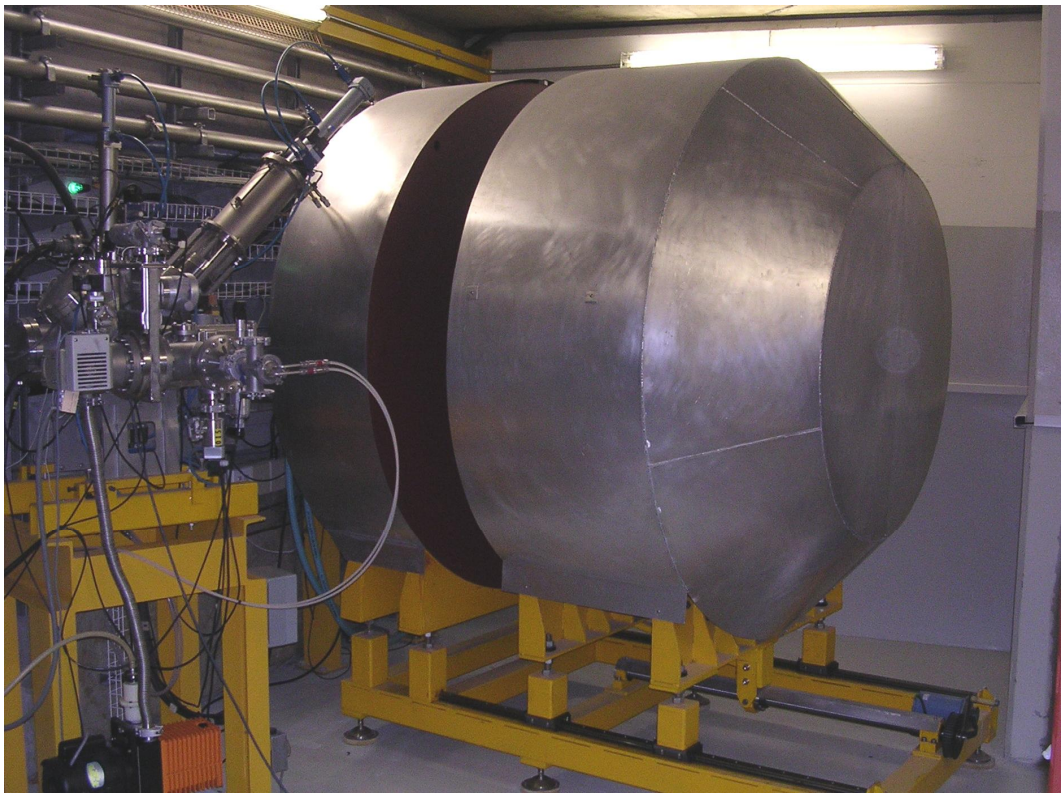

Fig. 2.2: An overall view of Babe[3], a bombardment station for semi-permanent targets utilizing a horizontal proton beam. The station is showed with the radiation attenuation shield, one section of which moves on rails, partially opened. The beam is incident from the left side of the station.

Common to both the Elephant and the VBTS is beam sweeping, in order to enlarge the area of the target directly exposed to the beam. This improves the thermal behaviour of targets, making it possible to increase the beam intensity. The beam is swept in a circular motion, at a frequency of 450 Hz in the case of the Elephant and 3000 Hz in the case of the VBTS.

Fig. 2.3: An overall view of the VBTS[4], a bombardment station for the irradiation of batch targets utilizing a vertical proton beam. The station is showed with the radiation attenuation shield closed. The remotely-controlled pneumatic robot arm which facilitates target transfers is shown in the foreground, while the electrified rail for target transport can be seen in the background. Note the beam diagnostics chamber on top of the target station.

2.3 Batch Targets at iThemba LABS

Most of the batch targets used at iThemba LABS consist of the target material of choice encapsulated in either aluminium, stainless steel or niobium. The infrastructure to encapsulate target material in aluminium is resident in the laboratory, whereas stainless steel and niobium encapsulation have to be outsourced. The encapsulation serves two purposes: 1) to protect the target material from the cooling water, and 2) to contain the target material, which often goes into a molten state during bombardment with high-intensity beams. The choice of encapsulation material depends on the target material to be contained. Molten target material may, for example, attack the aluminium capsule, in which case a more inert material, such as niobium, will be a better choice. Examples of this will be described in subsequent chapters.

The target holders presently in use at iThemba LABS can be used with either one target mounted, or with two targets mounted in tandem in the same holder. Fig. 2.4 is an exploded view of a VBTS target holder, showing the various components as well as two encapsulated targets in tandem. Note, in particular, the beam entrance window and beam stop. Fig. 2.5 compares the target holders of the Elephant and the VBTS. The outer dimensions of Elephant and VBTS target holders are exactly the same, however, the inner dimensions differ as VBTS targets are larger. Also, VBTS targets require a larger flow of cooling-water to dissipate the larger amount of heat generated by the beam, thus more water ports had to be provided (four inlet and four outlet ports in the case of VBTS targetry, compared to two inlet and two outlet ports in the case of Elephant targetry). Both type of target holder is compatible with all ancillary facilities, *e.g.* the target transporters, reception hot cells, target loading station and target store.

Note that in both types of target holder, the cooling water surrounds the target capsules in a 4π geometry. The water layers are thin (1 mm thick) and have a high velocity (about 32 m/s or higher) in order to remove the heat dissipated by the beam effectively. The high velocity is to suppress surface boiling, *i.e.* to remove steam micro-bubbles rapidly before a layer of steam can form on a surface. This is important, as a steam layer can effectively isolate the cooling water from the surface to be cooled, leading to rapid target burnout. A water flow rate through an inlet port is of the order of 30 liter/min. Elephant target holders, therefore, require a cooling water flow of about 60 liter/min and VBTS targets holders 120 liter/min. Only de-ionized water is used for cooling at a nominal pressure of 10 bar.

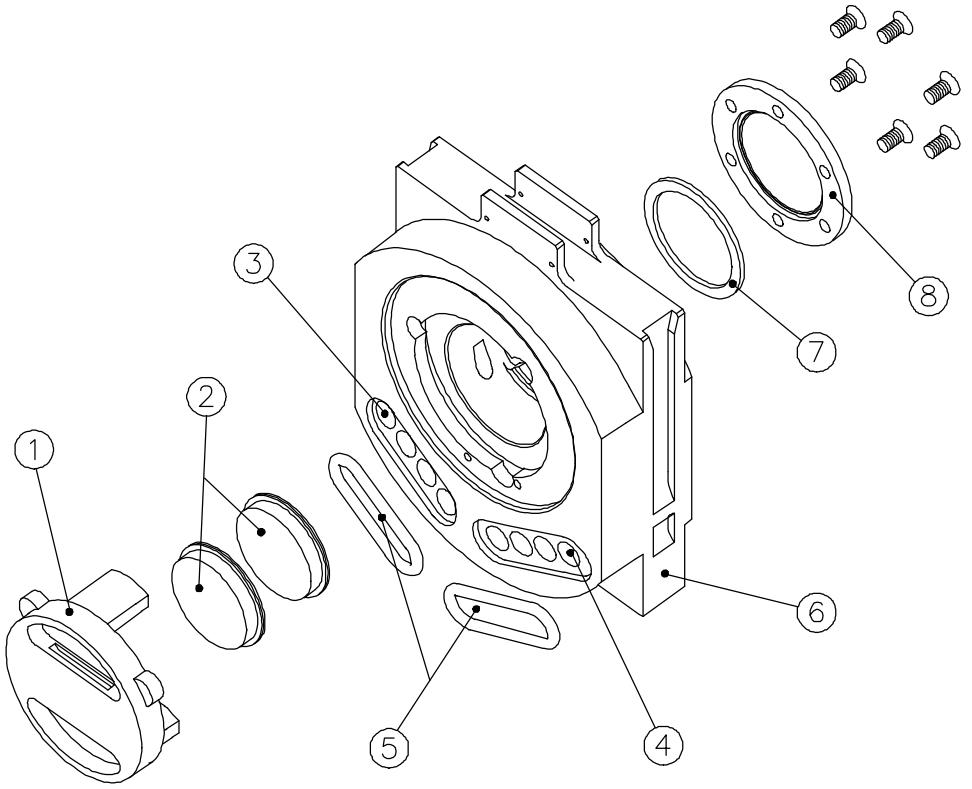

Fig. 2.4: Exploded view of a VBTS target holder, showing (1) the beam stop, (2) tandem stainless steel or Nb-encapsulated solid targets, (3) cooling water inlet ports, (4) cooling water outlet ports, (5) disposable rubber water seals, (6) target holder body, (7) Cu sealing ring, and (8) beam entrance window.

2.4 The RERAME Activation Chamber

Activation of foil stacks and experimental targets are often done at iThemba LABS in an irradiation chamber which is based on the design of the RERAME (REcoil RAnge MEasurements) facility of the Laboratory Nazionale del Sud (LNS) in Catania, Italy[5]. Although this facility was originally intended for recoil range measurements, it proved to be very versatile for many other kinds of activation studies also. A photograph of the RERAME chamber is shown in Fig. 2.6.

Fig. 2.5: Elephant (LEFT) and VBTS (RIGHT) target holders, with beam entrance windows and beam stops removed. The 20 mL serum vial on the left is for scaling purposes.

Fig. 2.6: The modified RERAME activation chamber at iThemba LABS, shown with the door in an open position. Targets or foil stacks are mounted on the door, in a vice moving on rails, in order to ensure good positional accuracy. The beam is incident from the left.

A collimator assembly with electron suppression for the chamber was designed and built at iThemba LABS[6]. This collimator is electrically insulated from the chamber in order to measure the beam current intercepted by it separately. A vice mechanism for holding the targets in the irradiation position, as well as the collimator assembly, are mounted on the door of the chamber. A novel feature is that the door can be opened and turned through 180º, thus, bringing parts which are normally inside the chamber outside. This allows for rapid and easy insertion and removal of targets. The door is also fitted with a rotatable handle which controls the opening and closing of the jaws of the vice, allowing for samples, targets or foil stacks of different thicknesses to be accommodated.

The chamber is equipped with insulated feed-through for electrical connections, vacuum connections and a transparent port for viewing a fluorescent beam monitor with a TV camera. A beryllium oxide (BeO) viewer can be placed in the target position, which is useful for the initial focusing when the beam is first brought into the chamber. The entire chamber is electrically insulated and is provided with electron suppression at the beam entrance. It is, therefore, a Faraday chamber and allows for accurate measurement of the integrated beam current. During irradiations, the beam current to the chamber and also the fraction of the beam which gets intercepted by the collimator are monitored continuously and logged.

The vacuum system of the chamber is completely independent because it has to be periodically isolated from the beam-line to insert or remove targets. A rotary pump provides fore vacuum (~ 10^{-3} mbar) and a turbo-molecular pump the high vacuum (~ 10^{-6} mbar).

2.5 References

1. Steyn G. F., van Rooyen T. J., Binns P. J., Hough J. H., Nortier F. M., Mills S. J., 1992. *Nucl. Instrum. Meth. A*, **316**, 128.
2. Mills S. J., Nortier F. M., Rautenbach W. L., Smit H. A., Steyn, G. F., 1989. In: *Proceedings of the 12th International Conference of Cyclotrons and their*

Applications (Martin B., Ziegler K., Eds). World Scientific: Singapore, p. 527.

3. Nortier F. M., Binns P. J., Hanekom J., Penny M. A., Quantrill R. E., Smit H. A., van Rooyen T. J., Xulubana V. M. P., 1999. In: *Proceedings of the 8th International Workshop on Targetry and Target Chemistry* (McCarthy T. J., Ed). St Louis, Missouri, U.S.A., p. 22.
4. Steyn G. F., Vermeulen C., Quantrill R., Crafford J. P. A., Delsink J. L. G., 2004. In: *Proceedings of the 10th Workhop on Targetry and Targetry Chemistry* (J. R. Nickles, Ed), Madison, Wisconsin, U.S.A.
5. Fresca Fantoni R., Gadioli E., Guazzoni P., Vergani P., Zetta L., Dellera P. L., Tomasi F., Campagna V., Ciavola G., Marchetta C., 1994. *Appl. Radiat. Isot.*, **45**, 325.
6. Szelecsényi F., Steyn G. F., Kovács Z., Vermeulen C., van der Meulen N. P., Dolley S. G., van der Walt T. N., Suzuki K., Mukai K., 2005. *Nucl. Instrum. Meth. B*, **240**, 625.

CHAPTER 3 ORGANIC ION EXCHANGE RESINS USED IN THIS WORK

Column ion exchange resins are regarded in many fields of chemistry as being obsolete. The same can not be said for radiochemistry, where the use thereof is effective, tidy and safe (from a radiation safety perspective). Most of the organic ion exchange resins in question are resistant to radiation and the research performed using these resins is to ensure an effective separation of the radionuclide in question from its target material, such that a chemically and radiochemically pure product is obtained. The use of ion exchange resins has proved to be the most effective in this regard compared to any other method used in radiochemistry over the years.

Ion exchange resins have different makeup (although many of them are based on a styrene divinylbenzene copolymer lattice) and, therefore, different properties. It is for this reason that it was thought prudent to briefly discuss each ion exchange resin used in this work.

3.1 Amberchrom adsorption resins

Amberchrom™ chromatographic resins are macroporous, polymeric resins for adsorption and reversed liquid phase chromatography. They have been designed for laboratory and process scale purification of proteins, peptides, nucleic acids, antibiotics and small molecular weight pharmaceuticals. They have unique surface chemistries which offer distinctive selectivity for biomolecules, resulting in excellent separation of difficult compounds while maximizing capacity and yield of the desired product[1]. Amberchrom™ CG161 is based on a polystyrene-divinylbenzene polymer, while its CG71 counterpart is based on an acrylic polymer. Each resin is packed in slurry form (in 20 % ethanol solution) in quantities ranging from 25 mL to 50 L[2].

Amberchrom resins provide advantages over silica-based packings due to their physically and chemically stable polymeric structure[3]. As a result, the resin provides the following benefits for production-scale chromatography:

- The ability to use aggressive mobile phases for selectivity optimization.
- The resin can be cleaned in place (CIP) easily with a strong acid or base.
- Allows for thermal or chemical sanitization.
- Allows for gradient elution, or cleaning, using a broad range of solvents with a minimal change in bed volume.
- Enables repeated cycles with assured column stability and reproducible performance.
- Has the ability to operate at high flow rates with moderate back pressure.

Amberchrom™ CG161 is an insoluble polystyrene divinylbenzene polymer (with no functional groups) manufactured for high value chromatographic applications[4]. Its high surface area, unique ideal pore size and pore volume distribution makes the resin ideal for the separation of peptides. The resin has a high capacity for many pharmaceutical compounds and can be used in high resolution, low pressure chromatography. It is suitable for use in pharmaceutical applications in the front end capture, purification and desalting modes of operation, depending on its particle size. Amberchrom CG161 is ideally suited for operation within the entire pH range and can be easily cleaned in place (CIP) using organic solvents and dilute acids or bases. In addition to its excellent chemical resistance, it also exhibits low swelling in the more common solvents used.

Amberchrom CG71 is an insoluble aliphatic (acrylic ester) polymer. It is claimed that the CG71 has similar properties to CG161 resin, with both being hydrophilic resins with similar uses[5].

3.2 Chelex 100 chelating resins

Chelex chelating ion exchange resins has an unusually high preference for most transition elements and other heavy metals over monovalent cations such as sodium or potassium[6]. Its selection for divalent over monovalent ions is ~5000:1 and it has a strong attraction to transition metals, even in highly concentrated salt solutions.

Chelex 100 has been exhaustively sized, purified and converted to make it suitable for accurate, reproducible analytical techniques. It is a styrene divinylbenzene copolymer containing paired iminodiacetate ions which act as chelating groups in binding polyvalent metal ions. Chelex chelating resin is classified with the weakly acidic cation exchange resins, due to its carboxylic acid groups, but it differs from ordinary cation exchangers in that it has a high selectivity for metal ions and much higher bond strength.

The resin is effectively regenerated in dilute acid and can operate in acidic, neutral and basic solutions of pH 4 or higher. The resin behaves as an anion exchanger at very low pH values. Selectivity of ions using this resin is dependent on pH, ionic strength and the presence of other complex-forming species.

If a cation is tightly held (complexed) by Chelex 100 resin and is to be isolated from a solution of weakly held cations, a flow rate in excess of 20 mL/min can be used. Separations between similar species require lower flow rates of less than 4 mL/min.

3.3 AG 50W-X4 and AG MP-50 cation exchange resins

AG 50W and AG MP-50 strong acid cation exchange resins are useful for single step purification methods, for concentrating cationic solutes and for analytical determinations of mixed cationic solutes.

AG 50W-X4 cation exchange resin is composed of sulphonic acid functional groups attached to a styrene divinylbenzene copolymer lattice[7]. The amount of resin

crosslinking determines the bead pore size. A resin with a lower crosslinkage (e.g. AG 50W-X4) has a more open structure permeable to higher molecular substances than a more highly crosslinked resin (e.g. AG 50W-X8).

AG MP-50 cation exchange resin is the macroporous equivalent to the AG 50W resins, with a porosity of 30-35 %. Both of the cation exchange resins described are thermally stable and resistant to solvents, such as alcohols, reducing agents and oxidizing agents.

Resins are obtained in different mesh sizes. Resins with coarse mesh sizes (20 – 50 mesh and 50 – 100 mesh) are primarily used for large preparative applications and batch operations between the resin and sample when slurried together. Medium mesh resin (100 – 200 mesh) is used in column chromatography for analytical and laboratory scale preparative applications, while finer mesh resins are used for high resolution analytical separations. 100 – 200 mesh cation exchange resins were used for experimental and production purposes throughout this work.

3.4 Purolite S950

Purolite S950 is a macroporous aminophosphonic acid chelating resin[8], designed for the removal of toxic metals from industrial effluents at low pH. It is more highly selective, under the necessary conditions, for a range of heavy metals and common divalent ions.

The chelating resin is insoluble in acids, alkalis and all common solvents at normal temperatures. Oxidizing agents, such as concentrated nitric acid and perchloric acid, will destroy the resin at elevated temperatures and it is recommended against using concentrated nitric acid with this resin, as it could have explosive consequences.

3.5 AG MP-1 anion exchange resin

AG MP-1 resin is a macroporous, strongly basic anion exchanger, capable of exchanging anions of acidic, basic and neutral salts. Strong anion exchange resins are generally used for sample preparation, enzyme assays, metal separations and peptide, protein and nucleic acid separations.

This resin is strongly basic as a result of quaternary ammonium functional groups attached to a styrene divinylbenzene copolymer lattice[9]. The amount of resin crosslinkage determines the bead pore size. A resin with a lower percentage of crosslinkage has a lower physical resistance to shrinking and swelling, so that it absorbs more water and swells to a larger wet diameter than a highly crosslinked resin of the same dry diameter. AG MP-1, although it is macroporous, has 20 % porosity.

The resin is thermally stable to 150 ºC and is resistant to acids and solvents. It is stated that the resin slowly dissolves in hot 15 % HNO_3 or concentrated hydrogen peroxide.

3.6 General resin preparation

When working with any resin, it is good chromatographic practice to remove the "fines" (the finer particles in the resin) from the resin, such that filters and frits do not get blocked when using them, thereby, increasing the pressure drop across the column. The following decantation process was followed before packing any column for experimental or production use:

- The resin was re-suspended in its original container by means of shaking.
- The resin was poured into a suitable vessel for defining. The length of time required for resin settling depended on the geometry of the container used, the dilution factor and the particle size of the resin in question.
- The supernatant was decanted off the resin, the "fines" not having settled and suspended in the supernatant solution.

- Fresh de-ionized water was added to the resin and shaken. It is wise not to use a magnetic stirrer, as this will generate more "fines". The resin was, once again, allowed to settle, following which the supernatant was, again, decanted.
- The above process was repeated three times before the required column was packed.

Ion exchange chromatographic resins should be equilibrated after packing to ensure optimum column performance. Equilibration need only be performed on fresh resin: normal clean-in-place (CIP) procedures can be used on the resin afterwards.

3.7 References

1. Amberchrom™ Chromatographic Resins: High Selectivity for Biomolecules. Rohm and Haas.
2. Amberchrom™ chromatographic resins: Instruction Manual for Packing and Use. Rohm and Haas.
3. Coppi S., Betti A., Caldari A., 1987. *J. Chromatogr.*, **395**, 159.
4. Amberchrom® CG161 Chromatographic Grade Resin, Product Data Sheet. Rohm and Haas.
5. Amberchrom® CG71 Chromatographic Grade Resin, Product Data Sheet. Rohm and Haas.
6. Chelex 100 and Chelex 20 Chelating Ion Exchange Resin: Instruction Manual. Bio-Rad Laboratories.
7. AG® 50W and AG MP-50 Cation Exchange Resins: Instruction Manual. Bio-Rad Laboratories.
8. Purolite Ion Exchange Resins: S950 Technical Data Sheet. Purolite.
9. AG® 1, AG MP-1 and AG 2 Strong Anion Exchange Resin: Instruction Manual. Bio-Rad Laboratories.

CHAPTER 4 THE PRODUCTION OF ^{82}Sr USING LARGER FORMAT RbCl TARGETS

4.1 Introduction

^{82}Sr ($T_{1/2}$ = 25.55 d), which can be produced by means of a cyclotron, is currently a sought after commodity for use in medical generators, with a growing world demand driven, particularly, by cardiologists in North America. It decays purely by electron capture[1] into its daughter, ^{82}Rb ($T_{1/2}$ = 75 s), which behaves physiologically like potassium and is effective for myocardial infusion imaging studies of patients with the use of Positron Emission Tomography (PET)[2,3]. PET can be used as a technique to monitor coronary disease patients, particularly as it has better image resolution and image contrast than its Single Photon Emission Computed Tomography (SPECT) counterpart[4]. ^{82}Rb is also used in the measurement of blood-brain barrier permeability[5].

Due to the fact that ^{82}Rb has such a short half-life, it can be injected into the patient at ten-minute intervals, with a minimum amount of radiation dose to the patient, as well as hospital staff treating the patient[6,7]. It, thus, justifies the use of a generator, where ^{82}Sr is loaded onto an ion exchanger and the daughter ^{82}Rb is eluted from it when required. A number of different ion exchange resins have been used for this type of generator over the years. Grant *et al.* reported using Chelex 100 when developing a ^{82}Sr/^{82}Rb generator[8], while Yano *et al.* performed comparisons between Chelex 100 and Bio-Rex 70 ion exchange resins[9,10]. The use of tin oxide as an ion exchanger for this type of system appears to be the most popular type available these days[11-13]. Sylvester *et al.*, however, reported the use of sodium nonatitanate as a replacement for tin oxide as substrate for the ^{82}Sr/^{82}Rb generator[14].

^{82}Sr has been obtained via various production routes, namely, spallation reactions on molybdenum metal targets[15], Rb metal targets[1,16] and natural Rb salts in the form of RbCl via the ^{85}Rb(p,4n)^{82}Sr (Q = -31.9 MeV) and ^{87}Rb(p,6n)^{82}Sr (Q = -50.4 MeV) reactions[7,17,18] (see Fig. 4.1). As both ^{85}Rb (72.2 % natural abundance) and ^{87}Rb (27.8

% natural abundance) contribute to the yield when a proton beam of 66 MeV is employed, the use of enriched ^{85}Rb for routine production purposes is not really justified - the enriched target material is expensive, the recovery of the target material is cumbersome and the benefit in terms of increased yield is relatively small.

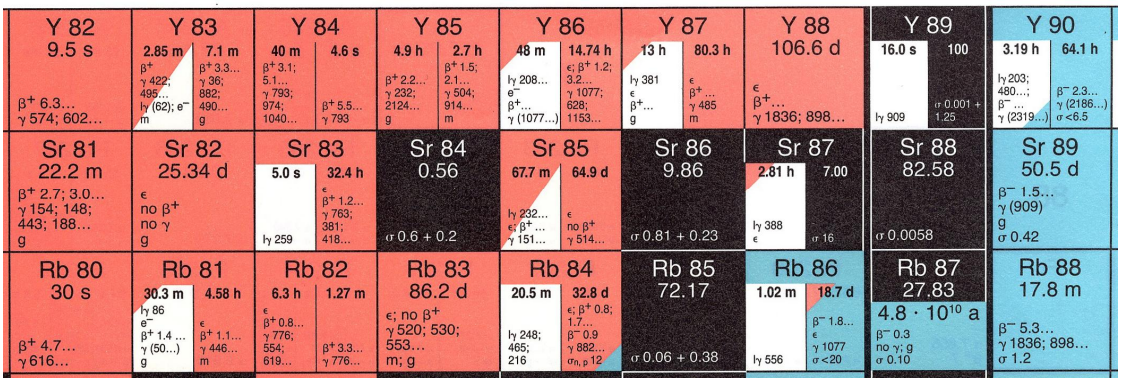

Fig. 4.1: Relevant part of the "Karlsruher Nuklidkarte" of 2006 for the production of ^{82}Sr.

Recent excitation function studies for the production of ^{82}Sr via ^{85}Rb + p by Kastleiner[19] *et al.*, ^{nat}Rb + p by Qaim[1] *et al.* and Buthelezi[20] *et al.* have been reported. As the impurity ^{85}Sr ($T_{1/2}$ = 64.9 d) is a bone of contention with the production of ^{82}Sr, it should be noted that this impurity can be kept below 20 % (EOB) when using ^{nat}Rb and a beam energy greater than 60 MeV. The ^{85}Sr/^{82}Sr ratio increases with time. It is important to have the ratio of ^{85}Sr/^{82}Sr less than 5 (an FDA regulation) as a generator cannot be used for medical purposes if the ratio exceeds that specification[16]. The evaluated excitation function of Qaim[1] *et al.* is shown in Fig. 4.2 and the corresponding thick-target production rate curves for ^{nat}RbCl + p and ^{nat}Rb + p, independently generated in this work from these cross-section values, are shown in Fig. 4.3. The calculation for ^{nat}RbCl confirms the results of Ref. 1.

As can be seen from these figures, the effective threshold is about 32 MeV and the excitation function reaches a maximum of about 112 mb at 50 MeV. With a RbCl target, a production rate of about 8.7 MBq/µAh is obtained with a proton energy window of 62 MeV down to threshold (because of energy losses inside target windows and encapsulation materials, the maximum beam energy of 66 MeV is not incident on the target material). With a Rb metal target, the corresponding thick-target production rate is 13.2 MBq/µAh. This is almost 52 % higher than in the case

of RbCl targets, which is very significant, especially for such a long-lived radionuclide. The initial experimental work at iThemba LABS was performed using RbCl salt targets, however, it is clear that future development work should also include Rb metal targets, because a much higher yield can be obtained.

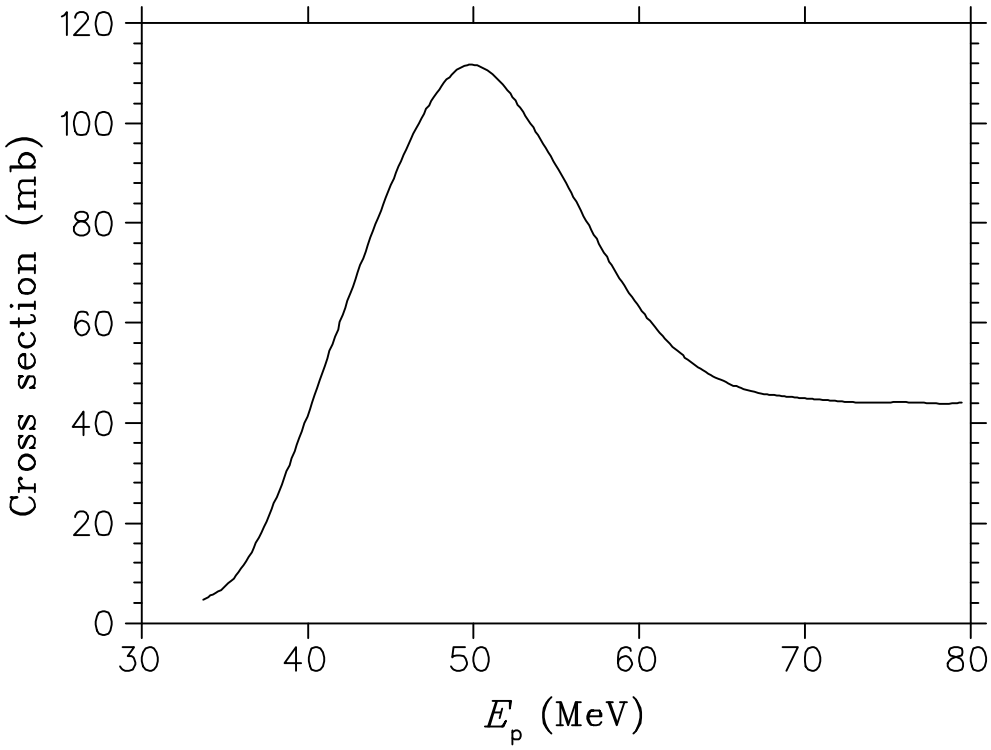

Fig. 4.2: Excitation function of ^{82}Sr formed in the reaction of protons with ^{nat}Rb. The curve is an evaluated excitation function by Qaim *et al.*[1]

Ironically, the requirement for the separation of ^{82}Sr is similar to that of the generator requirements, that is, for the Sr to be retained by the resin and the Rb to be easily eluted. As a result, many productions have been reported using Chelex 100 chelating resin[1,15-17]. Sylvester *et al.*[14] recently reported a separation method of ^{82}Sr from its target material using sodium nonatitanate ion exchanger, following their report of using the same material as sorbent for a ^{82}Sr/^{82}Rb generator. Vereshchagin *et al.* performed their production using Dowex-1 anion exchange resin[7], while Van der Walt and Vermeulen[21] and Aardaneh *et al.*[18] produced papers indicating the use of Purolite S950 as their resin of choice.

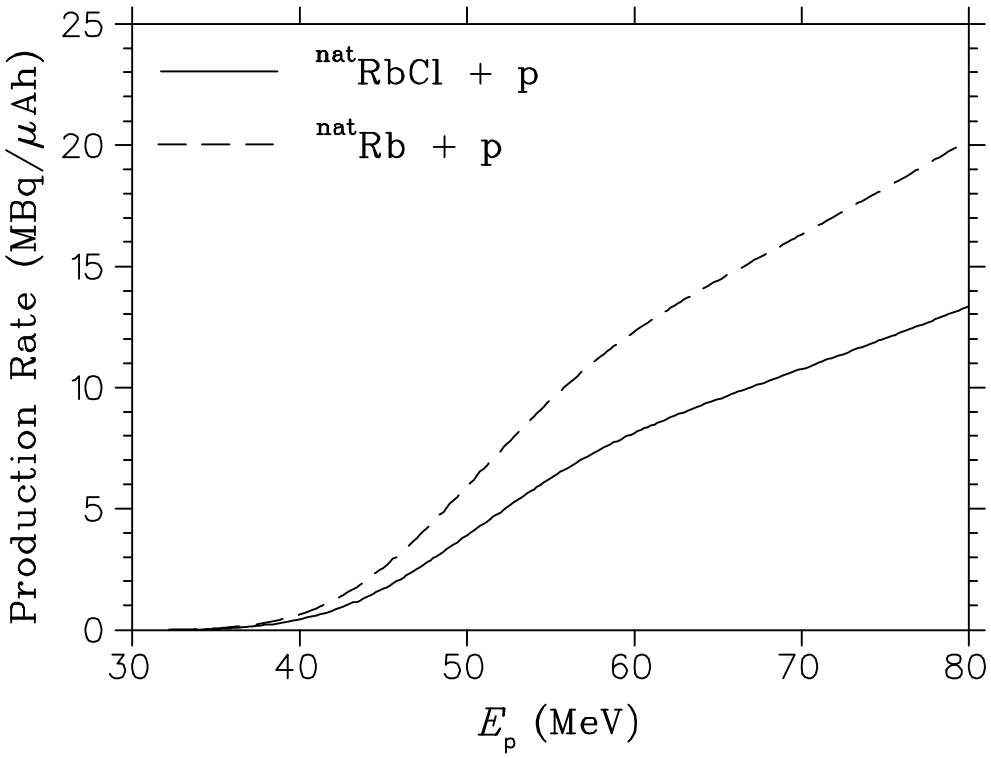

Fig. 4.3: Thick-target production rate curve of ^{82}Sr produced in the proton bombardment of ^{nat}RbCl and ^{nat}Rb metal, respectively. These curves were derived from the excitation function of Fig. 4.2.

iThemba LABS makes use of a 66 MeV primary proton beam for all its routine radionuclide productions. With the new Vertical Beam Target Station (VBTS) having recently been put into service for the production of longer-lived radionuclides, considerably higher beam intensities can be utilized, nominally 250 µA over extended periods of bombardment in contrast to a maximum of 100 µA previously. The main advantage of a higher beam intensity is, of course, a higher production rate. Unfortunately, a higher beam intensity also results in more energy dissipated in the target volume in the form of heat. The removal of the heat requires a larger surface in contact with a cooling medium (in this case fast flowing water). In practice, the RbCl salt is contained in a suitable metal capsule to prevent direct contact with the cooling water. Since the target thickness is determined by the required production energy window, it is not a parameter which can be adjusted to increase the contact surface. Instead, the target diameter has to be increased. This will result in larger targets and, consequently, more target material to be processed. The different sizes of the old target and a new VBTS target are shown in Fig. 4.4.

Fig. 4.4: Encapsulated RbCl targets for ^{82}Sr production. Both targets have nominally the same thickness but different diameters (outer diameters of 23 and 40 mm respectively). RIGHT: These capsules, made of aluminium, were used for many years at iThemba LABS to irradiate RbCl with a 66 MeV proton beam, up to a maximum beam current of 100 µA. LEFT: The new VBTS targets utilize stainless steel capsules, which are irradiated with a 66 MeV beam of nominally 250 µA. The increased surface area is necessary to effectively dissipate the increased heat load generated by the beam (see text).

4.2 Experimental

Analytical grade reagents were used throughout this work and were obtained from Merck (SA) Pty. Ltd or Sigma Aldrich GmbH, which included Sigma, Aldrich, Fluka and Riedel de Haen products. The Purolite S950 chelating resin used in this work was obtained from Purolite International, United Kingdom. Wherever water is referred to in the experimental descriptions, de-ionised water was used. This was obtained by de-ionising tap water using a Millipore MilliQ Reagent Grade Water System to a conductivity of greater than 10 megaohm cm^{-1}.

All radioactive determinations were performed using a standard calibrated HPGe detector, with a relative efficiency of 8 % (relative to three inch NaI), connected to a multichannel analyser.

10 g (Experiment 1), 20 g (Experiment 2) and 32 g (Experiment 3) of RbCl salt was weighed out, respectively. Each mass was treated in the following manner: the salt was dissolved in 200 mL 0.5 M ammonium chloride, containing 5 % methanol and 0.1 g o-phenanthroline monohydrate (to increase the distribution coefficient of Sr for a more effective retention on the resin). Tracer activities were added to the solution in the form of ^{85}Sr and ^{84}Rb and the solution activity measured.

The resultant solution was loaded on to a column (1.0 cm internal diameter) filled to a volume of 9 mL with Purolite S950, lightly crushed to decrease the particle size, and equilibrated with 50 mL 0.5 M ammonium chloride at a pH of 8. The elements were washed onto the resin using a further 50 mL 0.5 M ammonium chloride.

The Rb was eluted from the resin column using 150 mL 0.5 M ammonium chloride, before the column was rinsed with 100 mL water to remove any traces of ammonium chloride. The ^{85}Sr was eluted with 50 mL 2 M HCl. Two production runs were performed using bombarded RbCl targets once the experimental runs were completed, the first being an 8 g target and the second a 30 g target with 12000 μAh charge placed on it.

4.3 Results and Discussion

Each of the three experiments performed were done so successfully. The results of the experiments, as well as the two productions, are listed below in Table 4.1.

The difference in results between the two production runs is due to the types of encapsulation used for the target material. The first production run was performed using an 8 g RbCl target encapsulated in aluminium, bombarded in one of the horizontal-beam target stations (Elephant), while the second production run was performed using a 30 g RbCl target encapsulated in stainless steel, bombarded in the Vertical Beam Target Station (VBTS).

Table 4.1: Percentage impurity removal and percentage product yield using Purolite S950 resin.

	Experiment 1	Experiment 2	Experiment 3	Production 1	Production 2
% Sr removal in load step	0	0	0	0	5.7
% Rb removal in load step	97.0	94.5	95.2	96.5	95.5
% Sr removal in intial rinse step	0	0	0	0	0
% Rb removal in initial rinse step	3.0	5.5	4.8	3.5	4.5
% Sr removal in wash steps	0	0	0	0	0
% Rb removal in wash steps	0	0	0	0	0
% ^{82}Sr yield	100	100	100	100	94.338

The aluminium target capsule was cut open and removed from the target material, while the present infrastructure could not be used to open and remove the larger stainless steel capsule in a similar manner. Instead, the stainless steel capsule was simply punctured so that the target material could be dissolved. As a result, the dissolution of the target material in Production 2 turned a shade of orange, due to the o-phenanthroline monohydrate binding with iron and other impurities. When loading the solution on to the Purolite S950 resin, the impurities may have interfered with the ^{82}Sr being retained by the resin, resulting in the loss of *ca.* 5.7 % in the load step. The remainder of the product was successfully retained by the resin and eluted with the 2.0 M HCl. Although much of the colour was removed in the rinse steps of the production, there was still some colour in the final product, even when it was evaporated to dryness and picked up in 5 mL 0.1 M HCl.

Phillps *et al.*[15] reported a similar tendency in their separations. In this work, it may also have been due to the o-phenanthroline monohydrate increasing the iron distribution coefficient for the chemical separation[22], and the following method was employed to overcome this:

The ^{82}Sr product was evaporated to dryness and the salts dissolved in 100 mL 2.0 M HCl-70 % methanol. The solution was pumped through a column containing 10 mL AG MP-50 macroporous cation exchange resin (equilibrated with 50 ml 2.0 M HCl-70 % methanol). The elements were washed onto the resin using a further 50 mL 2.0 M HCl-70 % methanol. The impurities (Fe, Mn, Ni, Al and Cr) were eluted from the resin column using 50 mL 3.0 M HCl-45 % methanol, before the ^{82}Sr final product was eluted from the column with 50 mL 4.0 M HNO_3. This was evaporated to dryness, before being picked up in 0.1 M HCl.

The activity of ^{82}Sr was determined using the 776.5 keV γ-ray peak of the ^{82}Rb daughter, which reaches secular equilibrium with the parent nuclide only a few minutes after EOB. It was determined that the final product, other than the initial loss in the load step, was intact and devoid of impurities.

From the experiments and productions performed, elution curves of Rb and ^{82}Sr were plotted and are shown in Fig. 4.5.

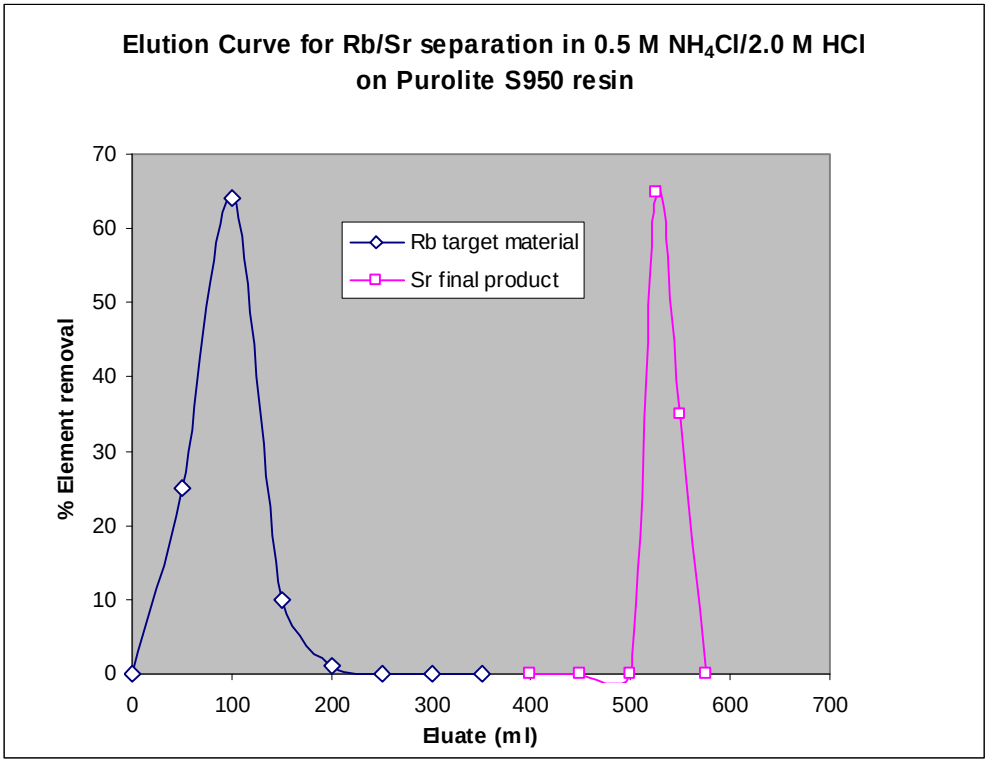

Fig. 4.5: Elution curves of ^{82}Sr and ^{84}Rb from Purolite S950 using 0.5 M NH_4Cl and 2.0 M HCl as eluents, respectively.

Aardaneh *et al.*[18] briefly described a method to produce ^{82}Sr comparing Chelex 100 and Purolite S950 chelating resins. While the authors determined Purolite S950 to be the resin of choice for their work, it differs from this work in that a 7 g target was used, while this work involved the use of a 30 g RbCl target. The main difference, however, was the fact that they used an "open" system with their ion exchange method, that is, applying gravity flow use of the column by dripping the solution into the column from the top at a flow rate of 2 mL per minute maximum. The flow rate had to be monitored carefully to prevent the column from running dry because of the bigger particle size of the resin beads. This work uses a "closed" system use of ion exchange, in that the column was sealed using a sinter on either end of the column and a Teflon plunger on one side. This allowed the resin to remain wet at all times, while being able to increase the pump speed up to 5 mL per minute without any side effects. The use of a "closed" system is also regarded as a safer method of performing a production, as any losses due to a broken tap or burst line can be kept to a minimum, while there is a danger of losing all of one's activity should it happen when using an open gravitational system. Furthermore, working with a closed system prevents external contamination and the smaller particle size of the resin results in better resolution.

Cackette *et al.*[16] described a method using Rb metal as target. Their hot cell production method of processing the target involved dissolving the target in n-butanol after piercing it in the processing hot cell, all taking place in a glass vessel purged with argon, before being processed further by means of ion exchange.

At the time of writing, several Rb metal targets (also encapsulated in stainless steel) have been bombarded successfully with beam intensities up to 250 µAh for extended periods. These targets were exported in an unprocessed form to the customer. The processing of Rb metal targets will also be implemented at iThemba LABS in due course, however, that development work falls outside the scope of this thesis.

4.4 Conclusion

A method was developed to effectively separate ^{82}Sr from the RbCl target material, producing a ^{82}Sr yield of over 94 %. The final product was determined to be of a very high purity, suitable for use in ^{82}Sr/^{82}Rb generators and, thus, this production method has been implemented for the routine productions at iThemba LABS.

Work on Rb metal targets has also been initiated in order to increase the production rate. Several targets have been bombarded successfully with beam intensities up to 250 µAh, however, the implementation of a suitable chemical separation infrastructure in the hot-cell complex is still to be performed in future.

Lastly, it should be mentioned that the yields obtained from both RbCl and Rb metal targets bombarded in the VBTS, were very close to the expected values based on the nuclear data of Figs. 4.2.and 4,3. This is very encouraging, and perhaps the first indication that a vertical beam has an advantage over a horizontal beam, in that molten target material remains better located in the beam strike.

4.5 References

1. Qaim S. M., Steyn G. F., Spahn I., Spellerberg S., van der Walt T. N., Coenen H. H., 2007. *Appl. Radiat. Isot.*, **65**, 247.
2. Mullani N. A., Goldstein R. A., Gould K. L., Marani S. K., Fisher D. J., O'Brian H. A. Jr, Loberg M. D., 1983. *J. Nucl. Med.*, **24** (10), 898.
3. Saha G. B., Go R. T., MacIntyre W. J., Marwick T. H., Beachler A., King J. L., Neumann D. R., 1990. *Int. J. Rad. Appl. Instrum. B.*, **17** (8), 763.
4. Sylvester P., Möller T., Adams T. W., Cisar A., 2004. *Appl. Radiat. Isot.*, **61**, 1139.
5. Brooks D. J., Beaney R. P., Lammertsma A. A., Leenders K. L., Horlock P. L., Kensett M. J., Marshall J., Thomas D. G., Jones T., 1984. *J. Cereb. Blood Flow Metab.*, **4** (4), 535.

6. Faβbender M., Nortier F. M., Phillips D. R., Hamilton V. T., Heaton R. C., Jamriska D. J., Kitten J. J., Pitt L. R., Salazar L. L., Valdez F. O., Peterson E. J., 2004. *Radiochim. Acta*, **92**, 237.
7. Vereshchagin Yu. I., Zagryadskiy V. A., Prusakov V. N., 1993. *Nucl. Instrum. Meth. Phys. Res. A*, **334**, 246.
8. Grant P. M., Erdal B. R., O'Brien H. A. Jr, 1975. *J. Nucl. Med.*, **16** (4), 300.
9. Yano Y., Chu P., Budinger T. F., Grant P. M., Ogard A. E., Barnes J. W., O'Brien H. A. Jr, Hoop B. Jr, 1977. *J. Nucl. Med.*, **18**, 46.
10. Yano Y., Budinger T. F., Chiang G., O'Brien H. A., Grant P. M., 1979. *J. Nucl. Med.*, **20** (9), 961.
11. Brihave C., Guillaume M., O'Brien H. A. Jr, Raets D., de Landsheere C., Rigo P., 1987. *Int. J. Rad. Appl. Instrum. [A]*, **38** (3), 213.
12. Alvarez-Diez T. M., deKemp R., Beanlands R, Vincent J., 1999. *Appl. Radiat. Isot.*, 50, 1015.
13. Klein R., Adler A., Beanlands R. S., de Kemp R. A., 2007. *Phys. Med. Biol.*, **52**, 659.
14. Sylvester P., Möller T., Adams T. W., 2006. *Appl. Radiat. Isot.*, **64** (4), 422.
15. Phillips D. R., Peterson E. J., Taylor W. A., Jamriska D. J., Hamilton V. T., Kitten J. J., Valdez F. O., Salazar L. L., Pitt L. R., Heaton R. C., Kolsky K. L., Mausner L. F., Kurczak S., Zhuikov B. L., Kokhanyuk V. M., Konyakhin N. A., Nortier F. M., van der Walt T. N., Hanekom J., Sosnowski K. M., Carty J. S., 2000. *Radiochim Acta*, **88**, 149.
16. Cackette M. R., Ruth T. J., Vincent J. S., 1993. *Appl. Radiat. Isot.*, **44** (6), 917.
17. Mausner L. F., Prach T., Srivastava S. C., 1987. *Appl. Radiat. Isot.*, **38** (3), 181.
18. Aardaneh K., van der Walt T. N., Davids C., 2006. *J. Radioanal. Nucl. Chem.*, **270** (2), 385.
19. Kastleiner S., Qaim S. M., Nortier F. M., Blessing G., van der Walt T. N., Coenen H. H., 2002. *Appl. Radiat. Isot.*, **56**, 685.
20. Buthelezi E. Z., Nortier F. M., Schroeder I. W., 2006. *Appl. Radiat. Isot.*, **64** (8), 915.
21. Van der Walt T. N., Vermeulen C., 2004. *Nucl. Instrum. Meth. Phys. Res. A*, **521**, 171.

22. Iyer S.G., Venkateswarlu Ch., 1976. *Indian J. Chem.*, **14A**, 437.

CHAPTER 5 THE PRODUCTION OF ^{28}Mg IN THE PROTON BOMBARDMENT OF ^{nat}Cl

5.1 Introduction and Background

^{28}Mg was discovered in 1953[1] and has a half-life of 20.9 h. Its mode of decay[2,3] is 100 % by β^- emission to ^{28}Al. Before then, all the known radionuclides of Mg were regarded as impractical for use as tracers because of their short half-lives, the longest being ^{27}Mg (9.3 minutes). As a result, the radiochemistry of Mg was largely neglected[4] until ^{28}Mg became an important tracer in biological research. Magnesium is an essential element which plays a pivotal role in animal and human physiology[5-9] and its metabolism is, even today, not fully understood.

The earliest studies using the radionuclide involved the investigation of serum Mg and urinary excretion of Mg in alcoholic subjects[10,11]. Attempts were made to study Mg absorption and excretion in humans with the use of ^{28}Mg[12], as well as retention of Mg in the body[13,14]. There have also been studies with regard to Mg losses[15] and Mg kinetics[15-18] in the human body, Mg distribution in the body[17-20] and intestinal peak absorption[21,22]. ^{28}Mg was also used as tracer in the study of primary hypomagnesemia, particularly in children[23-25].

The rather short half-life of ~ 20.9 h limits the usefulness of ^{28}Mg as a tracer to only about three days. It is, therefore, too short-lived for the determination of true adsorption[26] in certain types of processes in the body. Stable tracers are, therefore, more commonly used nowadays[25-30], especially in studies of processes having relatively long biological half-lives. Nevertheless, the simultaneous administration of ^{28}Mg with a stable Mg tracer remains useful for monitoring the initial Mg uptake and to evaluate the stable tracer[25].

^{28}Mg played an important role in studies of Mg bioavailability and nutrition. For example, its uptake has been measured in plants in studies pertaining to plant physiology and exchange processes in photosynthesis[5,30,31], while Mg uptake in the

leaves of sunflowers, as well as root uptake and the distribution of Mg to different parts of this plant were investigated[32-34]. ^{28}Mg has also been used to determine physiological disorders in plant species, particularly in apples and grapes, where it became evident that the specific Mg transport behaviour increases bitter pit necrosis primarily caused by calcium deficiency.

Interest was shown in this radionuclide for mineral uptake studies by the local Fruit and Fruit Technology Research Institute (FFTRI) of South Africa in the early 1990's. A project was started at iThemba LABS at that time to investigate its production with the 66 MeV proton beam, however, that project was never completed because priorities had changed. Recently, however, interest has been rekindled and the project to produce ^{28}Mg reopened.

The production of ^{28}Mg has been achieved with the use of neutrons from nuclear reactors, using Al as target material[35,36], following the reaction route ^{27}Al(n, p)^{27}Mg(n, γ)^{28}Mg or ^{27}Al(n, γ)^{28}Al(n, p)^{28}Mg (see Fig. 5.1). It has also been produced via the consecutive nuclear reactions ^{6}Li(n, t)^{4}He and ^{26}Mg(t, p)^{28}Mg with the use of Li/Mg alloy as target material[1,37,38]. The radionuclide has also been produced in accelerators via reactions of tritons on Mg, Al and Si[39,40], which has reportedly produced a product of high specific activity. Another method reported is via the reaction ^{27}Al(α,3p)^{28}Mg, providing a convenient means to produce carrier-free ^{28}Mg[24,25,35,41-43] in small to moderate quantities with relatively small cyclotrons (Q = -21.6 MeV). Cross-section experiments on the production of ^{28}Mg with the use of Si as target material have also been performed,[44,45] but the yields obtained were very low and this method has not been put into production. Spallation reactions, using Cl, to produce ^{28}Mg have been reported[46-48], using NaCl[46] and KCl[47] target material, precipitation with $Fe(OH)_3$ and separation by means of ion exchange chromatography. Unfortunately, not only is the yield low, but the product contains other impurities which makes the production cumbersome, as the purification of the product is labour intensive.

Nowadays, α-particle beams for radionuclide production purposes are becoming very rare as most modern medical cyclotrons are negative ion accelerators, unable to accelerate ^{4}He ions. The use of proton beams to produce ^{28}Mg, on the other hand, requires energies well over 50 MeV and, therefore, many commercial medical

cyclotrons are unable to produce this radionuclide. A number of larger accelerators in the world, however, do have the ability to produce useful quantities using proton beams. The options available for ^{28}Mg production in the proton energy region 50 - 200 MeV were revisited at iThemba LABS. Extensive new production rate and excitation function data were also measured for the ^{nat}Cl(p,6pxn)^{28}Mg nuclear process.

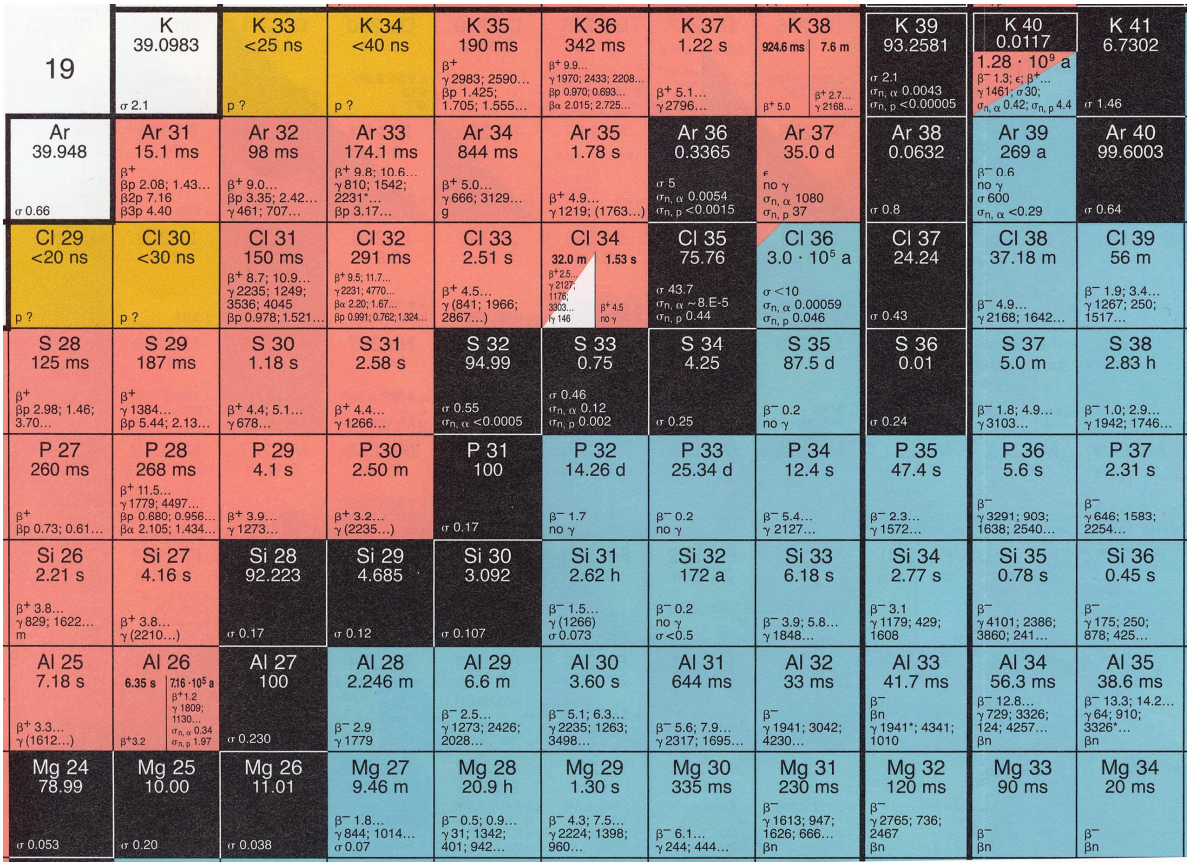

Fig. 5.1: Relevant part of the "Karlsruher Nuklidkarte" of 2006 for the production of ^{28}Mg. Note that not many neutron-rich radionuclides can be accelerator produced, ^{28}Mg being one of only a few exceptions.

It is interesting to note that (reportedly) no facility has produced ^{28}Mg routinely since 1990[49], although Brookhaven National Laboratory still had it listed as one of their products in 1995[50]. In 2002, the price of this radionuclide was reported to be approximately US$ 30 000 per mCi[49], explaining, perhaps, the shortage of the product worldwide. Currently, its status is "low demand, high price and hard to obtain".

5.2 Nuclear Data

5.2.1 Experimental Methods and Data Analysis

Usually, excitation functions are measured utilizing the well-known stacked-foil technique; the foils being sufficiently thin to ensure that the measured cross sections constitute microscopic data. From these microscopic data, production rates or yields can be deduced by means of a numerical integration procedure[51].

Occasionally, however, it is difficult to use the stacked-foil technique due to difficulties in preparing thin specimens of high integrity of a given material. This was experienced with the stable compounds of Cl, the chlorides being brittle salts. Thick-target yields were, therefore, measured in a range of different energy windows, using relatively thick NaCl discs as targets, in order to establish the thick-target production rate curve first. The corresponding excitation function was then deduced by means of a differentiation procedure, in order to obtain microscopic data for comparison with other literature cross sections. An important criterion of this approach is that the spacing of the measured points on the energy axis should be similar to what would have been appropriate in a conventional stacked-foil experiment.

Stacks of analytical grade NaCl (> 99 %, Merck) tablets were irradiated with proton beams of nominally 200, 100 and 66 MeV, delivered by the separated sector cyclotron of iThemba LABS. The NaCl target discs had thicknesses of nominally 870, 540 and 425 mg/cm^2, respectively, in the 200, 100 and 66 MeV stacks. The individual NaCl discs were separated by relatively thin monitor foils (99.9 %, Goodfellow, U.K.): 65 mg/cm^2 Al in the 200 and 100 MeV stacks and 44 mg/cm^2 Cu in the 66 MeV stack. The excitation functions of the ^{22}Na and ^{65}Zn formed in the Al and Cu foils, respectively, were used to monitor the accumulated proton charge. These well-established monitor reactions, recommended by the IAEA[52] gave consistent results with the readings of a calibrated Brookhaven Instruments Corporation Model 1000C current integrator.

The ^{28}Mg activities were determined by off-line γ-ray spectrometry using the 941.7 keV (38.3 %) and 1342.3 keV (52.6 %)[3] γ-lines. The ^{28}Mg sources were prepared by dissolving each NaCl tablet in 10 mL of water after irradiation. These solutions were sealed in standard serum vials. Activities were measured using an accurately calibrated HPGe detector with a relative efficiency of 13 % and a resolution of 1.8 keV at 1.33 MeV, connected to a Silena multi-channel analyzer. The thick-target production rate curve was obtained by summing the individual ^{28}Mg activities progressively. Corrections were made for the missing ^{28}Mg activities corresponding to the "dead layer" energy intervals occupied by the monitor foils. This was done by interpolating the activity values on both sides of each dead layer and scaling to the full energy region.

The total uncertainties of the measured activity values were obtained by summing all the contributing uncertainties in quadrature and are expressed with a 1σ (68 %) confidence level. The statistical uncertainties were insignificant compared to the systematic uncertainty, except near the reaction threshold, the latter of which was estimated to be about 7 %: beam current integration (3 %), detector efficiency (5 %), counting geometry (1 %), decay corrections (2 %) and target thickness (3 %).

5.2.2 Results and Discussion

The measured ^{28}Mg thick-target production rate curve for NaCl + p is shown in Fig. 5.2. Note that all target materials considered in this study are natural, non-enriched materials. The relatively high proton energies will make the correspondingly thick targets required prohibitively expensive should enriched target material be used. The reaction threshold is near 50 MeV and the production rate for the full energy region, *i.e.* from threshold up to the maximum energy of 200 MeV, is about 6 MBq/μAh. A standard polynomial function was fitted through the measured data using the code TableCurve[53].

The polynomial of Fig. 5.2 could be differentiated analytically, allowing the derivation of the excitation function for ^{nat}Cl + p, shown in Fig. 5.3. (Note that this

excitation function pertains to pure Cl and not NaCl.) The only other relevant data found in the literature are by Lundqvist and Malmborg[47], which currently is the only EXFOR data set for ^{28}Mg produced in ^{nat}Cl + p. Six of their nine values are in good agreement with the results obtained in this work, while three values are clearly somewhat higher. Generally, the agreement is satisfactory. The deduced cross-section values of this work as well as production rates for several possible target materials are presented in Appendix A1.

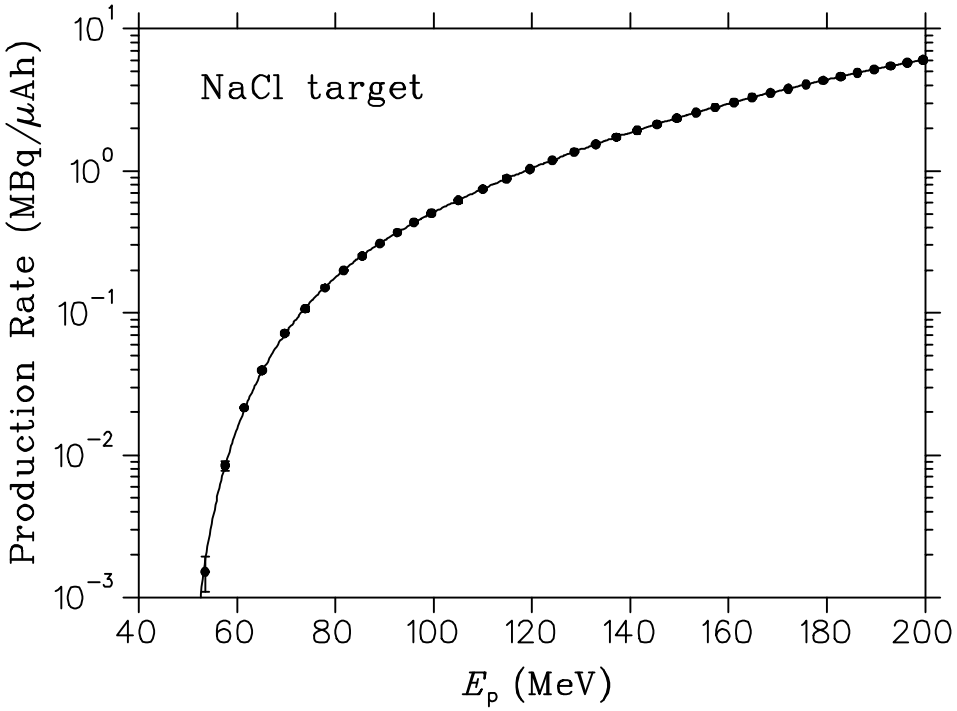

Fig. 5.2: **Thick-target production rate curve of ^{28}Mg produced in the proton bombardment of NaCl. The solid symbols are the measured values of this work while the solid curve is a polynomial fit. Error bars are shown when they exceed the symbol size.**

Lundqvist and Malmborg presented production cross sections for ^{28}Mg in the proton bombardment of silicon, phosphorus, sulphur, chlorine, argon and potassium. These were essentially all the possible target elements with potential in the energy region 50 – 180 MeV. The target materials and reactions are as follows: Si [^{30}Si(p,3p)^{28}Mg]; $Na_2P_2O_7$ [^{31}P(p,4p)^{28}Mg]; Na_2SO_4 [^{nat}S(p,5pxn)^{28}Mg]; LiCl [^{nat}Cl(p,6pxn)^{28}Mg]; Ar [^{nat}Ar(p,7pxn)^{28}Mg]; and K_2CO_3 [^{nat}K(p,8pxn)^{28}Mg]. From a practical targetry point-of-view, one can omit Ar. As a gas, Ar will be impossible to contain in a large enough energy window to make ^{28}Mg production viable, while it is impractical to keep it frozen under high-intensity bombardment conditions. One can also omit Si, S

and K, as with these elements, significantly lower cross sections were obtained than with Cl and P.

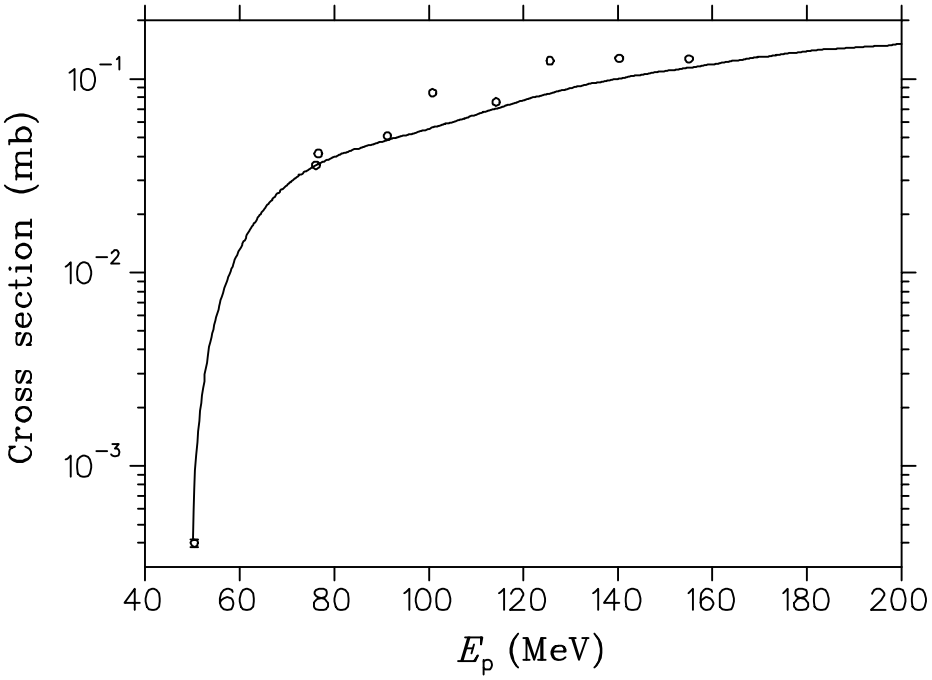

Fig. 5.3: Excitation function of ^{28}Mg formed in the reactions of protons with ^{nat}Cl. The solid curve was derived from the measured thick-target production rate data of this study (see Fig. 5.2). The open symbols are measured cross sections by Lundqvist and Malmborg[47].

Interestingly, the ^{nat}P + p process has higher cross sections for ^{28}Mg formation than ^{nat}Cl + p (about 30 % at 150 MeV). Unfortunately, no suitable compounds of P could be identified for use as target material, as they all seem to have poor thermal stability at higher temperatures and/or a relatively low P content. Many phosphorus compounds decompose at relatively low temperatures, rendering them unsafe to be used as target materials (as a high pressure build-up inside a target capsule can cause it to burst). One of the most stable compounds of P, namely, $Na_4P_2O_7$ (sodium pyrophosphate) has, for example, a reasonably high melting point of 880 °C but only contains 23 % of P by mass. In contrast, many of the chlorides have excellent thermal properties and a high Cl content. Several chlorides have boiling points at temperatures much higher than their melting points, thus, making excellent high-current targets if properly encapsulated and cooled. Also, both stable isotopes of Cl contribute significantly to the yield: ^{35}Cl[75.77 %](p,6p2n)^{28}Mg and ^{37}Cl[24.23 %](p,6p4n)^{28}Mg.

Figure 5.4 shows the expected thick-target production rates (or instantaneous yields) for several metal chlorides as well as pure chlorine for an energy window from threshold up to 200 MeV. Obviously, solid frozen chlorine will be the best choice in terms of yield, but it is quite impractical as a target. The next best choice in terms of yield is $BeCl_2$, however, this particular salt has less favourable thermal properties than the simpler chlorides, *viz.* LiCl, NaCl and KCl. LiCl was determined to be the target material of choice, as it has excellent thermal stability as well as a yield of about 80 % of the ^{nat}Cl + p theoretical maximum. LiCl has a melting point of 605 °C and a boiling point of 1325 °C, while the corresponding values for $BeCl_2$ are 405 °C and 488 °C, respectively. It also gives a 37 % higher ^{28}Mg yield than NaCl. The advantage of NaCl as target material is that significantly less ^{7}Be is co-produced (to be discussed later).

Once again, however, this is not the complete story as a production energy window of 50 – 200 MeV will result in a very thick LiCl target (about 32 g/cm^2). Such a thick target would be virtually impossible to cool sufficiently during high-intensity irradiation. A practical solution was to place several thinner targets (properly encapsulated) in series and to provide fast flowing cooling water around them in a 4π geometry[54]. This would reduce the cumulative production rate somewhat by introducing "dead layers" in the production energy window. Nevertheless, a higher operational beam intensity can more than adequately compensate for this loss.

It is interesting to compare the yields expected from thinner targets as a function of incident energy. This is shown in Fig. 5.5 for LiCl targets ranging in thickness from 2 to 32 g/cm^2. It is clear that, regardless of the target thickness, the highest yield is always obtained with the highest incident proton energy. This result may seem trivial, but it is not. There are no local minima or maxima, which is unusual. The production rate curve for an incident energy of 200 MeV is shown in Fig. 5.6, plotted as a function of target thickness.

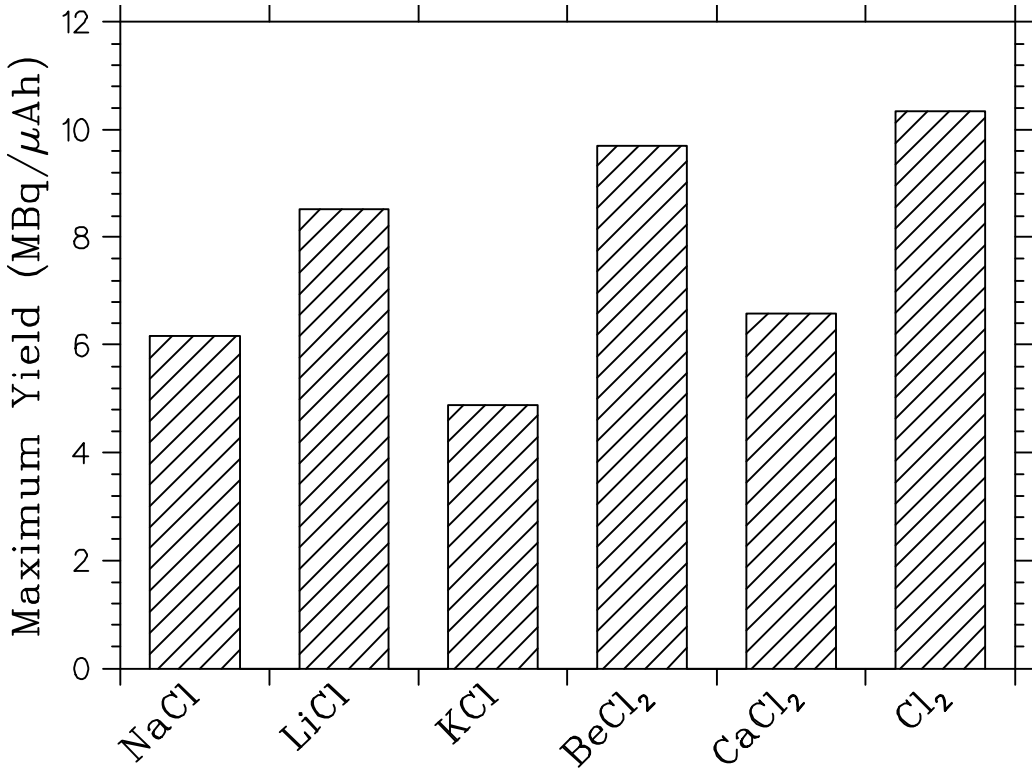

Fig. 5.4: Comparison of the expected thick-target production rates of ^{28}Mg in the proton irradiation of several Cl containing compounds, for an energy window 50 – 200 MeV, derived from the measured data of this work.

Salt targets, of nominally 4 g/cm^2 thickness and 20 mm in diameter and encapsulated in 0.5~mm thick Al, were successfully tested at iThemba LABS up to thermal loads of 2.5 kW. Cooling water layers of 1 mm thickness were provided to targets having a tandem geometry. This concept can easily be extended to more targets in series. As already mentioned, this kind of geometry will allow for effective cooling of the targets, however, one concern in such a long stack of targets should be the outscattering losses of protons due to radial beam spread, caused by Coulomb interactions inside the target material. It was decided to perform an experiment to investigate such losses and to test the target concept.

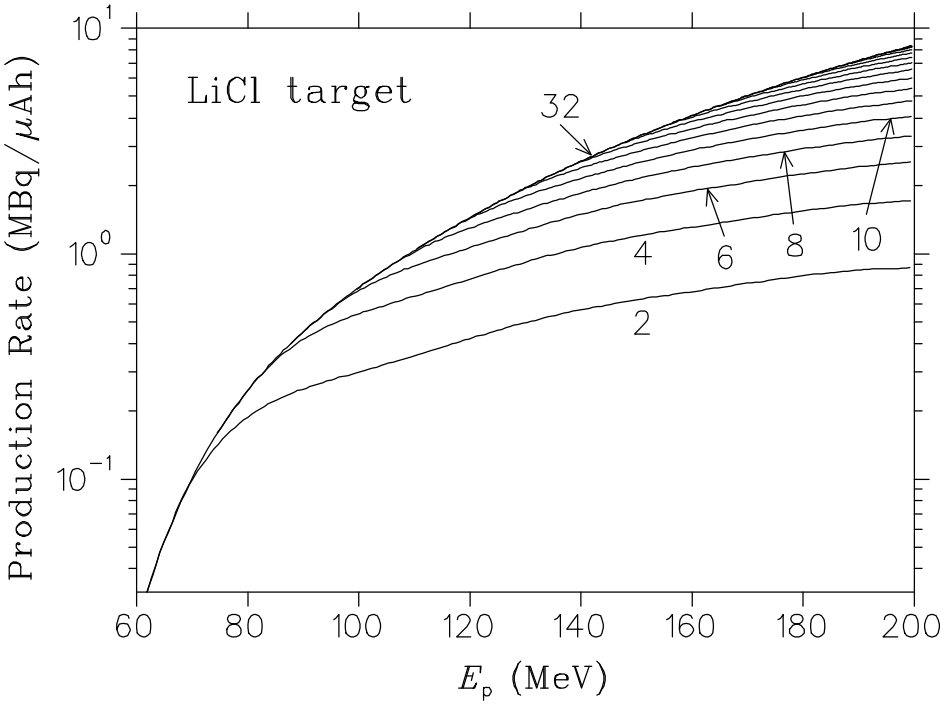

Fig. 5.5: Expected production rates of ^{28}Mg for various target thicknesses in the proton irradiation of LiCl, plotted as a function of incident energy. The target thicknesses range from 2 to 32 g/cm^2 in 2 g/cm^2 steps, as indicated.

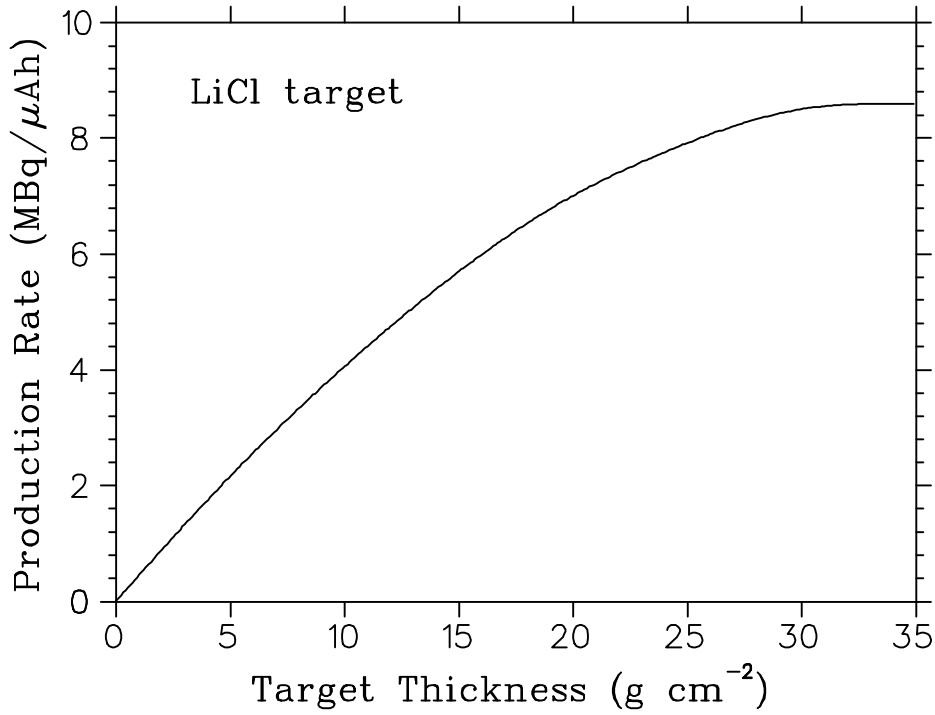

Fig. 5.6: Expected thick-target production rates of ^{28}Mg in the proton irradiation of LiCl with an incident energy of 200 MeV, plotted as a function of target thickness.

5.2.3 The Experimental Target

A target holder was designed to hold ten thick encapsulated LiCl targets (2.74 g/cm^2 each) in series. This is shown in Fig. 5.7 (expoded view) and Fig.5.8 (cutaway view). The targets were bombarded inside the RERAME[55] irradiation chamber (see Fig. 5.9) with a 200 MeV proton beam of 100 nA intensity for 80 minutes. The targets were then removed, decapsulated and the target material dissolved. Liquid sources in standard serum vials were prepared from a fraction of each solution, the rest used for the radiochemical investigations.

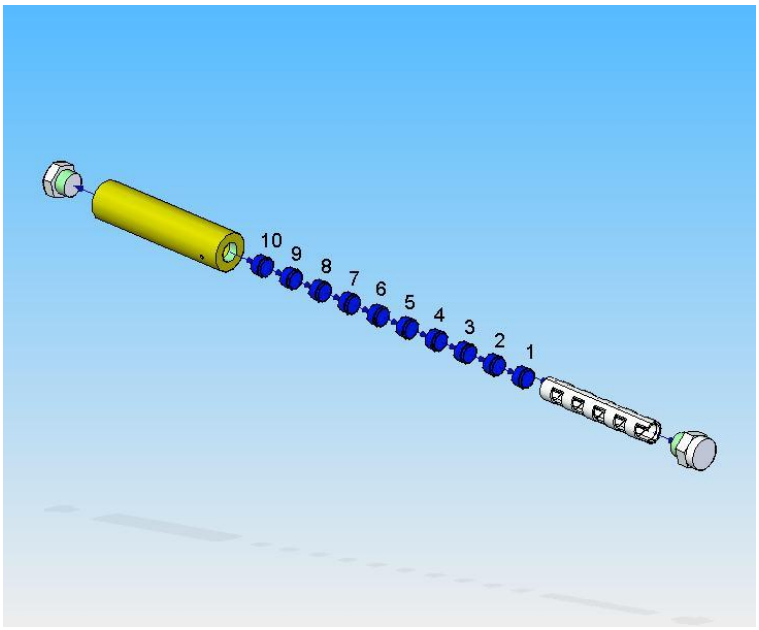

Fig. 5.7: **An exploded view of the LiCl target holder, showing the 10 encapsulated LiCl targets, an entrance window at one end and a beam stop at the other end. A rack was designed to keep the targets in position inside an aluminium sleeve while simultaneously providing cooling channels for cooling water. The cooling-water layers between targets had a thickness of 1 mm.**

The ten LiCl targets covered the entire energy region from 200 MeV down to threshold. The yield in each target was accurately measured and compared with the values expected from the nuclear data measurements. The ratio of these measured and predicted values are presented in Fig. 5.10, plotted versus the target number. Note that the target number increases with decreasing proton energy. A value of unity would indicate a situation where no beam losses have been incurred. As can be seen from the figure, this is indeed the case for targets number 1 through 8, within the

measured uncertainties. In the case of target no. 9, the ratio falls to about 0.72 and in the case of target no. 10, to 0.21. This sudden drop is thought to be mainly due to the radial beam spread, although an effect resulting from a slight energy mismatch towards the end of the target stack cannot be ruled out.

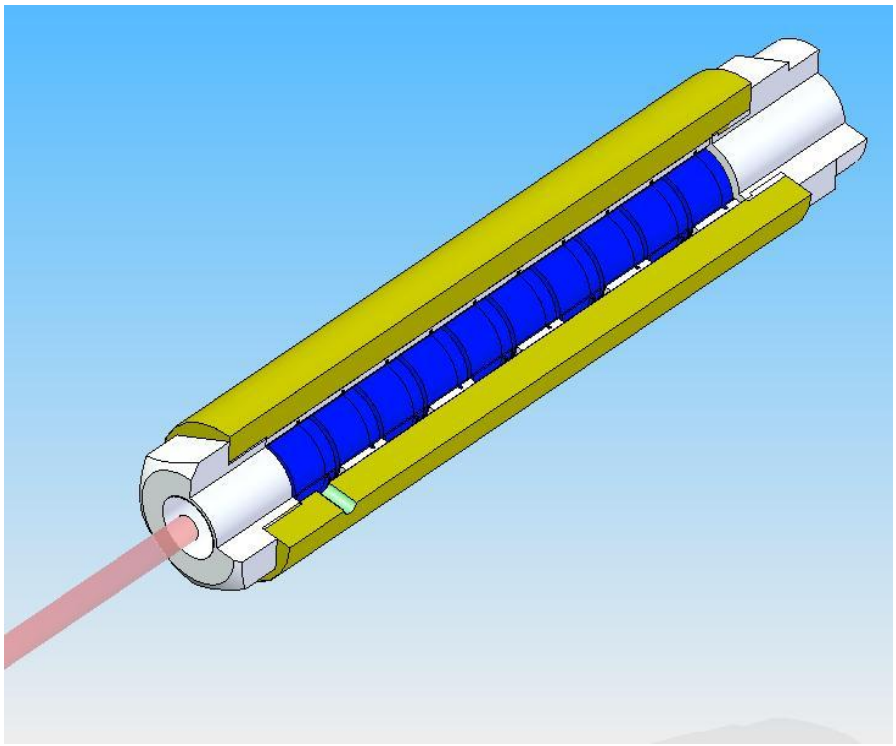

Fig. 5.8: A cutaway view of the the LiCl target holder showing the 10 LiCl targets, with the proton beam incident from the left.

During the bombardment, a Ni monitor foil placed directly behind the last target (*i.e.* target no. 10) was also activated. An idea of the beam profile at that point could be obtained by examining the ^{57}Ni ($T_{1/2}$ = 36 h) activity induced in that foil. For this purpose, the foil was cut up into smaller pieces, which were then individually counted for their ^{57}Ni activities. The activity distribution of a vertical cut through the foil is shown in Fig. 5.11. Note that the beam profile is expected to resemble a skew Gaussian distribution. From the figure, it is clear that the beam width has become significantly broader than the target diameter of 20 mm. It is evident, therefore, that the radial beam spread becomes a significant factor towards the low-energy side of the target stack.

Fig. 5.9: The LiCl target holder mounted on the door of the RERAME[55] irradiation chamber. The beamline is connected onto the chamber from the left side.

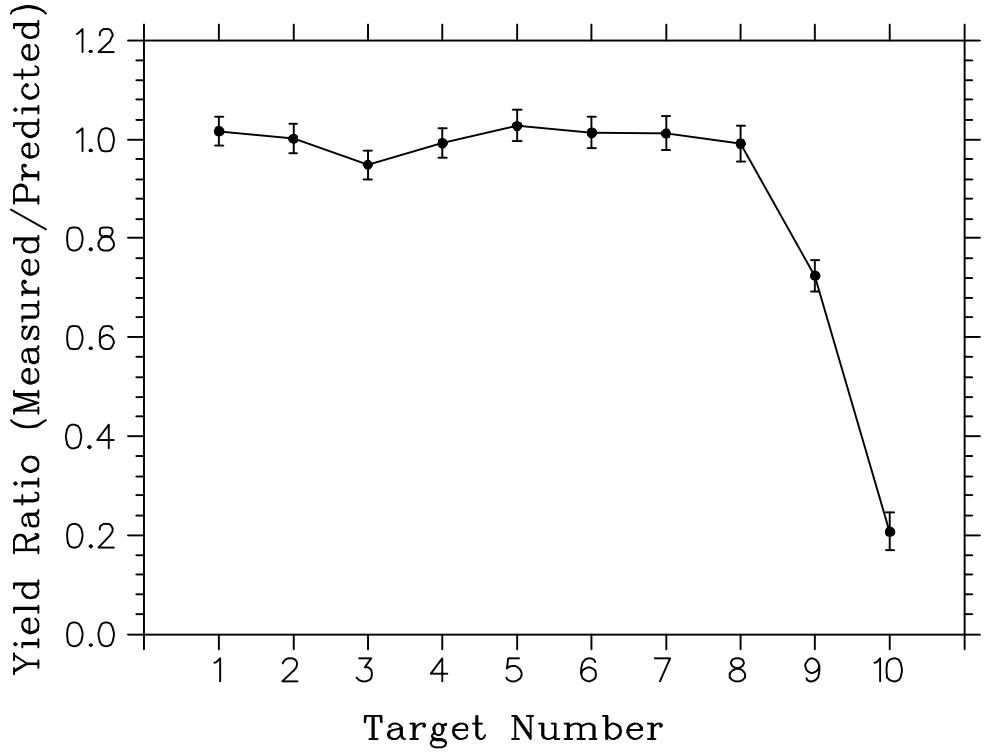

Fig. 5.10: The ratio of the measured ^{28}Mg activity and the corresponding predicted value based on the nuclear data measurements, plotted as a function of the target number. Note that the target number increases as the penetration depth into the target stack increases.

Finally, it is interesting to look at the cumulative ^{28}Mg yields obtained. The measured cumulative yield of all ten targets is 6.29 MBq/µAh at EOB. The expected yield is 6.40 MBq/µAh, thus very good overall agreement is obtained. Should one discard the last two targets in the stack, the total measured yield is 6.12 MBq/µAh. Thus, if only eight targets are used, a cumulative yield of about 97 % of that for ten targets is obtained. Clearly, it is not worthwhile having the last two targets in the stack. One may also consider reducing the number of targets in the stack further. The corresponding percentages (relative to 10 targets) are as follows: 7 targets (92 %); 6 targets (84 %); 5 targets (75 %); 4 targets (63%). A target system comprising six or seven encapsulated targets, therefore, seems to be the most sensible choice.

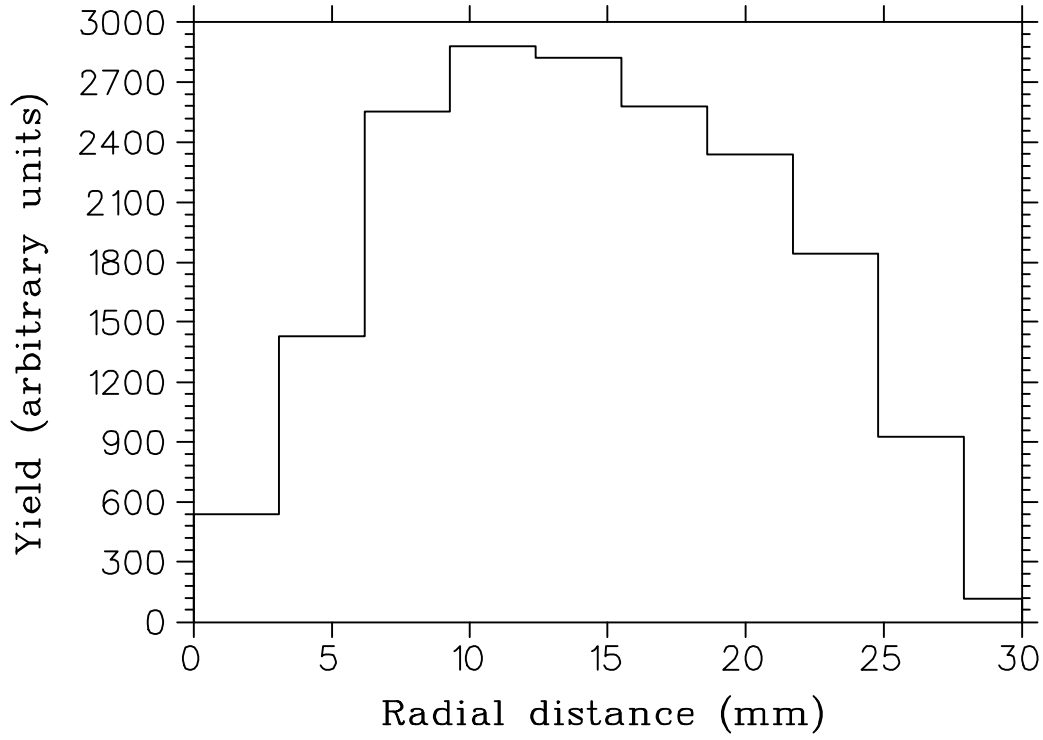

Fig. 5.11: The ^{57}Ni distribution of a vertical cut through the Ni monitor foil (see text), plotted as a function of the radial dimension. (Note that the target diameter was 20 mm).

5.3 Radiochemical Investigation

5.3.1 Chemical Separation Method

Experiment 1

An 8.6 g LiCl target was dissolved in 100 mL 0.01 M ammonium citrate and loaded onto a 10 mL column containing AG MP-1 macroporous anion exchange resin (equilibrated with 50 mL 0.1 M ammonium citrate). The Li was eluted from the column using 50 mL 0.1 M ammonium citrate, while the ^{28}Mg final product was eluted from the resin column using 50 mL 1.0 M HCl.

Experiment 2

A LiCl target (8.6 g) was dissolved in 100 mL 1.0 M ammonium chloride solution, at a pH of 8, to which 100 mg o-phenanthroline monohydrate was added. The resultant solution was pumped through a column containing 5.0 mL Purolite S950 chelating resin (the resin lightly ground to create finer particles for greater surface area), equilibrated with 50 mL 1.0 M ammonium chloride. The elements were washed onto the column with 20 mL 1.0 M ammonium chloride (pH 8), before the Li was eluted from the resin column with a further 50 mL 1.0 M ammonium chloride (pH 8). The ammonium chloride was washed out of the resin with water, before the ^{28}Mg was finally eluted with 50 mL 2.0 M HCl.

5.3.2 Results and Discussion

When dissolving each of the ten targets, it was noted that the beam was well focused on the first five targets, after which the area of "burning" on the target material began to spread. As a result, problems began to occur when dissolving the LiCl salt target. The targets situated at the front of the stack appeared to have reacted with the aluminium capsule, as a colloidal suspension occurred, instead of the salt going into solution. It was attempted to use dilute nitric acid to dissolve a target, but this had disastrous results as, oddly, the nitric acid reacted with the aluminium shavings from

the encapsulation, probably as a result of the Li reacting with the capsule. When each solution was filtered, however, all returned to normal. Luckily, the colloidal suspension did not contain any ^{28}Mg activity.

The targets used for the experiments were filtered and evaporated to incipient dryness, after which water was again added. This, too, was evaporated to dryness before the activity was picked up in the solution of choice for the necessary experiment.

Experiment 1 was pursued after perusing an article by Nelson *et al.*[56], where it was stated that the alkali metals would not be retained by anion exchange resins in dilute citrate media, while the alkali earth metals and Mg in particular, would be strongly retained by anion exchange resins in this mixture. After studying the distribution coefficients, it was decided to dissolve the target in 0.01 M ammonium citrate, as Mg had a particularly high distribution coefficient in this mixture. The experiment failed miserably, with 91.9 % of the ^{28}Mg activity passing through the resin column and the remaining 8.1 % being discovered in the rinse step. It was thought that the experiment would be successful, even though the literature stated that a 0.27 cm^2 x 44 cm column was used with 0.5 M ammonium citrate, where the Mg distribution coefficient was considerably less than in 0.01 M ammonium citrate. It was thought that a smaller column and more dilute solution would be as effective, but this was not the case.

The method devised for Experiment 2 was based on that for the ^{82}Sr separation from Rb salt targets (see Chapter 4), where an alkaline earth metal was effectively separated from an alkali metal. As with the ^{82}Sr production, o-phenanthroline monohydrate was added to the load solution such that the distribution coefficient of Mg would increase[57], thereby allowing the radionuclide to be more effectively retained by the resin. The experiment was considerably more successful than Experiment 1, but 18.72 % of the ^{28}Mg activity was still lost in the initial load step, while a further 1.55 % was lost in the rinse steps, yielding 79.73 % in the eluate.

It was deduced that the activity was migrating through the resin column and, as a result, a longer column would be necessary. Another option would be to dilute the LiCl and ammonium chloride mixture 10 times, but this idea was discarded due to the

volumes required for the separation process. A column of 12.5 cm in length and a diameter of 1 cm was used, packed with the same resin as before (Purolite S950, slightly ground). The same procedure was followed and the results were excellent, with a 100 % yield of ^{28}Mg being obtained, the product being radionuclidically pure, with the exception of some ^{7}Be being found in the product as a result of the (p,n) reaction on Li.

Another radionuclide that required separating in the procedure was that of ^{24}Na (1368 keV γ-ray), also produced in the bombardment process. While the initial procedure for Experiment 2 saw 90.2 % of ^{24}Na initially pass through the resin column, 6.60 % of the radionuclide was removed from the resin in the rinse step, while 3.20 % appeared in the final product. When the column was lengthened as described above, 82.1 % of the total ^{24}Na passed through the resin column in the initial load step, while 17.7 % was removed from the resin when performing the two rinse steps. 0.17 % was found in the final product, which would imply that should one use a further 20 mL of ammonium chloride, the remainder of the impurity would be removed.

5.4 Conclusion

New data were measured for the proton production of ^{28}Mg on ^{nat}Cl. Several chloride salts are suitable target materials, with LiCl perhaps being the best choice. An effective way was devised to bombard LiCl targets in series with a 200 MeV proton beam. Once removed from their encapsulation and filtered, the ^{28}Mg can be separated from its target material efficiently, using a 12.5 cm x 1cm^2 column containing Purolite S950 chelating resin, producing a 100 % yield of final product. There was some ^{7}Be found in the final product, as a result of the Li(p,n)^{7}Be reaction. In most applications this would not be a problem. Should this be a problem for potential users, however, NaCl targets can be used instead, although the yield of ^{28}Mg will not be as high as when LiCl target material is used.

The nuclear data part of this work was presented at the International Conference on Nuclear Data for Science and Technology 2007 in Nice, France[58] and will be published in the conference proceedings in due course.

5.5 References

1. Sheline R. K., Johnson N. R., 1953. *Phys. Rev.*, **89**, 520.
2. Qaim S. M., 2001. *Radiochim. Acta*, **89**, 223.
3. Firestone R. B., Ekström, L. P., 2004. WWW Table of Radioactive Isotopes, Version 2.1. URL: <http://ie.lbl.gov/toi>.
4. Fairhall A. W., 1961. The Radiochemistry of Magnesium. National Academy of Sciences – National Research Council. U. S. A.
5. Schwartz R., Wien E. M., Wentworth R. A., 1981. *J. Nutr.*, **111** (2), 219.
6. Van der Velden J. A., Kolar Z. I., Flik G., de Goeij J. J. M., 1989. *Final Programme and Book of Abstracts, XXth Annual Meeting ESNA*. Lunteren/Wageningen, The Netherlands. p 75.
7. Van der Velden J. A., Flik G., Kolar Z. I., de Goeij J. J. M., Bonga S. E. Wendelaar, 1990. *Final Programme and Book of Abstracts, XXIst Annual Meeting ESNA*. Kosice, Czechoslovakia. p 75.
8. Iwata R., Kawamura M., Ido T., Kimura S., 1992. *J. Radioanal. Nucl. Chem.*, **159** (2), 233.
9. Heijnen M. L., van den Berg G. J., Beynen A. C., 1996. *J. Nutr.*, **126** (9), 2253.
10. Martin H. E., Bauer F. K., 1962. *Proceedings of the Royal Society of Medicine - London*, **55**, 912.
11. Mendelson J. H., Barnes B., Mayman C., Victor M., 1965. *Metabolism: Clinical and Experimental*, **14**, 88.
12. Aikawa J. K., Rhoades E. L., Gordon C. S., 1958. *Proceedings of the Society for Experimental Biology and Medicine*, **10**, 29.
13. Kniffen J. C., Roessler C. E., Roessler G. S., Dunuvant B. G., Quick D. T., 1972. In *Radioaktive Isotope in Klinik und Forschung* (Ed: Felinger K., Höfer R.). Urban & Schwarzenberg. München.
14. Verhas M., de la Gueronniere V., Grognet J. M., Paternot J., Hermanne A., van den Winkel P., Gheldof R., Martin P., Fantino M., Rayssiguier Y., 2002. *Eur. J. Clinic. Nutr.*, **56**, 442.
15. Silver L., Robertson J. S., Dahl L. K., Heine M., Tassinari L, 1960. *J. Clinic. Invest.*, **39**, 420.

16. Wallach S., Rizek J. E., Dimich A., Prasad N., Siler W., 1966. *J. Clinic. Endocrinology*, **26**, 1069.
17. Avioli L. V., Berman M., 1966. *J. Appl. Physiol.*, **21**, 1688.
18. Watson W. S., Hilditch T. E. Horton P. W., Davies D. L., Lindsay R., 1979. *Metabolism: Clinical and Experimental*, **28**, 90.
19. Aikawa, Gordon G. S., Rhoades G. L., 1960. *J. Appl. Physiol.*, **15**, 503.
20. Choné B., Jahns E., Misri H. T., 1968. *Nuklearmedizin*, **7**, 107.
21. Graham L. A., Caesar J. J., Burgen A. S. V., 1960. *Metabolism: Clinical and Experimental*, **9**, 646.
22. Danielson B. G., Johansson G., Jung B., Ljunghall S., Lundqvist H., Malmborg P., 1979. *Mineral and Electrolyte Metabolism*, **2**, 116.
23. Lombeck I., Ritzl F., Schnippering H. G., Michael H., Bremer H. J., Feinendegen L. E., Kosenow W., 1975. *Z. Kinderheilk.*, **118**, 249.
24. Weinreich R., Bräutigam W., Machulla H. –J., Probst H. –J., Qaim S. M., Stöcklin G., 1975. In: *Proc. 7th Int. Conf. on Cyclotrons and their Applications* (Ed: Basel), Birkhäuser, Basel.
25. Schult O. W. B., 1977. *Nucl. Instr. Meth.*, **146**, 301.
26. Bohn T., 2003. *PhD. Thesis*, University of Frankfurt, Germany.
27. Currie V. E., Lengemann F. W., Wentworth R. A., Schwartz R., 1975. *Int. J. Nucl. Med. Biol.*, **2**, 159.
28. Schwartz R., Spencer H., Wentworth R. A., 1978. *Clinica Chim. Acta*, **87**, 265.
29. Schwartz R., Giesecke C. C., 1979. *Clinica Chim. Acta*, **97**, 1.
30. Schwartz R., Spencer H., Welsh J. E. J., 1984. *Am. J. Clinic. Nutri.*, **39**, 571.
31. Schwartz R., Grunes D. L., Wentworth R. A., Wien E. M. J., 1980. *J. Nutr.*, **110**, 1365.
32. Schimansky Chr., 1973. *Landw. Forschung*, **28/I**, 53.
33. Schimansky Chr., 1973. *Z. Pflanzenernährung u. Bodenkunde*, **136**, 68.
34. Schimansky Chr., 1975. *Landw. Forschung*, **31/I**, 109.
35. Probst H. J., Qaim S. M., Weinreich R., 1976. *Int. J. Appl. Radiat. Isot.*, **27**, 431.
36. Sekine T., Baba H., 1978. *J. Inorg. Nucl. Chem.*, **40**, 1457.

37. Van der Velden J. A., Kolar Z., Vollinga R. C., de Goeij J. J. M., 1989. *J. Label. Compd. Radiopharm.*, **26**, 172.

38. Kolar Z. I., van der Velden J. A., Vollinga R. C., Zandbergen P., de Goeij J. J. M., 1991. *Radiochim. Acta*, **54**, 167.

39. Malinin A. B., Levin V. I., 1973. *Radiokhimiya*, **15** (3), 422.

40. Nozaki T., Furukawa M., Kume S., Seki R., 1975. *Int. J. Appl. Radiat. Isot.*, **26**, 17.

41. Martens U., Schweimer G. W., 1970. *Z. Physik*, **233**, 170.

42. Weinreich R., Qaim S. M., Michael H., Stöcklin G., 1976. *J. Radioanal. Chem.*, **30**, 53.

43. Iwata R., Kawamura M., Ido T., Kimura S., 1992. *J. Radioanal. Nucl. Chem. Art.*, **159** (2), 233.

44. Bodemann R., Lange H.-J., Leya I., Michel R., 1993. *Nucl. Instr. Meth.*, **B 82**, 9.

45. Lange H.-J., Hahn T., Michel R., Schiekel T., Rösel R., Herpers U., Hofmann H.-J., Dittrich-Hannen B., Suter M., Wölfli W., Kubik P. W., 1995. *Appl. Radiat. Isot.*, **46**, 93.

46. Mellish C. E., Crockford G. W., 1957. *Int. J. Appl. Radiat. Isot.*, **1**, 299.

47. Lundqvist H., Malmborg P., 1979. *Int. J. Appl. Radiat. Isot.*, **30**, 33.

48. Mausner L. F., Prach T., Ku T., Richards P., 1984. *J. Nucl. Med.*, **25** (5), 120.

49. Maguire M. E., Cowan J. A., 2002. *BioMetals*, **15**, 203.

50. Facility Hazard Categorization Review for Brookhaven LINAC Isotope Producer, 1998. p I3.

51. Qaim S. M., 1982. *Radiochim. Acta*, **30**, 147.

52. Gul K., Hermanne A., Mustafa M. G., Nortier F. M., Obložinský P., Qaim S. M., Scholten B., Shubin Y., Takács S., Tárkányi F. T. and Zhuang Z., 2005. IAEA-TECDOC-1211, IAEA, Vienna, May 2001. Available from URL: http://www-nds.iaea.org/medical/.

53. TABLECURVE 2D, 1996. Automated Curve Fitting and Equation Discovery, Jandel Scientific, San Rafael, California.

54. Nortier F. M., Haasbroek F. J., Mills, S. J., Smit H. A., Steyn G. F., Stevens C. J., van Elst T. F. H. F., Vorster E., 1992. Proceedings 4th Int. Workshop

on Targetry and Target Chemistry, PSI-Proceedings 92-01, Villigen, Switzerland.

55. Szelecsényi, F., Steyn G. F., Kovács Z., Vermeulen, C., van der Meulen N. P., Dolley S. G., van der Walt T. N., Suzuki K., Mukai K., 2005. *Nucl. Instr. Meth*, **B** 240, 625.
56. Nelson F. A., Kraus K. A., 1955. *J. Amer. Chem. Soc.*, **77**, 801.
57. Iyer S.G., Venkateswarlu Ch., 1976. *Indian J. Chem.*, **14A**, 437.
58. Steyn G. F., van der Meulen N. P., van der Walt T. N., Vermeulen C., 2007. Proceedings of the International Conference on Nuclear Data for Science and Technology (Nice, France). *In press.*

CHAPTER 6 THE PRODUCTION OF ULTRAPURE ^{67}Ga

6.1 Introduction

^{67}Ga ($T_{1/2}$ = 78.3 h), which is usually produced in a cyclotron by means of the reactions ^{68}Zn(p, 2n)^{67}Ga or ^{nat}Zn(p,x)^{67}Ga (see Fig. 6.1), is extensively used in nuclear medicine[1]. Its main γ-emissions are 93.3 keV (37 %), 184.6 keV (20.4 %) and 300.2 keV (16.6 %). It is usually separated from Zn by means of ion exchange chromatography[2,3] or by liquid extraction[2,4]. The product is predominantly supplied in the citrate form and is mainly used for imaging soft tissue tumours and abscesses.

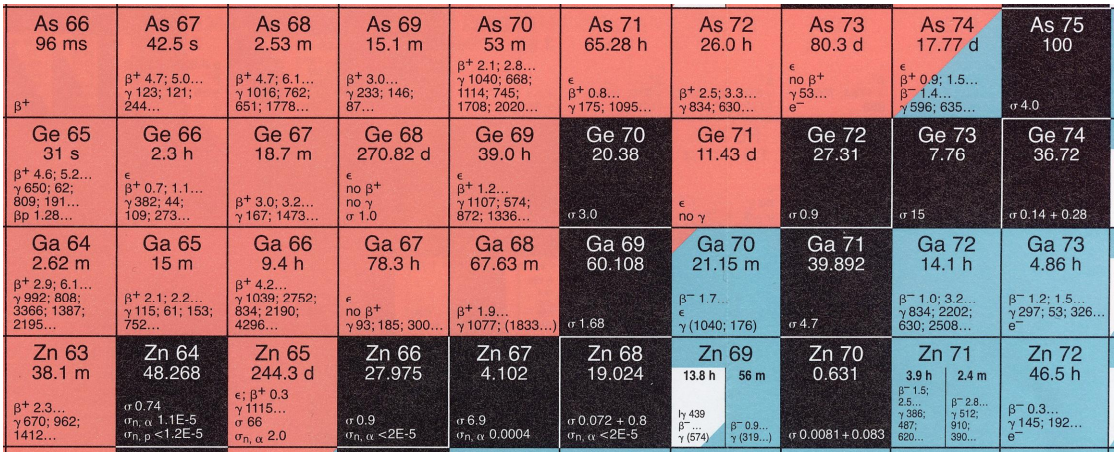

Fig. 6.1: Relevant part of the "Karlsruher Nuklidkarte" of 2006 for the production of ^{67}Ga.

When in citrate form, ^{67}Ga is known to concentrate in many types of tumours, as well as in non-malignant lesions. Although it is not a tumour-specific agent[5], it is used extensively for the localisation of a variety of human malignant tumours[6,7] and, due to its widespread application as a diagnostic tool in nuclear medicine, ^{67}Ga is one of the most widely employed cyclotron-produced radiopharmaceuticals.

A number of routes for the production of ^{67}Ga in large quantities, and their development into medical applications, have been reported[8-13]. At iThemba LABS, ^{nat}Ge targets (in tandem with ^{nat}Zn targets) have also been used for some time for routine production purposes but this practice has been terminated, temporarily, until a

problem concerning the release into the atmosphere of volatile radioarsenics has been solved satisfactorily. For the purposes of the present work, only ^{nat}Zn target will be considered. Several methods have been performed to separate ^{67}Ga from this target material by different ion exchange methods[14-18] and using the product in citrate form for medical applications.

The current production method in use at the RPG employs the bombardment of two ^{nat}Zn targets, in tandem. The bombarded targets are dissolved in hydrochloric acid and the resultant solution passed through a column containing Amberchrom CG-71cd resin. Any impurities contained on the resin are eluted, before the ^{67}Ga is eluted as the final product.

While the final product is deemed suitable for use in diagnostic nuclear medicine, the product has failed to label certain peptides efficiently due to the level of Fe impurity in the final product. The theory is that certain ^{67}Ga-labelled peptides may be effective for therapeutic purposes, thus, it was decided to investigate the possibility of producing an ultrapure product, such that this theory can be tested.

While descriptions of Ga and Fe separation from other elements have been reported in the literature[19-21], they do not adequately describe how Fe and Ga can be separated easily, as Fe(III) and Ga(III) have very similar chemical properties. It was thought prudent to adapt the method currently in use for production purposes at iThemba LABS.

6.2 Nuclear Data

It is interesting to peruse the excitation function for the production of ^{67}Ga in proton-induced nuclear reactions on ^{nat}Zn. For this purpose, two sets of data were combined and fitted with a polynomial function, in order to perform subsequent thick-target production rate calculations. The data are by Nortier *et al.*[22] and Szelecsényi *et al.*[23], shown in Fig. 6.2. The excitation function has a single peak, reaching a maximum of about 135 mb at 20 MeV. It falls away rapidly towards higher energies, therefore,

only the low-energy slot (of a tandem target geometry) will be suitable for its production.

Recently, two thin Zn targets (nominally 1.5 g/cm^2 each), located behind a Cu degrader, were bombarded without encapsulation (*i.e.* directly in contact with the cooling water). It is important to note that both Zn targets were located in the low energy slot. The reason why two thinner targets were used instead of a single thicker one is simply to increase the area in contact with the cooling water. It was found that thicker targets melt in the beam strike, in spite of being in direct contact with the cooling water, thereby, leading to production losses. The use of two thinner targets prevented the problem from reoccurring. The energy window of the two Zn targets was 5 – 45 MeV.

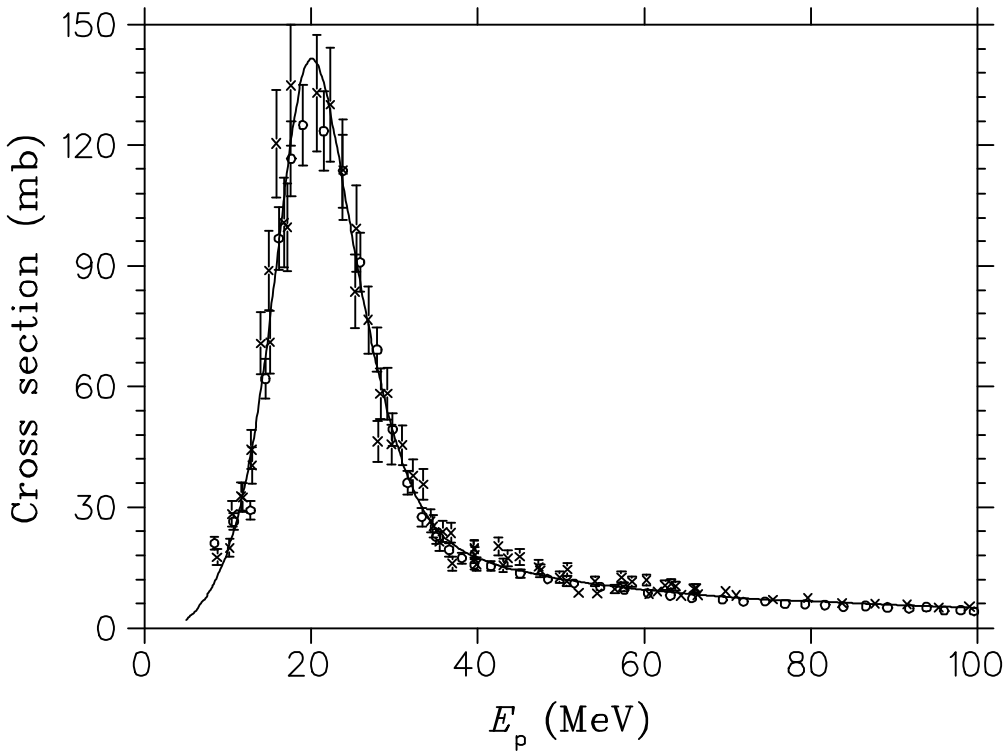

Fig. 6.2: Excitation function of ^{67}Ga formed in the reaction of protons with ^{nat}Zn. The open circles are the data of Nortier *et al.*[22] and the crosses the data of Szelecsényi *et al.*[23]. The curve is a polynomial fit through the data.

The thick-target production rate curve deduced from the polynomial of Fig. 6.2 is shown in Fig. 6.3. As can be seen from the figure, a production rate of about 75 MBq/µAh is predicted for the relevant production energy window. However, the

"dead layer" of the 1 mm thick cooling water layer between the two Zn targets should still be corrected for, reducing the expected production rate to approximately 68 MBq/µAh.

It is clear from these figures that only the so-called low-energy slot is useful using ^{nat}Zn as target material. Above 40 MeV, the ^{nat}Ge + p route is very promising and development work has again started at iThemba LABS to exploit it, however, that work falls outside the scope of this thesis project.

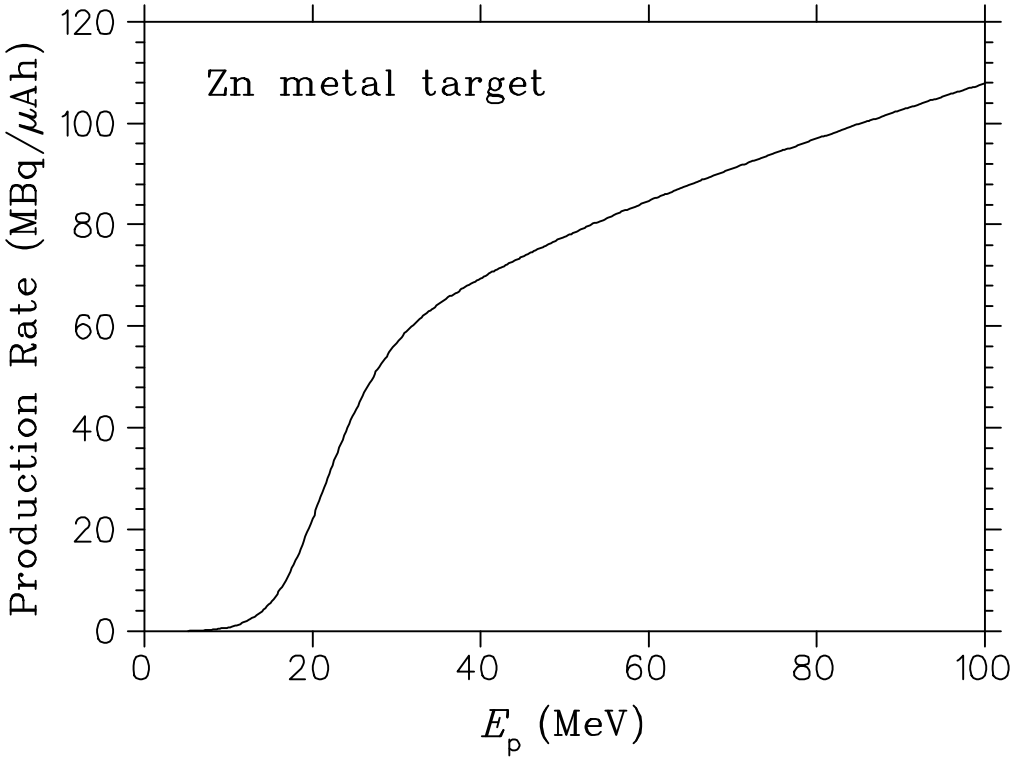

Fig. 6.3: Thick-target production rate curve of ^{67}Ga produced in the proton bombardment of ^{nat}Zn metal, as derived from the excitation function polynomial fit of Fig. 6.2.

6.3 Experimental

Analytical grade reagents were used throughout this work and were obtained from Merck (SA) Pty. Ltd or Sigma Aldrich GmbH, which included Sigma, Aldrich, Fluka and Riedel de Haen products. The Chelex 100 chelating resin used in this work was

obtained from BioRad Laboratories, Richmond, U.S.A., while the Amberchrom CG-161M resin was obtained from Rohm and Haas Company, Philadelphia, U.S.A.

Wherever water is referred to in the experimental descriptions, de-ionised water was used. This was obtained by de-ionising tap water using a Millipore MilliQ Reagent Grade Water System to a conductivity of greater than 10 megaohm cm^{-1}.

All radioactive determinations were performed using a standard calibrated HPGe detector, with a relative efficiency of 8 % (relative to three inch NaI), connected to a multichannel analyser. All Fe and Zn determinations were performed using a Varian graphite furnace atomic absorption spectrophotometer.

A good reducing agent is necessary to perform the experiments successfully. Comparisons were made using $TiCl_3$, $SnCl_2$ and ascorbic acid at different conditions. While $TiCl_3$ is a strong reducing agent, it contains traces of Fe when provided in 1 M HCl solution. As a result, the compound had to be purified, by means of cation exchange chromatography, prior to use.

Suprapur hydrochloric acid, which was used to perform the purification experiments with ^{67}Ga, was provided by Merck (SA) Pty. Ltd.

Reduction of Fe(III) with ascorbic acid

^{67}Ga tracer was added to a 10 mL solution of 0.01 M ascorbic acid containing 100 µg Fe. This solution was passed through a 2.5 mL column containing Chelex 100 resin. Fe was eluted using 50 mL 0.01 M ascorbic acid and the ascorbic acid rinsed from the resin using 20 mL water, before ^{67}Ga was eluted with 25 mL 2 M HCl.

Reduction of Fe(III) with $SnCl_2$

^{67}Ga tracer was added to 30 mL of a 0.1 M HCl solution containing 100 µg Fe and 2 mL $SnCl_2$ (0.01 g in 10 mL 1.0 M HCl) and heated to 60 ºC, before an additional 35 mL concentrated HCl was added to the solution. The resultant mixture was passed though a 2.5 ml column containing Amberchrom CG-161M resin (although this was also tested with Amberchrom CG-71cd resin). The resin was rinsed with 100 mL 6 M

HCl (to remove traces of Fe), before the ^{67}Ga was eluted with 30 mL 0.1 M HCl, collecting 5 mL fractions.

Reduction of Fe(III) with $TiCl_3$

As $TiCl_3$ solution is made up in dilute HCl, it was decided to purify it by means of ion exchange to remove any traces of Fe from it. Due to the fact that this project was part of an Innovation Fund Project Grant (from the local National Research Foundation), it was requested that this purification step not be divulged, as it could be claimed as intellectual property.

3 mL purified $TiCl_3$ was added to 30 mL 0.1 M HCl solution containing 100 µg Fe and ^{67}Ga tracer. The solution was well mixed. A further 45 mL of concentrated HCl was added to the solution, before the resultant solution was passed through a 2.5 mL column containing Amberchrom CG-161M resin. The resin was rinsed with 50 mL 6 M HCl (to remove traces of Fe and Ti), before the ^{67}Ga was eluted with 30 mL 0.1 M HCl, by collecting 5 mL fractions of the final eluant.

6.4 Results and Discussion

The experiments, using ascorbic acid as a reducing agent, proved to be successful to a degree. Initial runs saw 93 % of the ^{67}Ga removed in the first 10 mL of eluant, with an 88.3 % removal of Fe. The subsequent runs, however, proved to be less successful, with much of the Fe appearing in the first aliquot of eluant fractions. It was believed that this could possibly be due to the pump speed used for the experiments being too high. Even when the speed was decreased, however, the results did not improve much and this method was rejected.

The initial experiments involving $SnCl_2$ proved to be unsuccessful, as no heating was applied in the experimental process. While the yield was impressive, 10 µg/mL of Fe was found in the final product, a quantity deemed inappropriate to regard the experiment as successful. According to distribution coefficients obtained by Naidoo[24], Ga(III) is better retained by Amberchrom CG-161cd (with a polystyrene/divinylbenzene matrix) than when using Amberchrom CG-71cd (with an

acrylic ester matrix) as resin when the concentration of HCl increases. It was for this reason that most of the experiments performed on Amberchrom products were done using the CG-161 product, instead of the CG-71.

Subsequent experiments were performed by heating the solution to 60 ºC before the addition of the concentrated HCl. When using Amberchrom CG-161M, the results were found to be far more satisfactory, with 99 % removal of Fe and virtually all the ^{67}Ga found in the first 10 mL of eluant (see Fig. 6.4). The same could not be said when using Amberchrom CG-71cd: the Fe removal from the final product decreased to 70 % (it was deduced that Fe^{2+} was partially retained), while 20 mL of eluant was required to quantitively remove the ^{67}Ga from the resin (see Fig. 6.5).

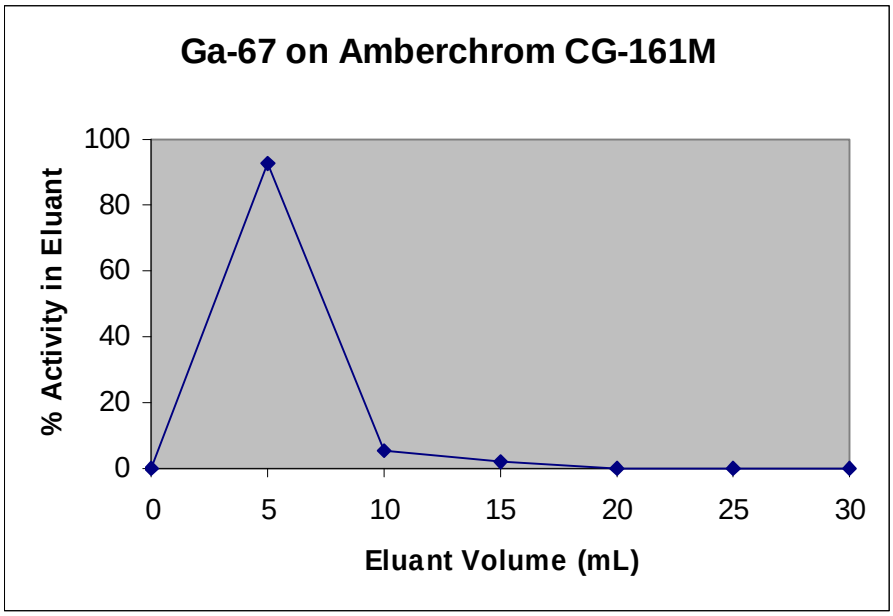

Fig. 6.4: Elution of ^{67}Ga from Amberchrom CG-161M using 0.1 M HCl.

It was decided to perform a comparison between the $SnCl_2$ and purified $TiCl_3$ as reducing agents. The results of the experiments using purified $TiCl_3$ as a reducing agent with Amberchrom CG-161M resin also provided very promising results. No heat was required upon adding the reducing agent and the final product (^{67}Ga) was yielded in the first 10 mL of eluant, while removing more than 99 % of the Fe added. With the results obtained from the comparison experiments, it was decided to take it a step further and perform a direct comparison under production simulation mode, that

is, using a similar method as currently used in routine production and add the experimental method to it. This implied that a double column separation had to be performed.

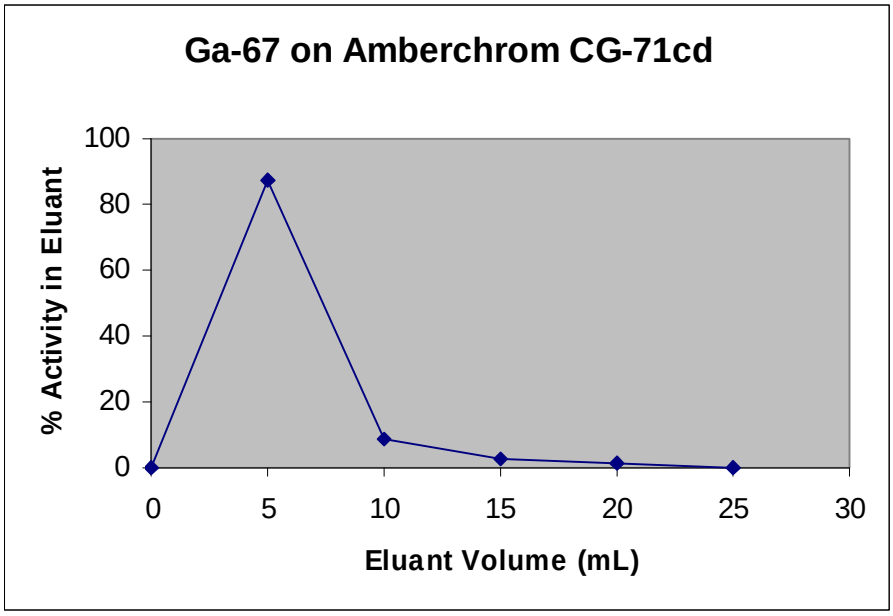

Fig. 6.5: Elution of ^{67}Ga from Amberchrom CG-71cd using 0.1 M HCl.

The experiment was, thus, conducted as follows: two pressed Zn targets, weighing *ca.* 9.46 g, were dissolved in 60 mL 32 % HCl (as used for routine production). Once complete dissolution was obtained a further 60 mL of 32 % HCl, containing 3 mL purified $TiCl_3$ solution, was added to the solution. The resultant mixture was passed through a column containing 2.5 mL Amberchrom CG-161M resin (100-200 mesh particle size and equilibrated with 7 M HCl). 150 mL 7 M HCl was passed through the resin column to elute the impurities such as target material and traces of Fe, before the ^{67}Ga was eluted with 30 mL 0.1 M Suprapur HCl. Each experiment was then conducted further according to the method described above.

Table 6.1: Fe and Zn contents of samples using different reducing agents on Amberchrom CG-161M resin.

Reducing agent	Product 1: Fe content (in µg/mL)	Product 2: Fe content (in µg/mL)	Percentage removed	Product 1: Zn content (in µg/mL)	Product 2: Zn content (in µg/mL)	Percentage removed
$SnCl_2$	1.86	0.071	99.23	20.30	0.088	99.91
$TiCl_3$	4.44	0.010	99.92	32.50	0.412	99.58

Samples were taken from the eluate of the first column (30 mL 0.1 M HCl – shown as "Product 1") and that of the second column (shown as "Product 2"), which was also the final product, and compared (see Table 6.1). As can be seen, the Fe and Zn contents in the first sample differed vastly between the experiments. This is due to the fact that no two Zn targets can have exactly the same make up, thus, it was regarded as more prudent to take the percentage removal of the impurity in question into account. As the percentage of Fe removals using the two different reducing agents were so similar, it was thought that a more definite decision could be made with regard to the most effective reducing agent should one take the Zn content in each product into account. This too, however, produced similar results.

It was finally decided that the most effective removal of impurities would be with the use of purified $TiCl_3$ as reducing agent, as the Fe removal is marginally better than when $SnCl_2$ was used as reducing agent, even though its removal of Zn is marginally less effective. Its ease of use in a hot cell environment, without requiring heat, was also a deciding factor in choosing $TiCl_3$ over $SnCl_2$ as reducing agent. Nevertheless, the use of both reducing agents with Amberchrom CG-161M resin produces a product that has vastly fewer impurities than the current production method in use, making this a product that can be regarded as ultrapure.

This method was devised as an addition to the current ^{67}Ga production, as to perform an ultrapure production on its own would require beam time that would overload the already heavily burdened schedule at iThemba LABS's Radionuclide Production Group. Should the targetry system be upgraded and beam time be available, the production could be performed as follows:

The two bombarded Zn targets would be dissolved in 60 mL concentrated Suprapur HCl, after which a further 60 mL (containing 3 mL purified $TiCl_3$) would be added. The resultant solution would be loaded onto a 2.5 mL column containing Amberchrom CG161M resin (equilibrated with 50 mL 7.0 M Suprapur HCl). Any remaining Zn and Fe impurities would be eluted with 150 mL 7.0 M Suprapur HCl, before the ^{67}Ga would be eluted from the resin column using 30 mL 0.1 M HCl. It can be assumed that this product would be required in this form for the labelling of peptides, as citrate would interfere with the labelling process. The main reason that this method would not be adopted for routine production purposes is the substantial increase in cost to produce the radionuclide, which would imply an increase in price for the consumers. This would not be well received by the local clinics and hospitals, particularly those subsidised by the government, as their budgets would not be able to cover this increase in cost.

6.5 Conclusion

Two alternate methods were tested and determined to be effective in the removal of Fe, as well as Zn, from ^{67}Ga. When using either $SnCl_2$ or purified $TiCl_3$ as a reducing agent in the process and applying a Amberchrom CG-161M resin column instead of a Amberchrom CG-71cd resin column, the results produced are excellent, with a removal of > 99 % of Fe and > 99.9 % of Zn from the final product.

While these methods were successful under production conditions for a quantity of 1.1 GBq (30 mCi) ^{67}Ga, further tests using much higher activities will be performed in the near future.

6.6 References

1. Green M. A., Welch M. J., 1989. *J. Nucl. Med. Biol.*, **16**, 435.
2. Helus F., Maier-Borst W., 1973. *J. Label. Compd. Radiopharm.*, 317.
3. Van der Walt T. N., Strelow F. W. E., 1983. *Anal. Chem.*, **55**, 212.
4. Hupf H. B., Beaver J. E., 1970. *Int. J. Appl. Radiat. Isot.*, **27**, 1.

5. Vallabhajosula S. R., Harwig J. F., Wolf W., 1981. *J. Nucl. Med. Biol.*, **8**, 363.
6. Taylor D. M., McReady V. R., 1986. In *Nuclear Techniques in Diagnostics Medicine* (Ed: van Rijk P. P.), Martinus Nijhoff, Dordrecht, p. 369.
7. Freeman L. M., 1999. In: *Nuclear Medicine Annual*, Lippincott Williams and Wilkens Publishers, Philadelphia, p. 165.
8. Silvester D. J., Thakur M. L., 1970. *Int. J. Appl. Radiat. Isot.*, **21**, 630.
9. Dahl J. R., Tilbury R. S., 1972. *Int. J. Appl. Radiat. Isot.*, **23**, 431.
10. Steyn J., Meyer B. R., 1973. *Int. J. Appl. Radiat. Isot.*, **24**, 369.
11. Vlatkovic M., Paic G., Kaucic S., Vekic B., 1975. *Int. J. Appl. Radiat. Isot.*, **26**, 377.
12. Neirinckx R. D., 1976. *Int. J. Appl. Radiat. Isot.*, **27**, 1.
13. Thakur M. L., 1977. *Int. J. Appl. Radiat. Isot.*, **28**, 183.
14. Strelow F. W. E., Victor A. H., van Zyl C. R., Cynthia E., 1971. *Anal. Chem.*, **43**(7), 870.
15. Boothe T. E., Tavano E., Munoz J., Carrol J., 1991. *J. Label. Compd. Radiopharm.*, **30**, 108.
16. Das M. K., Ramamoorthy N., 1995. *Calcutta Ind. J. Nucl. Med.*, **10**, 63.
17. Naidoo C., van der Walt T. N., 2001. *Appl. Radiat. Isot.*, **54**, 915.
18. El-Azony K. M., Ferieg Kh., Saleh Z. A., 2003. *Appl. Radiat. Isot.*, **59**, 329.
19. Strelow F. W. E., 1966. *Anal. Chim. Acta*, **34**, 387.
20. Strelow F. W. E., Victor A. H., 1972. *Anal. Chim. Acta*, **59**, 389.
21. Strelow F. E. W., Weinert C. H. S. W., van der Walt T. N., 1974. *Talanta*, **21**, 1183.
22. Nortier F. M., Mills S. J., Steyn G. F., 1991. *Appl. Radiat. Isot.*, 42, 353.
23 Szelecsényi F., Steyn G. F., Kovács Z., van der Walt T. N., Suzuki K., Okada K., Mukai K., 2005. *Nucl. Instrum. Meth. B*, **234**, 375.
24. C. Naidoo, 1998. *M.Sc. thesis*, University of Cape Town, South Africa.

CHAPTER 7 THE PRODUCTION OF ^{68}Ge USING LARGER VBTS FORMAT Ga TARGETS

7.1 Introduction

Positron Emission Tomography (PET), which provides information regarding blood flow and metabolism in patients non-invasively, is becoming a more common procedure in nuclear medicine. The detection of the two positron-annihilation photons (511 keV) in coincidence produces a significant reduction in background radiation, thereby, providing sharp tomographic images[1].

The availability of short-lived radionuclides from radionuclide generators provides an inexpensive and convenient alternative to in-house radionuclide production facilities, such as cyclotrons. ^{68}Ga, which has the physical characteristics desirable for PET, is obtained via the decay of ^{68}Ge, making the production of ^{68}Ge an important factor. ^{68}Ge, having a half-life of 288 days, decays entirely by electron capture[2] to produce ^{68}Ga ($T_{1/2}$ = 68 m), which disintegrates mainly by positron emission (90.5 %)[3]. The daughter (^{68}Ga) is obtained from ^{68}Ge when in secular equilibrium with the mother.

^{68}Ge has been used as a positron source in positron annihilation studies in nuclear physics and in metal radiography in industry[4]. The most recent application of this radionuclide, however, is as a ^{68}Ge/^{68}Ga generator for PET in nuclear medicine[5,6], with the use of ^{68}Ga as a PET tracer. The greater demand for ^{68}Ge is as a result of the increased use of ^{68}Ge/^{68}Ga generators for radiopharmaceutical purposes[7-13].

Two nuclear reactions have been utilized to produce ^{68}Ge routinely, namely, by ^{66}Zn(α,2n)^{68}Ge (^{66}Zn natural abundance being 27.8 %) giving a yield of up to 2 μCi.μAh^{-1}, or by ^{69}Ga(p, 2n)^{68}Ge (^{69}Ga natural abundance being 60 %) giving a yield of up to 20 μCi.μAh^{-1}. The latter reaction is regarded as the reaction of choice for medical cyclotrons due to the higher yields obtained and the fact that only two elements have to separated from each other, where with the former reaction a third element (Zn) has to be taken into consideration[14] (see Fig. 7.1).

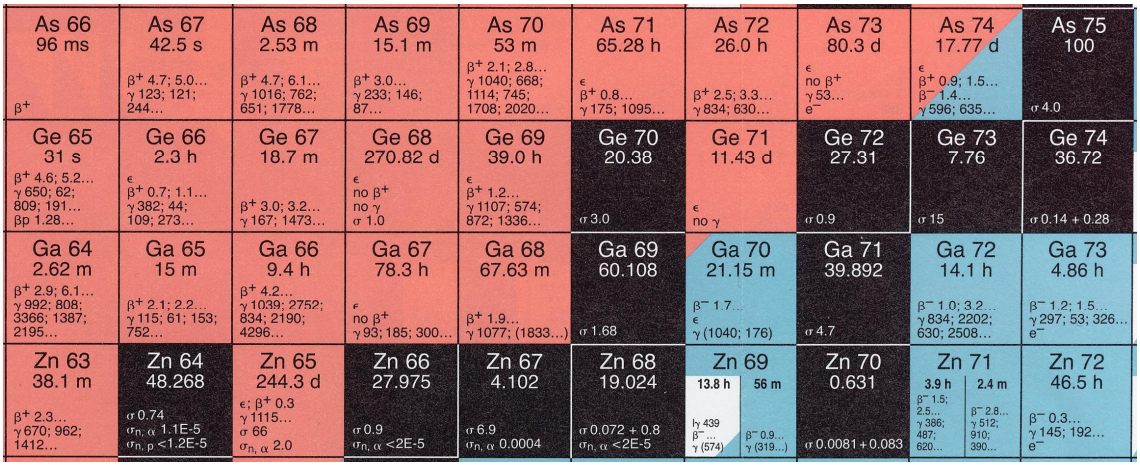

Fig. 7.1: Relevant part of the "Karlsruher Nuklidkarte" of 2006 for the production of ^{68}Ge.

Target materials used for the production of ^{68}Ge have included Ga_2O_3[14,15], Ga_4Ni[11], GaAg[16,17], RbBr[18], Ga_2O[13,19,20] and Ga metal[21-23]. The use of Ga_2O_3 has the disadvantage in that the material prohibits the use of a high-current proton beam. This is because the material changes from a hexagonal α-form to a monoclinic β-form at about 600 °C, leading to a volume increase which causes the target capsule to rupture. Because the target material has to be placed in a low energy slot in the VBTS (generally behind a Rb target), this material is not recommended as it is essential to utilise high-current beams for commercial production purposes. The use of alloys as target material (Ga_4Ni and GaAg) has the disadvantage of having to separate extra unnecessary impurities from the required final product, while the RbBr target also adds Rb as an extra impurity to remove, thereby, further complicating the proposed production method. The use of Ga_2O, while appearing to be useful, has been seen to be a long process which can turn to be cumbersome when performing the production in a hot cell environment, as well as the fact that it is a long, excruciating process to prepare the target material as a disc. Finally, Ga metal has been discovered to be corrosive to Al capsules. Elemental Ga has to be encapsulated due to its low melting point (29.8 °C), however, it has a tendency to dissolve most metals[11]. Should one encapsulate it in Nb, however, the Ga would not react with its encapsulation and one can bombard the target without incident[23,24].

Taking the advantages and disadvantages of all of the above target materials into account, it was decided to use Ga metal encapsulated in Nb, in the hope that the chemical separation will be easier, while at the same time using the target material

that produces the highest yield. The manufacture of these targets had to be partially outsourced as iThemba LABS does not yet have the infrastructure necessary to perform Nb encapsulation.

The radiochemical separation of ^{68}Ge from Ga targets by means of solvent extraction[11,15,16,19,25,26] and ion exchange chromatography, using organic[13,27] and inorganic[14,17,28] material, have been reported. It was decided to pursue ion exchange chromatography for this work, using a macroporous anion exchange resin, particularly after perusing Nelson *et al.*'s work[30] with regard to anion exchange separations involving hydrochloric acid, hydrofluoric acid and hydrochloric-hydrofluoric acid mixtures.

7.2 Nuclear Data

An evaluated excitation function data set for ^{nat}Ga + p was published by Takács *et al.* quite recently. This data (shown in Fig. 7.2) was adopted for making predictions of production rates at iThemba LABS.

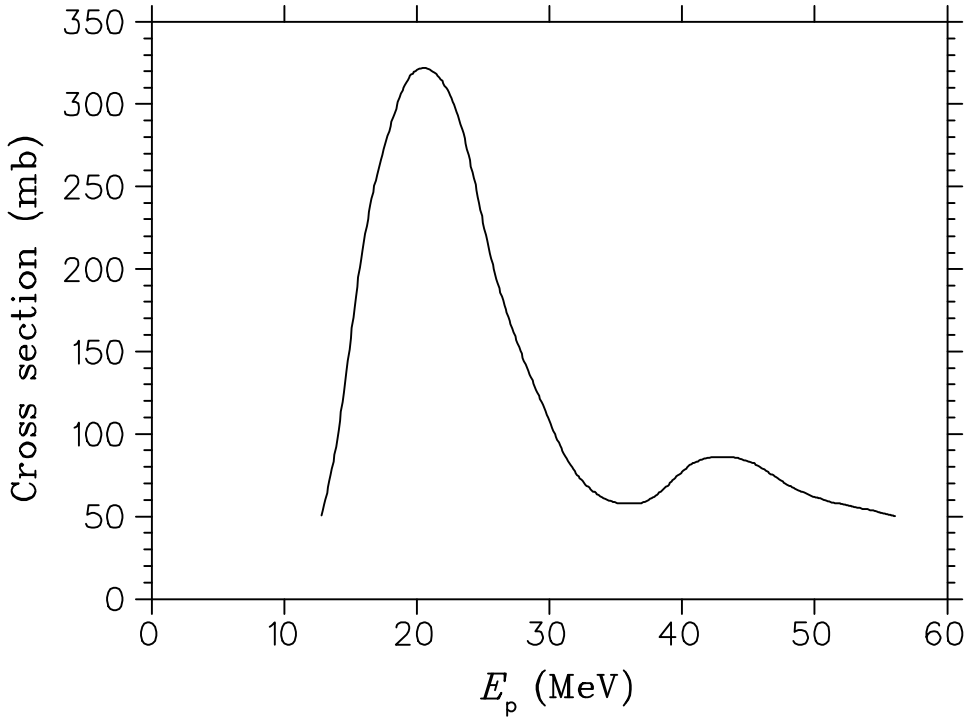

Fig. 7.2: Excitation function of ^{68}Ge formed in the reaction of protons with ^{nat}Ga. The curve is an evaluated excitation function[29] by Takács *et al.*

As can be seen from Fig. 7.2, the most prominent feature is a broad peak with a maximum of about 325 mb at 20 MeV, which is contributed to the excitation function by the reaction ^{69}Ga(p, 2n)^{68}Ge. A secondary peak towards higher energies corresponds to the contribution from the ^{71}Ga(p,4n)^{68}Ge reaction (see Fig. 7.1). Because of the large cross sections at energies below the effective threshold for the production of ^{82}Sr from ^{nat}Rb + p, *i.e.* about 33 MeV (see Chapter 4), it is extremely attractive to produce ^{68}Ge and ^{82}Sr simultaneously in a tandem target geometry. In other words, ^{68}Ge (from ^{nat}Ga + p) is an extremely attractive low-energy-slot companion for ^{82}Sr (from ^{nat}Rb + p), the latter target of which then occupies the high-energy slot. It is for this reason that a ^{nat}Rb/^{nat}Ga tandem target was introduced for the VBTS from the outset.

The thick-target production rate curve derived from the excitation function of Fig. 7.2, for a ^{nat}Ga metal target, is shown in Fig. 7.3. The energy window selected for the VBTS targetry is nominally 34 MeV down to threshold. The predicted production rate for this energy region is about 1.6 MBq/µAh. Actual production yields (EOB) of between 1.4 and 1.5 MBq/µAh (uncorrected for decay) have been obtained repeatedly, thus in excellent agreement with expectations. Once again, it was shown that a metal target with a low melting point, encapsulated with a metal having a high melting point, behaves extremely well in high-intensity irradiations of extended duration.

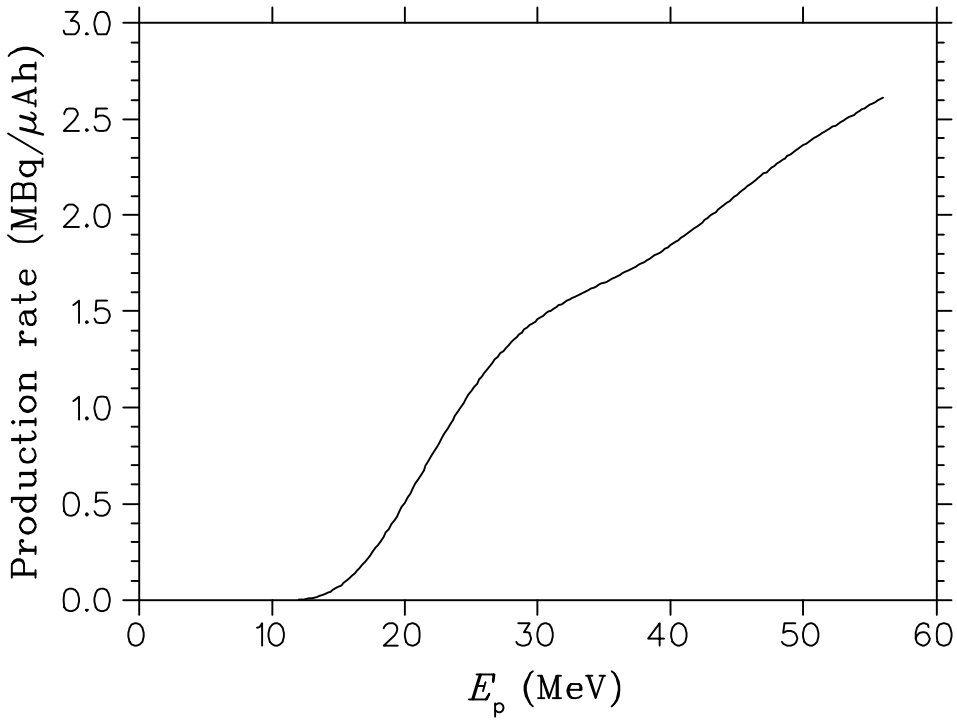

Fig. 7.3: Thick-target production rate curve of ^{68}Ge produced in the proton bombardment of ^{nat}Ga metal, derived from the excitation function of Fig. 7.2.

7.3 Experimental

Analytical grade reagents were used throughout this work and were obtained from Merck (SA) Pty. Ltd or Sigma Aldrich GmbH, which included Sigma, Aldrich, Fluka and Riedel de Haen products. The AG MP-1 anion exchange resin used in this work was obtained from BioRad Laboratories, Richmond, U.S.A.

De-ionised water from a Millipore MilliQ Reagent Grade Water System, to a conductivity of greater than 10 megaohm.cm^{-1}, was used for all experimental and production work.

All radioactive determinations were performed using a standard calibrated HPGe detector, with a relative efficiency of 13 % (relative to three inch NaI), connected to a multichannel analyser. As ^{68}Ge produces no gamma peaks, activity determinations were performed by measuring its daughter, ^{68}Ga, after 8 to 10 hours when equilibrium had been reached.

Experiment 1

A distillation system was set up in the hope that the target could be dissolved by means of sub-boiling, such that the Ge activity doesn't volatilize. The target was dissolved in 50 ml *aqua regia* and gently evaporated to dryness under vacuum. The activity was picked up in 100 ml 0.01 M HF and loaded on to a column containing 2.5 mL AG MP-1 resin. The column was rinsed with 50 mL 0.01 M HF, before the product was eluted with 20 ml 0.1 M acetic acid, followed by 20 mL 0.1 M HCl.

Experiment 2

A 20 mL aliquot was taken from a 1.0 M NaOH and 2 % ascorbic acid solution, containing ^{68}Ge/^{68}Ga activity. To this was added 50 µL ^{69}Ge activity and the activities of the sample measured. The resultant solution was loaded on to a 2.5 mL column containing AG MP-1 macroporous anion exchange resin, which had been equilibrated by the passage of 50 mL 1.0 M NaOH. Any impurities were removed from the column by rinsing the resin column with 50 mL 0.01 M HF, while the final product, ^{68}Ge, was eluted from the column with 20 mL 0.1 M acetic acid.

Experiment 3

A 20 mL aliquot was taken from a 1.0 M NaOH and 2 % ascorbic acid solution, containing ^{68}Ge/^{68}Ga activity. To this was added 1 mL concentrated HF (to equalize the ratio of F^- ions and OH^- at approximately 1:1), 50 µL ^{69}Ge activity and 50 µL ^{67}Ga activity, before the sample was measured. The resultant solution was loaded on to a 2.5 mL column containing AG MP-1 macroporous anion exchange resin, which had been equilibrated by the passage of 50 mL 0.2 M HF. Any impurities were removed from the column by rinsing with 50 mL 0.01 M HF, while the ^{68}Ge final product was eluted from the column with 20 mL 0.1 M acetic acid.

Experiment 4

A 20 mL aliquot was taken from a 1.0 M NaOH and 2 % ascorbic acid solution, containing ^{68}Ge/^{68}Ga activity. To this was added 1.5 mL concentrated HF (to bring the concentration of F^- ions into excess), 50 µL ^{69}Ge activity, 50 µL ^{67}Ga activity and 20 µL ^{22}Na activity before the sample was measured. The resultant solution was loaded on to a 2.5 mL column containing AG MP-1 macroporous anion exchange resin, which had been equilibrated with 50 mL 0.2 M HF. Any impurities were

removed from the column by rinsing with 50 mL 0.005 M HF, while the final product, ^{68}Ge, was eluted from the column with 20 mL 0.1 M HCl.

Experiment 5

A 20 mL aliquot was taken as described for Experiments 2 to 4 above. To this was added 1.5 mL concentrated HF (to bring the concentration of F^- ions into excess), 20 µL of ^{22}Na activity, 50 µL ^{67}Ga activity and 50 µL ^{69}Ge activity, before the sample was measured. This solution was then diluted to 200 mL, to decrease the concentration of Na^+ ions (which decreases the distribution coefficient of Ge by interference). The resultant solution was loaded on to a 2.5 mL column containing AG MP-1 macroporous anion exchange resin, which had been equilibrated with 50 mL 0.2 M HF. Any impurities were removed from the column by rinsing the resin column with 50 mL 0.01 M HF, while the final product, ^{68}Ge, was eluted from the column with 20 mL 0.1 M acetic acid, followed by 20 mL 0.1 M HCl.

Experiment 6

A 20 mL aliquot was taken as described for Experiments 2 to 5 above. To this was added 2.0 mL concentrated HF (to bring the concentration of F^- ions into excess), 20 µL of ^{22}Na activity, 50 µL ^{67}Ga activity and 50 µL ^{69}Ge activity, before various activities in the sample were measured. This solution was then diluted to 200 mL, to decrease the concentration of Na^+ ions. The resultant solution was loaded on to a 2.5 mL column containing AG MP-1 macroporous anion exchange resin, which had been equilibrated by the passage of 50 mL 0.2 M HF. Any impurities were removed from the column by rinsing with 50 mL 0.05 M HF, while the final product, ^{68}Ge, was eluted from the column with 20 mL 0.1 M acetic acid, followed by 20 mL 0.1 M HCl.

7.4 Results and discussion

When experiments were performed previously using ^{68}Ge solution supplied by Los Alamos National Laboratory, New Mexico, U.S.A., it was determined that AG MP-1 anion exchange resin could be used to retain the product and elute the ^{68}Ga daughter radionuclide using dilute HF in the form of a generator. While this will be discussed at a later stage, it was decided that this model should be used in production as well,

particularly as resins used in productions to separate the material of interest from the target material have often been carried over to the manufacture of the generator (the production of ^{82}Sr and the ^{82}Sr/^{82}Rb generator using Chelex 100 comes to mind).

While dissolving Ga target material is not generally problematic (one can use sulphuric acid or *aqua regia*), to obtain the radionuclides in the anion of interest did cause a few headaches. The use of sulphuric acid was discarded due to its high boiling point of over 300 ºC, therefore, it was thought to be more effective to use *aqua regia*. This brought forward another problem, in that Ge, as well as Ga, is volatile when in chloride form. As Faβbender *et al.*[23] used *aqua regia* to dissolve the target material and evaporated it to dryness before performing their solvent extraction method, it was decided to perform a similar method, but sub-boil the target solution under vacuum, such that volatility temperatures would not be reached.

The set-up, as a result, consisted of a reaction vessel connected to a condenser set at an angle, with a catcher at its base. Just above the catcher was a tube connected to a vacuum system, with a scrubber system containing 1.0 M NaOH and 2 % ascorbic acid in the event that the Ge and Ga radionuclides did volatilize and was not contained in the catcher vessel. A photographic view of this set up can be seen in Fig. 7.4.

Experiment 1

No Ge (or ^{68}Ga) activity was found in the load sample, load waste, wash waste or eluate samples. Upon checking the rest of the system, it was found to have collected in the scrubber system (90 %), with 10 % being picked up in the condensate. This implied that, even though the target solution was sub-boiled, the ^{68}Ge was still volatile, while the Ga radionuclides were not (^{68}Ga activity was the result of the decay of its parent, ^{68}Ge). It appeared that the nitrous oxide group from the *aqua regia* played a crucial role in the carrying over of the Ge activity. The experiments that followed were performed in the hope that the activity in the scrubber could be utilized, thereby still being able to use the experimental set-up effectively.

Experiment 2

The addition of ^{69}Ge tracer was such that one could determine the movement of the element. While ^{68}Ge produces no γ-rays, ^{69}Ge has a strong γ-line at 1116.6 keV, which is easily traceable for experimental purposes.

Using the solution as it was and equilibrating the resin column such that the system was slightly basic was not effective. The ^{69}Ge activity passed through the resin column, indicating that acidic conditions would be required to render an effective separation.

Experiment 3

The use of HF to acidify the scrubber solution proved to be effective to a degree, producing a 63.0 % yield of ^{68}Ge product. 35.7 % of the ^{69}Ge tracer was eluted in the load step, while 1.3 % was eluted in the rinse step with dilute HF. While only 2.2 % eluted with the 20 mL acetic acid, the remainder was eluted easily with another 20 mL 0.1 M HCl.

^{67}Ga was added in the eventuality that it would be in the load solution and Ga radionuclides would have to be separated from the Ge final product. 11.8 % of the ^{67}Ga tracer was eluted in the initial load step, while a further 65.5 % of the tracer was eluted when the column was rinsed with 0.01 M HF. The remainder of the radionuclide was eluted with 20 mL 0.1 M acetic acid.

Experiment 4

When the initial solution was mixed, it produced a precipitate. The experiment proceeded as with Experiment 3 and the precipitate measured. It was found to contain some 70 % of the ^{67}Ga tracer and approximately 6 % ^{22}Na. No ^{69}Ge tracer was found in the precipitate, presumed to be NaF as a result of more HF being added to the mixture.

The result of this experiment was an improvement over the previous ones, in that there was only 21.1 % breakthrough of the ^{69}Ge tracer from the resin column, over the 35.7 % from the previous experiment. 7.9 % of the tracer was eluted from the resin column when rinsing with dilute HF, however. No ^{69}Ge was found in the 20 mL 0.1

M HCl and when attempting to elute the product with a further 20 mL 0.1 M acetic acid, less than 1 % was gleaned from the column. When reverting to another 20 mL 0.l M HCl in a desperate attempt to remove the activity from the resin, success was achieved and the remainder of the activity was eluted. It would appear that one would have to "rinse" the column with acetic acid to assist the Ge to move through the column, before converting the Ge to the chloride form such that it can be eluted from the resin column effectively.

While much of the ^{67}Ga tracer was in the precipitate as stated above, the remainder of the tracer was removed in the load and rinse steps, with 8.6 % of the radionuclide being removed in the load step and 22.3 % in the rinse step, respectively.

The same can be said for the ^{22}Na tracer, placed in the initial load solution to ensure that the Na^+ ions did not play a role as an impurity in the final product if one used the scrubber solution in a production procedure. 75.3 % of the tracer was eluted from the resin column in the load step, while 18.4 % was eluted in the dilute HF rinse step. None of the tracer was found to be in the final eluate.

Experiment 5

While diluting the solution such that the NaF formed would stay in solution, interestingly, the result of this experiment was remarkably similar to Experiment 4 with regard to the Ge tracer, in that 23.1 % of the ^{69}Ge went through the column in the load step, while a further 5.1 % of the tracer was eluted when using 0.01 M HF: an improvement over Experiment 4 when 0.005 M HF was used, indicating that more concentrated HF should be considered to ensure the Ge is not eluted. No Ge tracer was found in the acetic acid eluent, however, and the remainder (71.8 %) was eluted with the 20 mL 0.1 M HCl.

Almost half of the ^{67}Ga tracer, 44.9 % to be exact, was eluted with the load waste, while 53.5 % of the total amount of tracer was eluted when using dilute HF. The remaining trace of the element was removed when eluting the resin column with 20 mL 0.1 M acetic acid.

The removal of Na also proved to effective, with 97.0 % of the ^{22}Na tracer added being removed in the load step. 1.6 % of the tracer was removed when rinsing the column with the dilute HF, while the remaining trace of the element was removed in the 20 mL acetic acid elution step.

Experiment 6

The increase in F^- ions in the load solution, as a result of the extra HF added, proved to be the turning point in the experimental process. As a result, no ^{69}Ge tracer was eluted from the resin column and found in the load waste. The increase of HF concentration to 0.05 M also proved to be beneficial, as no tracer was detected in the waste resulting from the dilute HF rinsing of the column. No tracer was found in the acetic acid rinse step, while 91.5 % of ^{69}Ge was found in the 20 mL 0.1 M HCl eluate. A further 1.6 % was removed from the resin column with the introduction of another 10 mL aliquot of 0.1 mL HCl to the resin column.

Should ^{67}Ga be found in the load solution, one can rest assured that it will not play a role in the final product. 10.6 % of the tracer was eluted with the load waste, while a further 85.6 % of the element was eluted with the dilute HF rinse step. The remaining 3.8 % was eluted with the 20 mL 0.1 M acetic acid rinse step.

It would appear that Na will also not play a vital role in the production of ^{68}Ge with regard to the final product, as 98.4 % of Na, as indicated by the ^{22}Na tracer, was not retained by the AG MP-1 macroporous anion exchange resin and was found in the load waste solution. The remaining 1.6 % of the tracer was eluted with the 0.05 M HF rinse step.

To ensure that the experiment was reproducible, the method was repeated and the results obtained were very similar to that obtained in Experiment 6. As a result, it was assured that the system used to dissolve the target would be effective, in that the Ge activity would volatilize to the scrubber system containing NaOH and that an effective separation could still be obtained. Production runs were performed to ensure that the volatilization of the ^{68}Ge is reproducible and is described below.

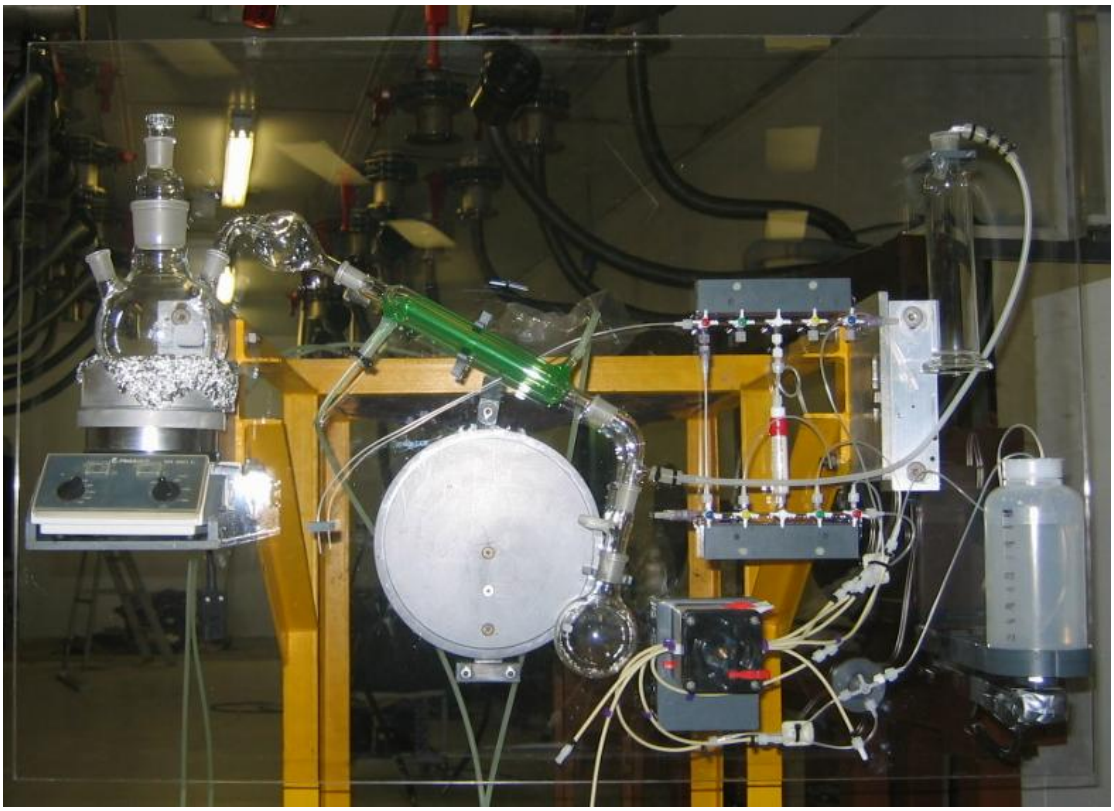

Fig. 7.4: The ^{68}Ge production panel, consisting of a reaction vessel (see left) connected to a condenser set at an angle, with a catcher at its base. Just above the catcher is a tube connected to a vacuum system via a scrubber system. After the reaction, the scrubber content is pumped to the plastic bottle (see right), mixed and pumped through the resin column.

Production 1

An 8.0 g Ga target, cut open and separated from its niobium encapsulation, was placed in the reaction vessel and dissolved in 50 mL *aqua regia*. The target material was left to react and dissolved for 1.5 hours, before the solution was gently heated for another hour to bring the reaction to completion and to ensure the ^{68}Ge had indeed volatilized. The solution was left to cool for 5 minutes.

10 mL of concentrated HF was pumped into the scrubber solution, containing 100 mL 1.0 M NaOH and 2 g Na_2SO_3 (used as a reducing agent, such that the Ge activity carried over stays in solution). This proved to be an error in judgement, as a precipitate formed after the HF was pumped into the scrubber solution, presumably NaF. As the solution was pumped out into a 1 L bottle containing 900 mL water, some of the solution was pumped back into the scrubber to ensure that the precipitate re-dissolved and that no ^{68}Ge activity would be lost in the process.

The resultant solution was pumped through a 10 mL column containing AG MP-1 macroporous anion exchange resin, equilibrated by the passage of 50 mL 0.2 M HF. A bigger column was chosen because the concentration of the HF in solution was lower, resulting in a lower distribution for Ge and, therefore, production losses. The column was rinsed with 50 mL 0.05 M HF, followed by 20 mL 0.1 M acetic acid, before the ^{68}Ge final product was eluted from the resin column using 20 mL 0.1 M HCl.

It was determined that all of the ^{68}Ge activity had been carried over to the scrubber solution but, interestingly, none of the Ga radionuclides had volatilized and was still found in the reaction vessel. It was also determined that the reaction vessel did not need to be evaporated to dryness. Once all the brown nitrous oxide fumes had been carried over to the scrubber system it could be seen, with the use of detectors, that 90 % of the activity had been carried over and it was deemed that the remainder in the reaction vessel was due to the Ga radionuclides left in the target solution.

Due to the increase in "dead" volume within the resin column, as a result of the increase in column size from 2.5 mL to 10 mL, the use of 20 mL 0.1 M HCl to remove the final product did not suffice and the volume was increased to 50 mL to ensure that all of the ^{68}Ge activity was removed from the column.

Approximately 10.9 % of the total ^{68}Ge activity from the target solution was collected in the catcher at the base of the condenser system. It was radionuclidically pure and it was assumed that it was in approximately 6 M HCl solution, as a result of the decay of ***aqua regia*** in the gentle heating process. No ^{68}Ge activity was found in the load and rinse wastes and the column was found to be devoid of activity once the final product was eluted with 0.1 M HCl, indicating that all of the activity in the scrubber solution was collected in the final product, which was radionuclidically pure.

Production 2

The method as described in Production 1 was repeated but, instead of pumping 10 mL HF into the scrubber solution, the scrubber solution was pumped into a container holding 900 mL of water and 10 mL concentrated HF. 50 mL 0.1 M HCl was used to elute the final product. No precipitate was found in the container, thereby keeping the

NaF in solution and there was no breakthough of ^{68}Ge while loading the 10 mL AG MP-1 anion exchange resin column. Once again, there was no breakthough of ^{68}Ge when performing the dilute HF column rinse, while all of the ^{68}Ge activity found in the scrubber solution was eluted with the 0.1 M HCl. The first 20 mL of the eluate yielded no ^{68}Ge and that was probably due to the larger column in use, as well as the "dead" volume of the larger column. The entire yield came out between 25 mL and 45 mL (an elution curve can be seen in Fig. 7.5 below). As with Production 1, approximately 10.8 % of the total ^{68}Ge activity was found in the catcher vessel at the base of the condenser. While there were losses to the catcher vessel, the separation produced a 100 % product yield, with the possibility of neutralizing the product "caught" in the catcher vessel with ammonia, to create germanic acid, such that it is stabilized and can be evaporated to dryness. As with Production 1, the final product was determined to be radionuclidically pure.

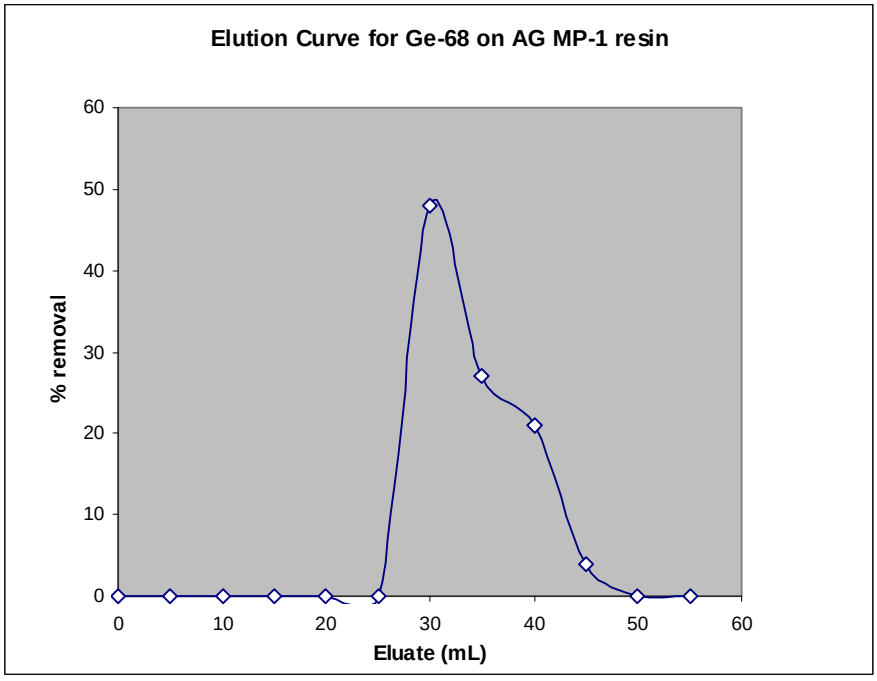

Fig. 7.5: The elution curve for ^{68}Ge from AG MP-1 resin using 0.1 M HCl as eluent.

The results obtained from the experiments and the two production runs are listed below in Table 7.1.

Table 7.1: Percentage impurity removal and percentage product yield using AG MP-1 resin.

	Experiment 3	Experiment 5	Experiment 6	Production 1	Production 2
% ^{68}Ge removal in load step	35.8	23.1	0	0	0
% ^{22}Na removal in load step	N/A	97.0	98.4	N/A	N/A
% ^{67}Ga removal in load step	11.8	44.9	10.6	N/A	N/A
% ^{68}Ge removal in initial rinse step	1.3	5.0	0	0	0
% ^{22}Na removal in initial rinse step	N/A	1.6	1.6	N/A	N/A
% ^{67}Ga removal in initial rinse step	65.5	53.5	85.6	N/A	N/A
% ^{68}Ge removal in 2nd rinse step	2.2	0	0	0	0
% ^{22}Na removal in 2nd rinse step	N/A	1.4	0	N/A	N/A
% ^{67}Ga removal in 2nd rinse step	22.7	1.6	3.9	N/A	N/A
% ^{68}Ge yield	60.8	71.8	93.0	89.1 (100)	89.2 (100)

While it was thought that the column size and the ion exchange separation method would not have to change when using the upsized 32 g target bombarded in the VBTS at iThemba LABS, as the activity is carried over to the scrubber system, the volume of *aqua regia* had to be increased such that the target material could react effectively to dissolve the Ga and, thereby, release the ^{68}Ge. As 50 mL was used to react with the 8 g target material, it was decided to use 200 mL *aqua regia* to react with the larger target. This would prove to have disastrous consequences.

Once the target material was removed from its niobium capsule and added to the reaction vessel, *aqua regia* was added and the target left to dissolve for three hours. After the three hours had passed, the reaction vessel was gently heated at 50 ºC, as before. After a further 30 minutes, chaos ensued within the reaction vessel as a violent reaction took place, spilling hot *aqua regia* out of the reaction vessel on to the floor of the hot cell, as well as into the catcher vessel and into the scrubber system. As a result, much activity was lost and damage control had to take place to extract what activity one could from the production.

The chloride in the scrubber system proved to be an enemy, as the ^{68}Ge readily began to break through the resin column. The load solution had to be modified by neutralizing the solution and adding more HF to the solution such that the final fluoride concentration was 1 mol L^{-1}. Once this was done, the solution was loaded through a 20 mL resin column, to ensure that no further breakthrough would take place. As a result, 85 % of the activity in the load solution was yielded.

To ensure that the violent exothermic reaction would not reoccur, further experiments were conducted with regard to the dissolution of the target material. It was thought that the nitric acid determined the reaction rate and, therefore, the exothermic reaction with the target material. 32 g of Ga, therefore, was added to 150 mL HCl and 10 mL HNO_3 added to the reaction (instead of 50 mL) and the solution gently heated to 50 ºC. It was noted that the Ga globule slowly, but surely, broke up into hundreds of little balls, thereby, increasing the surface area for reaction exponentially. The solution then turned a murky, darker yellow colour, before the exothermic reaction occurred, dramatically, with smoke and solution pouring from the vessel. The murkiness was later determined as effervescence due to the smaller Ga balls reacting with the *aqua regia*.

Following this failure, it was concluded that the HCl did have a vital role to play in the reaction, after all, and, therefore, the HCl volume was decreased, beginning the reaction with 50 mL, in order to reduce the "fuel" for the vigorous reaction. 50 mL concentrated HCl was added to 32 g Ga and heated to 70 ºC, before 2 mL concentrated nitric acid was added. The solution was left for 30 minutes and the exothermic reaction took place, albeit with greatly reduced vigour, leaving a fair amount of target material still to dissolve. Another 2 mL of HNO_3 was added to the reaction solution, where another vigorous reaction took place. The solution turned colourless, indicating that the HCl was depleted. A further 50 mL HCl was added to the reaction solution and the process repeated, although more nitric acid had to be added than previously due to the fact that the solution was more dilute than before. Once the HCl was depleted, the last 50 mL was added to the reaction vessel, along with the remainder of the HNO_3. The reaction did not affect the scrubber system, while the ^{68}Ge activity did, indeed, carry over to the scrubber system. The ion exchange separation was carried out successfully, without further incident.

Target encapsulation

From experience gained when performing productions using this product, it became apparent that bench experiments and productions differed greatly. Initially, target capsules were cut open and the target provided for processing. In this case, however, the gallium was fused to the niobium capsule after the bombardment, thereby, making it very difficult to remove for processing. Placing the "fused" capsule in hot water proved to be an effective way of removing the Ga from the capsule.

As mentioned previously, Ga has a tendency of reacting with its encapsulation when using stainless steel or aluminium. Ideally, it would be better to encapsulate the target material in a more inert capsule, such as niobium, but this proved to be costly as it required the transportation to Pelindaba, outside Pretoria, to ensure that the capsules could be sealed, under vacuum, using an electron-beam welder.

While the Merck Index[31] stated that niobium was inert to strong acids, including ***aqua regia***, the capsule did indeed react, creating black oxide particles at the bottom of the reaction vessel, thereby, making it very messy with regard to the load step. It was discovered that 37.2 % of the capsule had either gone into solution or reacted with the capsule to form an oxide. As a result, it was decided to change the HCl:HNO_3 ratio in the ***aqua regia*** from 3:1 to 9:1, ***i.e.*** decrease the nitric acid concentration in the target reaction. While it took longer for the target material to dissolve, it had a markedly better effect on the niobium capsule; with a mere 1.5 % of Nb going into solution (no oxide particles were discovered). It was, therefore, decided to use the method of removing the gallium with hot water (where Ga becomes liquefied) and remove the niobium before the dissolution of the Ga was performed.

Adopted production method

32 g of Ga was removed from its niobium encapsulation by placing it in hot water and letting it flow out, ***sans*** water and capsule, into the reaction vessel containing 50 mL concentrated HCl. 3 mL of concentrated HNO_3 was added to the vessel and the reaction solution heated to 70 ºC for 30 minutes, such that the target material can react vigorously. This was followed by the addition of a further 3 mL HNO_3. A further 50 mL concentrated HCl was added to the vessel and left for 15 minutes to warm, before 3 mL HNO_3 was added and left to react further for 20 minutes. Another 4 mL HNO_3

was added to the reaction vessel and the solution left for a further 20 minutes. Once the HCl was depleted, the final 50 mL of HCl was added and the solution left for 15 minutes, before 10 mL HNO_3 was added to the reaction, followed by the final 17 mL after 30 minutes.

Once the reaction was completed, the scrubber solution, consisting of 100 mL 1.0 M NaOH containing 2.0 g Na_2SO_3 and containing the ^{68}Ge activity, was pumped to a bottle containing 900 mL water and 10 mL concentrated HF. The resultant solution was stirred for 10 minutes, before being pumped through a column containing 10 mL AG MP-1 macroporous anion exchange resin (equilibrated with 50 mL 0.2 M HF). Any impurities, such as Na^+ ions, were removed by rinsing the column with 50 mL 0.05 M HF, before 20 mL acetic acid was pumped through the resin column to assist in the elution of the final product. The final product, ^{68}Ge was eluted from the resin using 50 mL 0.1 M HCl, in 10 mL fractions, where the first 20 mL was discarded.

While this production method has been put in place such that $^{68}Ge/^{68}Ga$ generators can be made using SnO_2 as matrix[20], the panel can be streamlined further should one adopt a method of constructing generators using AG MP-1 macroporous anion exchange resin (to be discussed later), by attaching the constructed generator to the panel such that the ^{68}Ge is loaded directly on to the resin column, thereby, not requiring the elution process.

7.5 Conclusion

The yields from several production runs were found to be in very good agreement with predictions based on an evaluated excitation function recently published in the literature. An energy window of 34 MeV down to threshold was adopted for ^{68}Ge production, in order to utilize the low-energy slot in a tandem target configuration where the high-energy slot was reserved for ^{82}Sr production. Several of these tandem targets have been irradiated in the VBTS with beam currents of nominally 250 µA for extended periods (up to one month with fractionated beam, the accumulated charge typically of the order of 30 000 µAh.)

An elegant method to separate ^{68}Ge from Ga target material, and its Ga radionuclides, has been developed. The ^{68}Ge is carried over, by means of volatilization, to a scrubber system containing 1.0 M NaOH and 2 % Na_2SO_3. The scrubber solution is acidified with HF before loading the resultant solution onto a 10 mL column containing AG MP-1 anion exchange resin. The column is rinsed with dilute HF to remove any remaining impurities, such that a radiochemically pure product is obtained. The 10 % (maximum) ^{68}Ge contained in the catcher, also radiochemically pure, can also be used, even though the solution is in concentrated HCl, by adding NH_3 and evaporating to dryness. This method of production has been adopted by Radionuclide Production at iThemba LABS.

7.6 References

1. Marinsky J., 1961. The Radiochemistry of Germanium. National Academy of Sciences – National Research Council.
2. Firestone R. B. and Eckström L. P., 2004. WWW Table of Radioactive Isotopes, Version 2.1. URL: <http://ie.lbl.gov/toi>.
3. Iwata Y., Kawamoto M., Yoshizawa Y., 1983. *Int. J. Appl. Radiat. Isot.*, **31**, 1537.
4. Hughes E., 1980. *Mat. Eng.*, **2**, 34.
5. Lambrecht R. M., Sajjad M., 1988. *Radiochim. Acta*, **43**, 171.
6. Lambrecht R. M., 1984. *Radiochim. Acta*, **34**, 9.
7. Hnatowich D. J., 1977. *Int. J. Appl. Radiat. Isot.*, **28**, 169.
8. Hnatowich D. J., Kulprathipana S., Evans G., Elmaleh D., 1979. *Int. J. Appl. Radiat. Isot.*, **30**, 335.
9. Yvert J. P., Maziere B., Verhas M., Comar D., 1979. *Eur. J. Nucl. Med.*, **4**, 95.
10. Loc'h C., Maziere B., Comar D., 1980. *J. Radioanal. Chem.*, **21**, 171.
11. Loc'h C., Maziere B., Comar D., Knipper R., 1982. *Int. J. Appl. Radiat. Isot.*, **33**, 267.
12. Qaim S. M., 1987. *Radiochim. Acta*, **41**, 111.
13. Naidoo C., van der Walt T. N., Raubenheimer H. G., 2002. *J. Radioanal. Nucl. Chem.*, **53** (2), 221.
14. Pao P. J., Silvester D. J., Waters S. L., 1981. *J. Radioanal. Chem.*, **64**, 267.

15. Barong B., Yinsong W., 1992. *Nucl. Sci. Tech.*, **3**(3), 202.
16. Borong B., Song M., 1996. *J. Radioanal. Nucl. Chem.*, **213**, 233.
17. Cheng W. L., Jao Y., Lee C. S., Lo A. R., 2000. *J. Radioanal. Nucl. Chem.*, **254**, 25.
18. Grant P. M., Miller D. A., Gilmore J. S., O'Brien H. A., 1982. *Int. J. Appl. Radiat. Isot.*, **33**, 415.
19. Van der Walt T. N., Vermeulen C., 2004. *Nucl. Meth. Phys. Research*, **A 521**, 171.
20. Aardeneh K., van der Walt T. N., 2006. *J. Radioanal. Nucl. Chem.*, **268**(1), 25.
21. Gleason G. I., 1960. *Int. J. Appl. Radiat. Isot.*, **8**, 90.
22. Mirzadeh S., Kahn M., Grant P. M., O'Brien H. A., 1981. *Radiochim. Acta*, **28**, 47.
23. Faβbender M., Nortier F. M., Phillips D. R., Hamilton V. T., Heaton R. C., Jamriska D. J., Kitten J. J., Pitt L. R., Salazar L. L., Valdez F. O., Peterson E. J., 2004. *Radiochim. Acta*, **92**, 237.
24. Arzumanov A. A., Alexandrenko V. V., Borissenko A., Ignatenko D. N., Koptev V. K., Lyssukhin S., Popov Y. S., Volkov B. A., 2004. *17th Int. Conf. on Cyclotrons and their Applications*, Tokyo, Japan.
25. Ehrhardt G. J., Welch M. J., 1978. *J. Nucl. Med.*, **19**, 925.
26. Egamediev S. Kh., Khujaev S., Muminov A. I., 2001. In *CP600, Cyclotrons and their Applications 2001* (F. Marti *Ed.*), Sixteenth International Conference.
27. Clement R., Sandmann H., 1955. *Z. Anal. Chem.*, **145**, 325.
28. Arino H., Skraba W. J., Kramer H. H., 1978. *Int. J. Appl. Radiat. Isot.*, **29**, 117.
29. Nelson F., Rush R. M., Kraus K. A., 1960. *JACS*, **82**, 339.
30. Takács S., Tárkányi F., Hermanne A., Paviotti de Corcuera R., 2003. *Nucl. Instrum. Meth. B*, **211**, 169.
31. Merck Index, 12th Ed, Whitehouse Station, NJ, 1996.

CHAPTER 8 THE PRODUCTION OF A ^{68}Ga GENERATOR

8.1 Introduction

Positron emitters occupy a special place in the world of radionuclides and nuclear medicine, in particular, as a result of the emission of two coincident annihilation photons in opposite directions when the positron decays, thereby, providing good quality images in Positron Emission Tomography (PET).

Specific targeting agents offer the potential for earlier diagnosis of disease if an increased amount of the targeting-detectable conjugate is localised to a greater extent in tissue to be imaged compared to background tissues. In practice, the detectable agent in background tissue needs to be minimised, while the detectable agent in the target tissue needs to be maximised. Radioactive medicines are preferred detectable agents. Superior imaging modality is offered with the use of PET, with a dramatic increase in sensitivity and, therefore, the ability to detect disease at an earlier stage.

PET radionuclides are generally labelled to an organic substance, such that the resultant radiopharmaceutical, when injected into the patient, is "organ specific" *i.e.* the radiopharmaceutical will accumulate (at a maximum) in the specified organ with minimum background from surrounding tissue.

These radionuclides are generally short-lived, an advantage from a patient dose point-of-view, but disadvantageous for clinical use in hospitals not equipped with the means necessary for their production. An exception to this is the PET radionuclide ^{68}Ga, a positron emitter with a half life of 68.3 minutes[1] produced by electron capture from ^{68}Ge ($T_{1/2}$ = 270.99 d)[2]. If the daughter, ^{68}Ga, can be separated rapidly from ^{68}Ge, one obtains a self-contained, short-lived positron source which can be used several times per day, as the ^{68}Ge/^{68}Ga secular equilibrium is reached within a few hours.

A generator is a self-contained system housing a parent/daughter radionuclide mixture in equilibrium, which is designed to yield the daughter separate from the parent. The principal utility of a generator is to produce certain radionuclides on site which, because of their short half-lives, cannot be shipped by commercial sources. For the generator to be useful, the parent radionuclide's half-life should be long in comparison to the travel time required to transport it to the recipient[3].

Ideally, the generator should have the following properties[3,4]:

- The chemical properties of the daughter must be different from those of the parent such that the daughter can be separated from the parent radionuclide.
- The daughter radionuclide should be short-lived and γ- or positron-emitting.
- The design should be simple and, reproducibly, give a high yield of the desired radionuclide with a very large separation factor from the parent radionuclide.
- The collection of the daughter nuclide should be possible with a small volume of reagent.
- The physical half-life of the parent radionuclide should be short enough so that daughter re-growth within the generator system after elution is rapid, but long enough for practicality.
- The parent radionuclide must be retained quantitively on the ion exchanger column during the whole period of usage of the generator, i.e. no breakthough should occur.
- The chemical form of the daughter radionuclide should be suitable for the preparation of a wide variety of labelled compounds, particularly for those in kit form.
- The system should contain a very long-lived or stable granddaughter, such that no radiation dose is conferred to the patient by the decay of subsequent generations.
- The generator should contain effective and, if possible, inexpensive shielding, such that the radiation dosage to users is minimised.

The high potential of a $^{68}Ge/^{68}Ga$ generator for PET applications has been enhanced as of late, with a great demand for the product from iThemba LABS. The use of

$^{68}Ge/^{68}Ga$ generators in nuclear medicine is attractive for a number of reasons, namely:

- The 271-day half-life of the parent, ^{68}Ge, allows the generator to be used over a long period, for up to one year.
- The PET radionuclide ^{68}Ga is continuously available, at a reasonable cost, from a $^{68}Ge/^{68}Ga$ generator, also at centres without a cyclotron.
- The 68-minute half-life of ^{68}Ga matches the pharmacokinetics of many peptides and other small molecules due to rapid diffusion, localisation at the target and fast blood clearance.

The first $^{68}Ge/^{68}Ga$ generator was produced in 1960 and the process involved solvent extraction[5]. Further methods of extracting Ge using solvent were developed[6-9], while distillation of Ge, in various ways, also manifested[10-13]. Commercial generators today, however, are of the column chromatographic type and a number of different sorbents to bind ^{68}Ge and release its daughter upon elution have been released to date.

Generators containing an alumina column, with a claimed yield of 70 %, have been developed[14-16], but the ^{68}Ga daughter is eluted in complex form, which must be destroyed before being incorporated into the required radiopharmaceutical. Attempts were made to elute the alumina column with HCl[17], as well as NaOH[18], without success. There were attempts to further development of $^{68}Ge/^{68}Ga$ generators by using the hydroxides of zirconium, tin and titanium as adsorbents[19], while using HCl, HNO_3 and acetic acid as eluents. A yield of 35 % ^{68}Ga was obtained, with a breakthrough of Ge of 0.03 % and this was deemed inappropriate for clinical use. A system was developed with the use of polyantimonic acid[20], eluting the product with oxalate solution, but this, too, was regarded as inappropriate as the loss of ^{68}Ge was too high and the eluent was regarded as toxic and, therefore, had to be chemically manipulated before it could be used for clinical purposes.

Further tests were performed using the oxides of titanium, zirconium and silicon[21]. Interestingly, the use of titanium dioxide was deemed inappropriate for use in a generator, but a great deal of further development has seen this compound being patented for use in a $^{68}Ge/^{68}Ga$ generator by GE Healthcare[22], using dilute HCl as

eluent. Following comparison tests performed with the radionuclide, using various adsorbents as generator material[23,24], it was determined that the generator using tin oxide as adsorbent would be the most appropriate[25]. While further developments have been performed in the attempt to obtain a more effective generator, such as the use of alpha ferrous oxide[26] and the polymer pyrogallol-formaldehyde[27,28] as matrix, the tin dioxide commercial generator is still the most prominent[29].

A ^{68}Ge/^{68}Ga generator has been produced using anion exchange resin[30,31] while, more recently, a generator has been produced using cation exchange chromatography[32]. Ion exchange columns have also been used to concentrate the ^{68}Ga eluent obtained from a generator[33-38].

While dilute HCl has been in use as the most popular eluent of ^{68}Ge/^{68}Ga generators, a proposal was put forward to elute ^{68}Ga using 0.1 M HF from AG1-X8 anion exchange resin[30]. The breakthrough of ^{68}Ge was determined at <0.001 %, with a ^{68}Ga yield of >95 %. While it was later determined that radiation damage to the resin could result in breakthrough, as well as discolouration, as the generator got older, it was still decided to attempt to produce a generator using AG MP-1 macroporous anion exchange resin, as this is more resistant to radiation damage than the microporous gel-type anion exchange resins, using dilute concentrations of HF such that the ^{68}Ga eluted from the generator can be effectively, and directly, used for the labelling of peptides.

8.2 Experimental

Analytical grade reagents were used throughout this work and were obtained from Merck (SA) Pty. Ltd or Sigma Aldrich GmbH, which included Fluka and Riedel de Haen products. The AG MP-1 anion exchange resin used in this work was obtained from BioRad Laboratories, Richmond, U.S.A., while the ^{68}Ge was obtained, in 0.1 M HCl, from Los Alamos Laboratories, New Mexico, U.S.A. De-ionised water from a Millipore MilliQ Reagent Grade Water System, to a conductivity of greater than 10 megaohm cm^{-1}, was used for all experimental and production work.

All radioactive determinations were performed using a standard calibrated HPGe detector, with a relative efficiency of 13 % (relative to three inch NaI), connected to a multichannel analyser. As ^{68}Ge produces no gamma peaks, activity determinations were performed by measuring its daughter, ^{68}Ga, after 8 to 10 hours when equilibrium had been reached.

For each experiment, a column containing 1.0 mL AG MP-1 macroporous anion exchange resin was prepared and equilibrated by the passage of 50 mL 5.0 M HF, followed by 50 mL 0.1 M HF.

Experiment 1

200 μL of ^{68}Ge activity (in 0.1 M HCl) was mixed with 4.3 mL of water and 0.5 mL concentrated HF. The activity was measured before it was loaded on to the resin column. The load waste was collected in 1 mL fractions and each fraction measured.

The "load" vial was rinsed with 5x 1 mL 0.1 M HF and each fraction was pumped through the column, collected and measured. Each measurement was repeated hourly for three hours.

Experiment 2

The same method was applied in this experiment as with Experiment 1, but 5 mL 0.05 M HF was used to rinse the resin column.

Experiment 3

The same method was put to use as the previous experiments, the only difference being that 5x 1 mL 0.01 M HF was used to rinse the resin column.

Experiment 4

While the same method was applied to load the ^{68}Ge activity on to the resin column as that of the previous experiments, 5x 1 mL 0.005 M HF was used to rinse the AG MP-1 column.

Experiment 5

The same method was used to load the resin column as previously, but 5 mL 0.1 M acetic acid, in 1 mL fractions, was used to rinse the resin column.

8.3 Results and discussion

The ^{68}Ge activity was successfully loaded on to the AG MP-1 macroporous anion exchange resin, with the load waste indicating that all of the activity was quantitively retained by the resin.

^{68}Ga was successfully eluted using the various concentrations of dilute HF, with yields ranging between 95 and 98 % being obtained. The yields were generally obtained within 5 mL of eluate (see Fig. 8.1), thereby, improving on the quantity of eluent required for tin oxide matrices[22,34]. No breakthrough of ^{68}Ge was initially detected, although it was hoped that breakthrough would be kept to a minimum with the more dilute concentrations of HF, such that the pH of the solution would not adversely affect any ^{68}Ga-labelling processes.

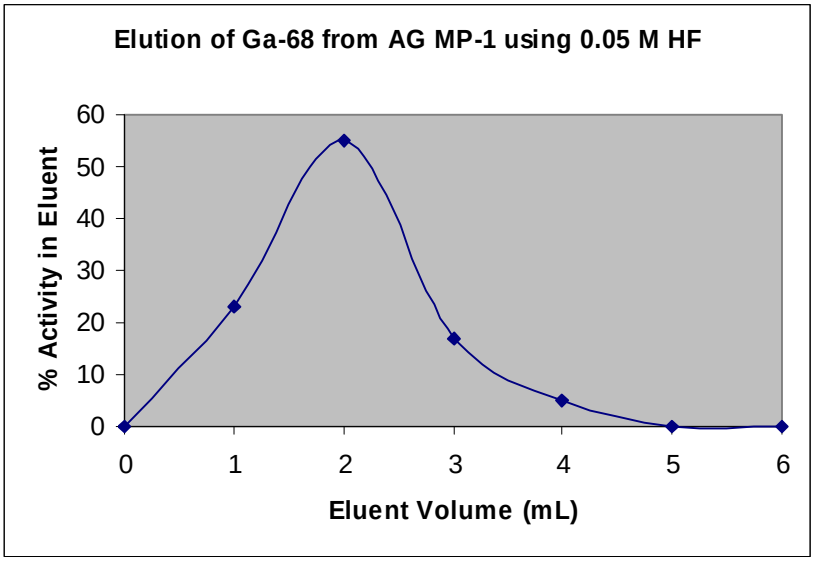

Fig. 8.1: Elution curve of ^{68}Ga from 1 mL AG MP-1 column

The use of acetic acid as eluent of ^{68}Ga was immediately rejected, as there was massive breakthrough of ^{68}Ge, thereby, disqualifying the use of this method.

Breakthrough of ^{68}Ge was determined at least 24 hours after elution, using the closest distance possible at which the Ge detector was calibrated. This was determined to be negligible for HF concentrations 0.1, 0.05 and 0.01 M, with percentages in the order of 1x 10^{-4} %, although 0.005 M HF indicated that there may be slightly more ^{68}Ge breakthrough than with the more concentrated solutions, with a 7x 10^{-4} % breakthrough.

From the results obtained, it was decided to load a generator with about 1110 MBq (30 mCi) ^{68}Ge, eluting the ^{68}Ga continuously with 0.01 M HF. The activity was prepared by mixing with water and HF, as previously, and loaded on to a 1.0 mL column containing AG MP-1 anion exchange resin (in the fluoride form, equilibrated with 0.01 M HF). The column was eluted twice a day, 6 hours apart, with 5 mL 0.01 M HF in 1 mL fractions. The fractions were measured continuously to observe any ^{68}Ge breakthrough. After a period of two and a half months, the generator was still behaving well, with no visible sign of breakthrough of ^{68}Ge or resin discolouration.

A generator was built in the hope that it could be used commercially. The kit was supplied by NTP Radioisotopes (Pty) Ltd and features a converted commercial ^{99}Mo/^{99m}Tc generator (Fig. 8.2, 8.3 and 8.4) by replacing the alumina column with an AG MP-1 resin column. This generator has been loaded in-house with ^{68}Ge and is still under evaluation at the time of writing.

The generator has been designed such that the user can elute the generator with ease, with a tray placed above the generator such that sterile vials (under vacuum) can be placed upon it (Fig. 8.2). A plastic “sump” is situated just under the tray which contains the dilute HF for elution. Filters have been placed in position such that any air allowed into the system when eluting is filtered and cleaned.

Fig. 8.2: The $^{68}Ge/^{68}Ga$ generator

Fig. 8.3: The aerial view of the generator showing a tray carrying sterile vials.

The needle protruding through the centre of the tray originates from the generator itself (Fig. 8.3) and the rubber bung of the vial can be impaled on the needle for elution purposes. Needless to say, the generator (i.e. the AG MP-1 resin column) is shielded with lead and there are tubes protruding from the shielding such that the elution solution from the "sump" can access the resin column.

Fig. 8.4: The tray cover removed to show the shielded generator with protruding needle.

Interestingly, no company in Europe has a marketing authorization for a ^{68}Ge/^{68}Ga generator, which is a strict requirement as stated by the European Parliament and European Council[39]. The granting of a marketing authorization is dependent on the fact that it is manufactured under the conditions of good manufacturing practice (GMP), as the eluate of the generator is considered to be an active substance used as a starting material for a radiopharmaceutical product for human use.

Apart from the need of a ^{68}Ge/^{68}Ga generator that is of "medicinal" quality, the use of ^{68}Ga-labelled radiopharmaceuticals is dependant on many conditions, rules and laws, but a manufacturer may obtain a marketing authorization for one or more labelling

kits for the preparation of ^{68}Ga-labelled radiopharmaceuticals and to make these kits commercially available. It has been determined that it would take a minimum of 5 years from the present date for an approved ^{68}Ga-radiopharmaceutical or labelling kit to become commercially available.

8.4 Conclusion

A ^{68}Ge/^{68}Ga generator has been constructed using AG MP-1 macroporous anion exchange resin as adsorbent. The breakthough, or preferable lack thereof, is regarded as acceptable and an average of 95 % yield ^{68}Ga was obtained. While these results indicate an improvement over many generators commercially available, further bench testing is required to determine whether this type of generator will be able to withstand higher activities of ^{68}Ge/^{68}Ga over a period of one year.

8.5 References

1. Firestone R. B. and Eckström L. P., 2004. WWW Table of Radioactive Isotopes, Version 2.1. URL: <http://ie.lbl.gov/toi>.
2. Schönfeld E., Schötzig U., Günther E., Schrader H., 1994. *Appl. Radiat. Isot.*, **45** (9), 955.
3. Karesh S., 1996. URL: <http://lunis.luc.edu/nucmed/tutorial/radpharm/sect-d1.htm>.
4. Neirinckx R. D., Davis M. A., 1979. *J. Nucl. Med.*, **20**, 1075.
5. Gleason G. I., 1960. *Int. J. Appl. Radiat. Isot.*, **8**, 90.
6. Senise P., Sant' Agostino L., 1956. *Mikrochim. Acta*, 1445.
7. Brink G. O., Kafalas P., Sharp P. A., 1957. *J. Am. Chem. Soc.*, **79**, 1303.
8. Senise P., Sant' Agostino L., 1959. *Mikrochim. Acta*, 572.
9. Erhardt G. J., Welch M. J., 1978. *J. Nucl. Med.*, **19**, 925.
10. Coase S. A., 1934. *Analyst*, **59**, 747.
11. Bartelmus G., Hecht F., 1954. *Mikrochim. Acta*, 148.
12. Rayner H. B., 1963. *Anal. Chem.*, **35**, 1097.

13. Mirzadeh S., Khan M., Grant P. M., 1978. In: *Abstracts of the Second International Congress of the World Federation of Nuclear Medicine and Biology*. Washington D.C. 82.
14. Greene M. W., Tucker W. D., 1961. *Int. J. Appl. Radiat. Isot.*, **12**, 62.
15. Yano J., Anger H. O., 1964. *J. Nucl. Med.*, **5**, 484.
16. Hnatowich D. J., 1975. *J. Nucl. Med.*, **16**, 764.
17. Kopecky P., Mudrova B., 1974. *Int. J. Appl. Radiat. Isot.*, **25**, 263.
18. Lewis R. E., Camin L. L., 1981. *J. Label Compd. Radiopharm.*, **18**, 164.
19. Malyshev K. V., Smirnovv, 1975. *Radiokhimiya*, **17**, 137.
20. Arino H., Skraba W. J., Kramer H. H., 1978. *Int. J. Appl. Radiat. Isot.*, **29**, 117.
21. Neirinckx R. D., Davis M. A., 1979. *J. Nucl. Med.*, **20**, 1075.
22. United States Patent 20070031329: Method of obtaining gallium-68 and use thereof and device for carrying out said method. URL: <www.freepatentsonline.com/20070031329.html>
23. Hanrahan T., Yano Y., Welch M. J., 1982. *J. Label Compd. Radiopharm.*, **19**, 1535.
24. McElvany K. D., Hopkins K. T., Welch M. J., 1984. *Int. J. Appl. Radiat. Isot.*, **35**, 521.
25. Loc'h C., Mazièré, Comar D., 1980. *J. Nucl. Med.*, **21**, 171.
26. Ambe S., 1988. *Appl. Radiat. Isot.*, **39**, 49.
27. Schuhmacher J., Maier-Borst W., 1981. *Int. J. Appl. Radiat. Isot.*, **32**, 31.
28. Neirinckx R. D., Layne W. W., Sawan S. P., Davis M. A., 1982. *Appl. Radiat. Isot.*, **33**, 259.
29. Aardeneh K., van der Walt T. N., 2006. *J. Radioanal. Nucl. Chem.*, **268** (1), 25.
30. Neirinckx R. D., Davis M. A., 1979. *J. Nucl. Med.*, **20** (6), 681.
31. Neirinckx R. D., Davis M. A., 1980. *J. Nucl. Med.*, **21**, 81.
32. Zhernosekov K. P., Filosofov D. V., Baum R. P., Aschoff P., Bihl H., Razbash A. A., Jahn M., Jennewein M., Rösch F., 2007. *J. Nucl. Med.*, **48** (10), 1741.
33. Hofmann M., Maecke H., Börner A. R., Weckesser E., Schöffski P., Oei M. L., Schumacher J., Henze M., Heppeler A., Meyer G. J., Knapp W. H., 2001. *Eur. J. Nucl. Med.*, **28**, 1751.

34. Meyer G.-J., Hofmann M., Schumacher J., Harms T., Knapp W. H., 2003. *J. Label Compd. Radiopharm.*, **46**, S272.

35. Nakayama M., Haratake M., Ono M., Koiso T., Harada K., Nakayama H., Yahara S., Ohmomo Y., Arano Y., 2003. *Appl. Radiat. Isot.*, **58**, 9.

36. Meyer G.-J., Mäcke H., Schuhmacher J., Knapp W. H., Hofmann M., 2004. *Eur. J. Nucl. Med. Mol. Imaging*, **31**, 1097.

37. Velikyan I., Beyer G. J., Långström B., 2004. *Bioconjugate Chemistry*, **15**, 554.

38. Velikyan I., 2005. Ph. D. Thesis, University of Uppsala, Sweden.

39. Breeman W. A. P., Verbruggen A. M., 2007. *Eur. J. Nucl. Med. Mol. Imaging*, **34**, 978.

CHAPTER 9 THE SEPARATION OF ^{227}Pa FROM A Th TARGET BY MEANS OF ION EXCHANGE CHROMATOGRAPHY

9.1 Introduction

Cluster radioactivity is the phenomenon where a radioactive nucleus decays spontaneously by the emission of composite particles heavier than α particles. This mode of radioactive decay, also called exotic radioactive decay, was first discovered in 1984 by Rose and Jones[1] when they observed the spontaneous emission of ^{14}C clusters from ^{223}Ra decay. It is an astonishing fact of history that this remarkable discovery was made almost a century after radioactivity was first discovered and studied by Henri Becquerel and the Curies. Cluster radioactivity is now a well-established phenomenon from both experimental and theoretical perspectives[2] with close to two dozen cases having been reported, the observed clusters ranging from ^{14}C to ^{32}Si. One of the most important achievements in this field has been the discovery of the sensitivity of the partial half-life to the microscopic properties of the parent-daughter nuclei. In particular, physicists can investigate this sensitivity by studying the emissions from odd-*A* nuclei. This will be discussed in more detail later.

^{223}Ac is regarded as a special case in this type of investigation, as it allows the study of the effect of the odd particle wave function in both the residual nucleus and in the cluster itself. Sources of the radioisotope ^{223}Ac, therefore, were required for the purpose of studying its possible exotic radioactive decay via ^{14}C and ^{15}N emission. This radioisotope has a rather short half-life of only 2.2 minutes, however, its precursor, ^{227}Pa, has a substantially longer half-life of 38.3 minutes. It was, therefore, experimentally more appropriate to produce sources of ^{227}Pa, which would continuously feed ^{223}Ac (in secular equilibrium with its precursor) by means of α-decay. A collaboration to investigate this possibility was formed by researchers from The University of Milan, Italy, the Joint Institute of Nuclear Research (JINR), Dubna, Russia, the Kurchatov Institute, Moscow, Russia and iThemba LABS.

To produce ^{223}Ac for these experiments, a number of Th targets were bombarded with 66 MeV protons delivered by the separated sector cyclotron of iThemba LABS, utilizing the reaction ^{232}Th(p, 6n)^{227}Pa → α + ^{223}Ac (see Fig. 9.1). Due to the relatively short half-life of ^{227}Pa, the chemical separation required to isolate ^{227}Pa from the Th target material had to be completed within approximately 70 minutes from the end of bombardment (EOB), *i.e.* within two half-lives of the precursor radioisotope.

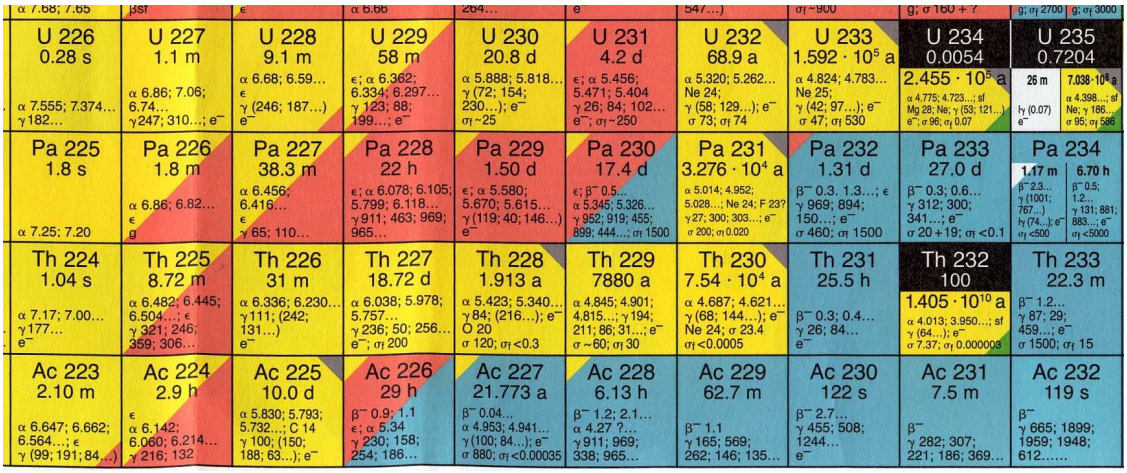

Fig 9.1: Relevant part of the "Karlsruher Nuklidkarte" of 2006. Note the stable target nucleus ^{232}Th (100% natural abundance), the product nucleus ^{227}Pa which is formed via a (p,6n) reaction, and ^{223}Ac which is obtained by a subsequent α-decay. Some of the nuclear data used in this work may differ slightly from the information given in this chart of the nuclides.

The experimental investigation was designed to have two distinct stages. The first stage, or *radiochemistry stage*, involved the bombardment of Th targets, separation of the Pa from the target material and producing small-area ^{227}Pa sources. During the second stage, or *nuclear physics stage*, two arrays of solid-state nuclear track detectors[2] were exposed to the emissions from these sources, followed by the commencement of the search for ^{14}C and ^{15}N tracks. While the radiochemistry is more the topic of this chapter and will be discussed in detail, some aspects of the nuclear physics will also be discussed briefly.

While Pa has been separated from various compounds and other elements using solvent extraction[3,4], acid and alkali leaches[5], fractional distillation[6], co-precipitation

with a variety of compounds[5,7-11] and precipitation[7], these methods are not regarded as practical when working with high activities in a hot-cell environment, where ion exchange methods are preferred for speed, ease of use and safety reasons. Experiments have been performed using anion exchange resins to determine how well Pa and Th are sorbed to the resin in question. These include Dowex-1[12,13], AG1-X10[14], AG MP-1[5,15] and Dowex 1 X10[16].

Previous research has indicated that no adsorption of Pa(V) on cation exchange resin is observed[16]. Pa(V) can be strongly absorbed by anion exchange resins using concentrated hydrochloric acid solutions[14] (with a sharp reduction in adsorption as the concentration is decreased[17]), but was found to be poorly absorbed from HCl-HF mixtures at high HCl concentrations[12] in comparison. When using a constant HF concentration (0.5 M), adsorption increased with an increase in HCl concentration, with moderately good adsorption at 10 M HCl, after which adsorption reached a plateau[18]. When Solache-Rios[5] performed experiments to separate Pa from other elements using AG MP-1 resin, it was discovered that 35 % of the total Pa was lost when traces of fluoride were on the resin. Systematic studies of the behaviour of Pa in anion exchangers using mixed solutions with hydrofluoric, hydrochloric and nitric acids, as well as thiocyanate, have shown that the use of more than one complexing agent may often promote effective separation from other selected elements[19-23].

Pa(V) tends to hydrolyse or precipitate in fairly concentrated acid solution, but HCl-HF solutions were found to be suitable media for reversing this effect. Various radiochemical and ion exchange techniques have been performed using various Pa radioisotopes[24-26].

Adsorption of Th(IV) from HCl solutions is negligible[14,22,26-28]. While thorium fluoride is rather insoluble, no difficulties were found in measurements at trace Th concentrations in media containing 1 M HF and 0.1 M to 11 M HCl. Under these conditions adsorption of Th was negligible[5].

Methods exist in the literature for the separation of Pa from irradiated thorium nitrate[28], but many of the procedures mentioned are time consuming and, unless care

is taken, they frequently result in losses due to the hydrolytic condensation of Pa(V) from aqueous acidic media other than those containing fluoride or sulphate[7].

9.2 Nuclear Data

An ^{223}Ac nucleus possibly has two exotic decay modes, namely, $^{223}\text{Ac}\rightarrow{}^{14}\text{C} + {}^{209}\text{Bi}$ (Q = 33.08 MeV) and $^{223}\text{Ac}\rightarrow{}^{15}\text{N} + {}^{208}\text{Pb}$ (Q = 39.49 MeV). Neither of these has been experimentally observed prior to this study. It is important to note that the residual nucleus ^{208}Pb is doubly magic while ^{209}Bi is singly magic, thus, they may constitute very stable cores within the original mother nuclei. Several theoretical predictions exist for the branching ratios of the respective cluster emissions; $B(^{14}\text{C}) = \lambda(^{14}\text{C})/\lambda(\alpha)$ and $B(^{15}\text{N}) = \lambda(^{15}\text{N})/\lambda(\alpha)$, where it is customary to express this quantity relative to the dominant α-decay ($\lambda(x)$ refers to the partial decay constant for the emission of a cluster of type x).

Firstly, Poenaru *et al.* produced their Superasymmetric Fission theoretical model[29], predicting $B(^{14}\text{C}) = 2.5 \times 10^{-11}$ and $B(^{15}\text{N}) = 1.0 \times 10^{-12}$ for ^{223}Ac radioactive decay. According to this prediction, ^{15}N emission is expected to be 25 times less abundant than ^{14}C emission. The prediction includes the tremendously small probabilities for the decay by heavy-cluster emission compared to that for α-decay (11 to 12 orders of magnitude lower). Blendowske *et al.*, on the other hand, treated all cluster emissions similar to the original Gamow theory of α-decay, namely, as a two-body decay process where large amplitude motions of a fragment inside the nucleus causes it to tunnel through the Coulomb barrier, whose height is always much higher than the available kinetic energy. They produced two theoretical predictions: a favoured version and an unfavoured version[30]. The favoured model predicted $B(^{14}\text{C}) = 3.8 \times 10^{-11}$ and $B(^{15}\text{N}) = 2.2 \times 10^{-12}$, while the corresponding values according to the unfavoured model are $B(^{14}\text{C}) = 2.5 \times 10^{-12}$ and $B(^{15}\text{N}) = 9.4 \times 10^{-14}$, respectively.

The data compilation of Firestone and Eckström[31] describes the radioactive decay of ^{223}Ac as α-decay (99 %) and electron capture (1 %), while for ^{227}Pa decay the corresponding values are α-decay (85 %) and electron capture (15 %), respectively, thus, 85 % of ^{227}Pa decays will produce ^{223}Ac nuclei.

The only excitation function data found in the literature for proton-induced reactions on ^{232}Th, in the energy region of interest, were measured by Suk *et al.*[32] A polynomial curve was fitted through the listed EXFOR ^{227}Pa point data (subentry B0037002) using the TABLECURVE software (see Fig. 9.2). The excitation function rises rapidly from a threshold near 37 MeV to a maximum of ~ 42 mb at about 48 MeV, whereafter it again falls significantly. It is clear that the 66 MeV proton beam for the routine radionuclide production is ideally suited to exploit this reaction. From the curve of Fig. 9.2, the thick-target production rate curve of ^{227}Pa induced in a metallic Th target was derived (see Fig. 9.3). An energy window of 62 → 40 MeV could easily be accommodated within the standard target holder for radionuclide production in the horizontal bombardment station, using Al as encapsulation to isolate the Th target material from the cooling water. Such a target would contain approximately 8 g of Th metal, pressed as a disc with a diameter of 15 mm. The technology to produce such targets already existed at iThemba LABS, making it an ideal laboratory for this study.

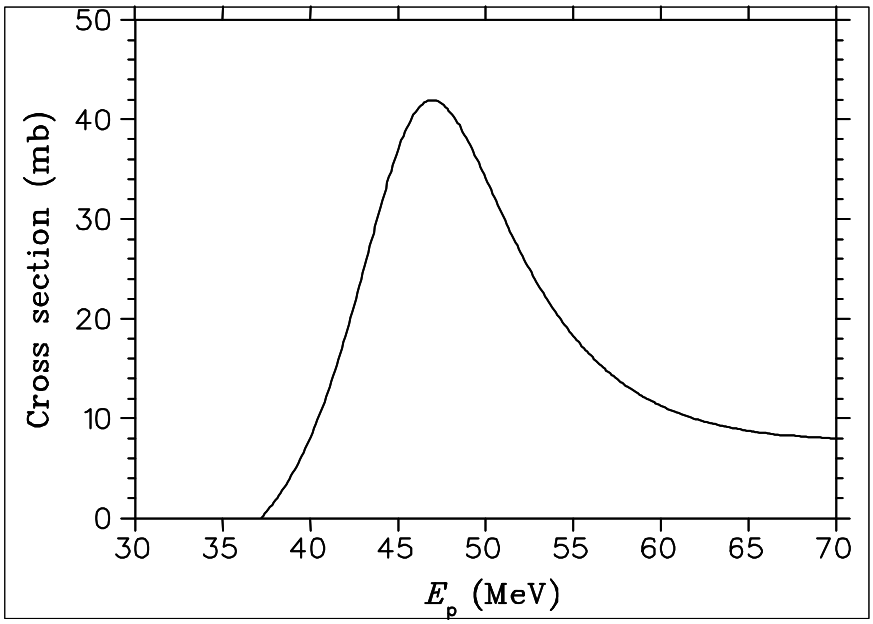

Fig. 9.2: Excitation function for the production of ^{227}Pa in the bombardment of ^{232}Th with protons. The curve was produced by fitting a polynomial function through the measured point data of Suk *et al.*[32]

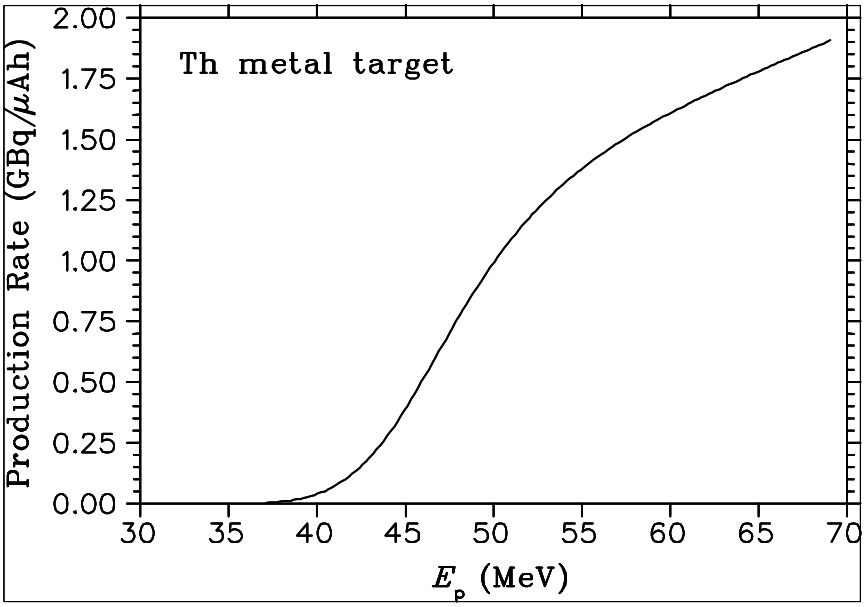

Fig. 9.3: Production rate curve of ^{227}Pa formed in the bombardment of ^{232}Th with protons.

From Suk's ^{232}Th(p, 6n) experimental cross section data, a production rate of 1.65 GBq/µAh was predicted for the energy window selected. With a two hour irradiation time at a beam intensity of 80 µA, the predicted ^{227}Pa yield is 107.5 GBq (2.9 Ci) at EOB, taking decay during bombardment into account. This ^{227}Pa activity corresponds to 3.56 x 10^{14} atoms at EOB. If one assumes that the entire chemical separation and source making can be performed in 70 minutes (*i.e.* under two half lives of ^{227}Pa), about 1 x 10^{14} ^{227}Pa atoms will be available for the nuclear physics experiment (assuming, of course, negligible radiochemical losses).

As already mentioned, only 85 % of these atoms will decay to ^{223}Ac. If one further assumes that only one hemisphere of space (*i.e.* a solid angle of 2π sr) will be used in the experiment and that the detection efficiency will be ~ 80 %, one can finally estimate the number of expected cluster events, using the branching ratios discussed above. In the case of the Blendowske model, $N(^{14}C) = 79 \rightarrow 1215$ and $N(^{15}N) = 2 \rightarrow 69$, depending on whether the transition is favoured or unfavoured. These numbers are rather small, demanding a high radiochemical yield and a fast radiochemical separation for the success of the experiment.

9.3 Chemical Separation Experiments

A summary of the basic method implemented is as follows: An 8.0 g quantity of Th metal was placed into a reaction vessel and 100 mL concentrated HCl added to it and stirred. To this was added ^{230}Pa tracer. The solution was heated to 60 ºC and 2.0 M HF added drop-wise, at 5 minute intervals, until all of the grey thorium had gone into solution.

The solution was cooled, before it was loaded onto a 2 mL column containing AG MP-1 macroporous anion exchange resin, equilibrated by the passage of 50 mL 7.0 M HCl. Any remaining impurities were removed by rinsing the column with 50 mL 7.0 M HCl, before the ^{230}Pa tracer was eluted from the resin column with 10 mL 0.1 M HCl, taking 1 mL fractions. Each fraction, including the load and rinse wastes, was measured quantitatively using standard off-line γ-ray spectrometry.

The experiment was repeated several times, with various eluting agents tried out during each repetition. 10 mL 0.1 M HNO_3, 0.1 M HF and 0.1 M acetic acid were used as eluting agents, respectively.

9.4 Results and Discussion

With the information gleaned from the literature and the required time constraint in the production of ^{227}Pa from Th targets taken into account, one also had to consider possible losses of the final product. Thorium oxide was found to take too long to dissolve in acid media, while thorium metal was not much better when using concentrated (32 %) HCl, unless 2.0 M HF was added drop-wise to the heated reaction solution[33]. The disadvantage was that there was still a small amount of residue once dissolution was complete (approximately 10 %), probably due to thorium fluoride being formed.

Initial experimental runs were performed using ^{230}Pa as tracer, because of its convenient half-life (17.4 days) and γ-emissions, and Th dissolved in concentrated

HCl media containing a few drops of 2.0 M HF. Experiments performed using Amberchrom CG71c ion exchange resin were soon discarded once it was discovered that, while the Th was not retained by the resin, the Pa tracer was also found in the load solution. Trials performed using the macroporous anion exchange resin AG MP-1, proved to be more successful and the remaining runs were concentrated using this as the resin of choice.

It was determined that the Th target to be pressed would be 8.0 g in mass and experiments performed took this fact into account. Once the method was refined, it took 100 mL concentrated HCl and 27 drops of 2.0 M HF to dissolve the target material (which would later be found to be detrimental) and 50 mL 7.0 M HCl to elute Th and other impurities from the resin column.

To allow for the creation of a small-area dry source from the final product, it was vital to elute the ^{227}Pa using as small a volume of eluate as possible. The eluate ultimately chosen was 0.1 M acetic acid, as only 3 mL would be required to remove Pa in its entirety from the resin column. Once the elution curve was plotted (see Fig. 9.4), it was noted that the first 1 mL of the eluate contained virtually no activity and that the majority of the activity was contained in the remaining 2 mL.

The initial production run was successful, but when a second production run was performed, approximately 50 % of the Pa activity was lost, even though the bombardment conditions were the same. Initial problem-solving attempts pointed to the concentration of the hydrochloric acid not being high enough, but the fact that too much HF was added to the dissolution process probably also played a significant role, thereby, confirming Solache-Rios's results[4].

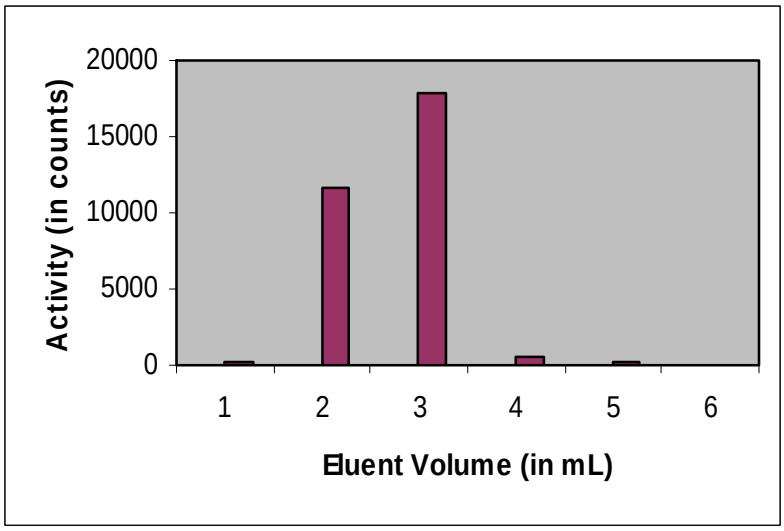

Fig. 9.4: Elution of ^{227}Pa from AG MP-1 resin using 0.1 M acetic acid.

The effect of fluoride was investigated further, using 37 % HCl instead and decreasing the number of drops of 2 M HF added to the solution to 15. This proved to be more effective and the final production run was performed without significant losses (less than 8 %) of Pa activity.

The 8.0 g Th target was bombarded, using the 66 MeV proton beam provided by the SSC of iThemba LABS, for two hours at a beam current of 80 μA. Once it was removed from the beam, it was placed in a reaction vessel containing a heated mixture of 100 mL 37 % HCl and 15 drops 2.0 M HF. The reaction took place vigorously while the solution was being stirred, although a slight residue remained after complete dissolution of the target material. The reaction solution was left to cool slightly for two minutes before passing the solution through a column containing 2 mL AG MP-1 macroporous anion exchange resin, on which the ^{227}Pa was quantitively retained by the resin.

Th impurities from the target material were eluted using 50 mL 9.0 M HCl, before ^{227}Pa was eluted using 3 mL 0.1 M acetic acid, of which the first 1 mL was discarded. The final product was removed and was placed, 1 mL at a time, on to a small, round source plate (25 mm in diameter) manufactured from Cu and plated with Au. The plate was put under a lamp in a fume booth, where the solution was allowed to evaporate (see Figure 9.5).

The time elapsed from the EOB to the drying of the source was 71 minutes, which was deemed adequate for these particular experimental purposes. By acquiring both α-particle and γ-ray spectra, it was determined that only Pa and its daughters were present in the final product, thereby achieving radiochemically pure sources. The nominal source strength obtained was 81 GBq (~ 2.2 Ci) of ^{227}Pa at the start of the exposure of the detectors. This is about 75 % of the expected source strength based on the predictions performed using the excitation data of Suk *et al.*

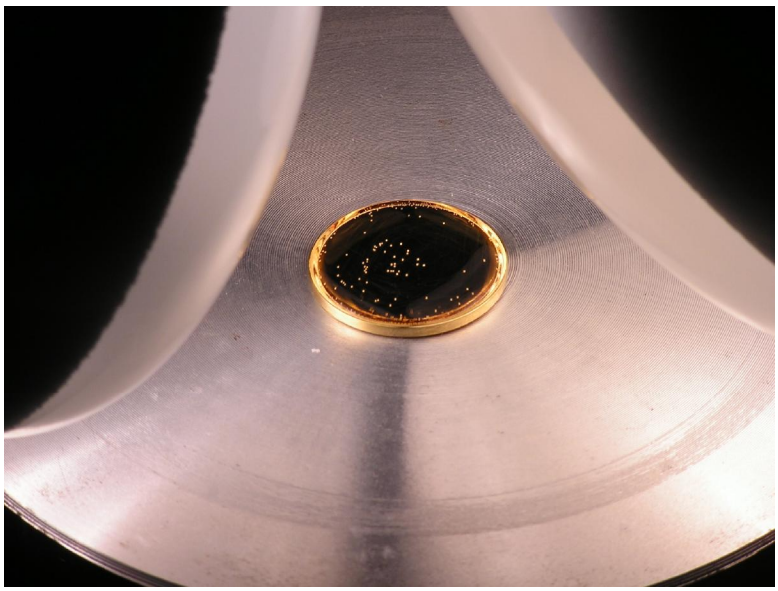

Fig. 9.5: Cu small-area source plate, coated with Au, under evaporator.

While the product was radiochemically pure and one was confident that there was no Th in the final product, a thin yellow layer formed on the gold-plated source plate during drying, which caused some energy degradation of the emitted clusters. Fortunately, this layer was too thin to stop any clusters, therefore their detection and identification were not compromised. It was later determined to be Fe (probably in the form of $FeCl_3.3H_2O$), with which our physicist colleagues could cope, even though it did make the data analysis more complicated. Although it would have been ideal to remove the Fe from the final product, it could only have been done using sulphuric acid and within a time frame of a few hours[25], which would not have been suitable for this particular experiment.

9.5 The Physics Experiment

The technique most widely used in cluster radioactivity experiments is one which uses passive, solid state nuclear track detectors (SSNTD) to comply with the unusual efficiency and selectivity requirements necessary to detect clusters with an abundance many orders of magnitude lower than that of the dominant α-particle emissions. Use is made of certain plastic or glass plates which are able to register the passage of an ionizing particle in the form of a damage track only when the particle ionizing rate is higher than a given threshold, characteristic of the detector material. An appropriate choice of the threshold and, therefore, of the detector material can largely eliminate the effect of low-ionizing α-particles and favour the heavier clusters under investigation.

Immediately after preparation of a ^{227}Pa source, it was placed in the centre of a 23.5 cm diameter hemisphere (hollow dome), whose inner surface was covered with phosphate BP-1 glass track detectors, for a period of two hours such that the glass track detectors could be exposed to the radioactive decay emissions from the source. For this purpose, the detectors and source were placed inside a vacuum chamber (see Fig. 9.6), specially designed and built for the experiment, and pumped down to a fore vacuum of about 10^{-3} mbar. A standard Si surface barrier detector could also be mounted in the chamber to measure accurate energy spectra of the emitted α particles, using a standard 4K-channel analyzer (MCA) system. The details of that analysis, however, fall outside the scope of this thesis.

After the exposure of the BP-1 glass track detectors, they were carefully packed and shipped to the University of Milan for further analysis. They were subsequently etched in a 50 % HBF_4 solution at a temperature of 65 °C for about 2 days in order to enlarge the tracks made by the heavy ionizing clusters and make them visible under an optical microscope. The etching process enlarges the damaged track regions on the detector (glass) from the Å to μm scale as a result of the competition established between the etching velocity in the non-irradiated part of the material and the etching velocity in the irradiated part, giving rise to conical tracks which appear as black spots in the bright light of the microscope.

Fig. 9.6: The vacuum chamber assembly used to expose the solid state nuclear track detectors (SSNTD) to the radioactive emissions from a ^{227}Pa source (LEFT). Also shown is the multi-channel analyzer system used to acquire the α-particle spectra (RIGHT).

The entire surface of the irradiated track detectors (about 730 cm^2) was scanned at 200 x magnification with an automated image analyzer system, which allowed for a faster search for "good" ion tracks. The entire search still took almost a year to complete. The good tracks were investigated further and their geometric parameters determined. A comparison with calibration curves obtained by irradiating similar samples of BP-1 glasses with ions of known mass, charge and energy, delivered by a Tandem accelerator, finally allowed the unique identification of most of the track events found.

At the time of writing, a still preliminary but well advanced analysis yielded 350 ^{14}C events and zero ^{15}N events. In the case of ^{14}C emission, a branching ratio of $B(^{14}C) = 3.2 \times 10^{-11}$ can be inferred with an uncertainty of about 30 %. Since no ^{15}N tracks were found, only an upper limit on the branching ratio can be inferred at this stage: $B(15N) \leq 2.2 \times 10^{-13}$, with a confidence level of 90 %.

9.6 Conclusion

The objective, namely to obtain radiochemically pure ^{227}Pa from a Th target in as short a period possible, was achieved. Under severe radiological conditions, the target was removed from the bombardment station, moved to the selected hot cell for processing, the separation process completed, the final product removed and dried on a small-area source plate using an infra red lamp, before being placed in a vacuum chamber containing the solid-state nuclear track detectors, in less than two half-lives of ^{227}Pa. The quality of the tracks obtained from these very strong small-area sources was deemed to be adequate for determining ^{14}C and ^{15}N events uniquely. The analysis of the tracks to date resulted in 350 ^{14}C events and no ^{15}N events, making it possible to determine the ^{14}C branching ratio quite well and to determine an upper limit for ^{15}N emission, with a 90 % confidence limit.

It is clear that the ^{14}C emission from the odd-*A* ^{223}Ac isotope cannot be much unfavoured as it rather resembles emissions from even-even nuclei, therefore the decay can be interpreted as a ground-state to ground-state favoured one. In the case of ^{15}N emission, the non-observance of any events is compatible with an unfavoured transition: here the unpaired odd nucleon goes from the heavy nucleus ^{223}Ac to the much lighter cluster ^{15}N, the ground state configurations of which are very different, thus this transition is largely hindered.

The results of the radiochemical investigation were presented at the 15th Radiochemical Conference at Mariánské Lázně, Czech Republic, and subsequently published in the Czech Journal of Physics in 2006[34]. Preliminary results of the nuclear physics investigation were presented at the "Cluster 07" International Conference[35]: a paper of which was submitted for publication in the Conference Proceedings.

9.7 References

1. Rose H. J., Jones G. J., 1984, Nature **307**, 245.

2. Bonetti R., Guglielmetti A., 1999. In: *Heavy Elements and Related New Phenomena* (Greiner W. and Gupta R.K., Ed.), Vol II. World Scientific, Singapore.
3. Kandil A. T., Ramadan A., 1978. *Radiochim. Acta*, **25**, 107.
4. Andrews J. E., Baisden P. A., 1986. *J. Radioanal. Nucl. Chem., Lett.*, **108**, 77.
5. Solache-Rios M., 1992. *J. Radioanal. Nucl. Chem*, **165**, 159.
6. Solache-Rios M., 1988. *J. Radioanal. Nucl. Chem*, **125**, 221.
7. Brown D., Whittaker B., 1978. *Journal of the Less Common Metals*, **61**, 161.
8. Katz J. J., Seaborg G. T., 1957. The Chemistry of the Actinide Elements. Methuen, London.
9. Haissinsky M., Bouissières G., 1958. In: *Nouveau Traité de Chimie Minérale* (Pascal P., Ed.), Masson, Paris.
10. Brown D., Maddock A. G., 1963. *Q. Rev. Chem. Soc.*, **17**, 289.
11. Brown D., Maddock A. G., 1967. *Prog. Nucl. Energy*, **8**, 1.
12. Kraus K. A., Moore G. E., 1951. *J. Am. Chem Soc.*, **73**, 2900.
13. Kraus K. A., Moore G. E., 1950. *J. Am. Chem Soc.*, **72**, 4293.
14. Kraus K. A., Moore G. E., 1955. *J. Am. Chem Soc.*, **77**, 1383.
15. Monroy-Guzman F., Trubert D., Le Naour C., 2002. *J. Radioanal. Nucl. Chem.*, **254**, 431.
16. Chetham-Strode A. Jr., Keller O. L. Jr., 1966. Physico-Chimie du Protactinium. Centre National de la Recherche Scientifique, Paris. p 189.
17. Kraus K. A., Nelson F., 1956. In: *Proceedings of the International Conferences on the Peaceful Uses of Atomic Energy P/837*, Vol VII, United Nations. p 113.
18. Nelson F., Rush R. M., Kraus K. A., 1960. *J. Am. Chem. Soc.*, **82**, 339.
19. Wish L., 1959. *Anal. Chem.*, **31**, 326.
20. Caletka R., Hausbeck R., Krivan V., 1989. *J. Radioanal. Nucl. Chem.*, **131**, 353.
21. Caletka R., Hausbeck R., Krivan V., 1990. *J. Radioanal. Nucl. Chem.*, **142**, 383.
22. Kim L., Lagally H., Born H. J., 1973. *Anal. Chim. Acta*, **64**, 29.
23. Caletka R., Hausbeck R., Krivan V., 1990. *Anal. Chim. Acta*, **229**, 127.
24. Trubert D., Monroy-Guzman F., Le Naour C., Brillard L., Hussonnois M., Constantinescu O., 1998. *Anal. Chim. Acta*, **34**, 149.

25. Monroy-Guzman F., Trubert D., Brillard L., Kim J. B. Hussonnois M., Constantinescu O., 1996. *J. Radioanal. Nucl. Chem.*, **208**, 461.
26. Kraus K. A., Moore G. E., Nelson F., 1956. *J. Am. Chem. Soc.*, **78**, 2692.
27. Kluge E., Lieser K. H., 1980. *Radiochim. Acta*, **27**, 165.
28. Goble A. G., Maddock A. G., 1958. *J. Inorg. Nucl. Chem.*, **7**, 94.
29. Poenaru D. N., Ivascu M. A., 1989. In: *Particle Emission from Nuclei* (Ed: Poenaru D. N., Ivascu M. A.), Vol. II. Chemical Rubber Company, Boca Raton, Florida, U.S.A.
30. Blendowske R., Walliser H., 1988. *Phys. Rev. Lett.*, **61**, 1930.
31. Firestone R. B., Eckström, L. P., WWW Table of Radioactive Isotopes, Version 2.1. URL:<http://ie.lbl.gov/toi>.
32. Suk H. C., Crawford J. E., Moore R. B., 1974. *Nucl. Phys.*, **A218**, 418; EXFOR subentry B0037002.
33. Greenwood N. N., Earnshaw A., 1997. Chemistry of the Elements. Butterworth-Heinemann, Oxford. p 1264.
34. Van der Meulen N. P., Steyn G. F., van der Walt T. N., Shishkin S. V., Vermeulen C., Tretyakova S. P., Guglielmetti A., Bonetti R., Ogloblin A. A., McGee D., 2006. *Czech. J. Phys.*, **56**, D357.
35. Guglielmetti A., Faccio D., Bonetti R., Shishkin S. V., Tretyakova S. P., Dmitriev S. V., Ogloblin A. A., Pik-Pichak G. A., van der Meulen N. P., Steyn G. F., van der Walt T. N., Vermeulen C., McGee, 2008. Proceedings of the 9th International Cluster Conference (Stratford-Upon-Avon, U. K.), *In Press*.

CHAPTER 10 THE PRODUCTION OF ^{88}Y IN THE PROTON BOMBARDMENT OF ^{nat}Sr

10.1 Introduction

^{88}Y ($T_{1/2}$ = 106.6 d), which can be produced by means of a cyclotron, is not currently being mass produced and is, at times, sought after for calibration sources and other experimental purposes. There appears to be a renewed interest in the product, as potential customers increasingly request iThemba LABS's Radionuclide Production Group to supply it on a regular basis. With protons, it can be produced via the reaction ^{88}Sr(p, n)^{88}Y (see Fig. 10.1). Its mode of decay is predominantly by means of electron capture and the decay emissions include the strong γ-rays of 898.0 keV (93.7 %) and 1836.1 keV (99.2 %), respectively[1]. Initially, ^{88}Y was only produced in no-carrier-added form via the spallation process at the Los Alamos National Laboratory, but has since been produced with the use of small-sized cyclotrons[2]. It is formed in proton-induced reactions, using ^{nat}Sr as target material, only via the ^{88}Sr(p, n)^{88}Y reaction[2], although ^{87}Rb(^{3}He, 2n)^{88}Y and ^{85}Rb(^{4}He, n)^{88}Y routes have also been reported[3,4].

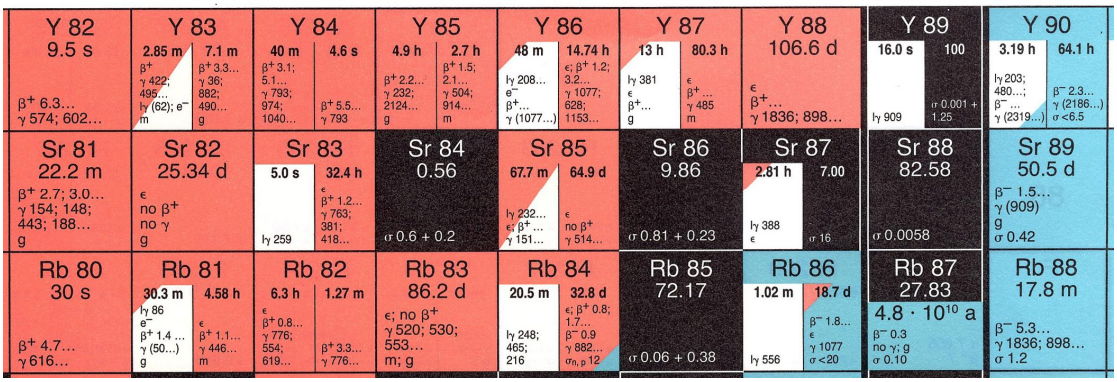

Fig. 10.1: Relevant part of the "Karlsruher Nuklidkarte" of 2006 for the production of ^{88}Y.

The separation of Y from Sr has been described in the literature by using two preferred methods, namely, by means of ion exchange chromatography[2,5-9] or by liquid extraction[10]. Electrochemical separation of their radioisotopes has also been described to obtain a product of high radiochemical and radionuclidic purity[11,12]. ^{88}Y

has also been obtained as a product from $^{88}Zr/^{88}Y$ generators[13], separating ^{88}Zr from bombarded niobium capsules.

^{88}Y is used as small point sources in the calibration of instruments, as well as in the determination of mixtures containing Sr radionuclides[14], the accurate determination of yttrium in superconductive oxide ceramics[10,15] and as a substitute for ^{90}Y (a β-emitter radionuclide used for therapy) to quantify the biodistribution of Y-pharmaceuticals in animals[16-19]. It is used effectively as tracer for the chemical yield determination of ^{90}Y [20].

A production method recently used at iThemba LABS to separate ^{88}Y from $SrCl_2$ target material has been reported[8]. Briefly, the target was dissolved in 0.01 M HNO_3, after which it was loaded onto a column containing Chelex 100 chelating resin (in H^+ form) at a pump speed of 1 mL/min. The remaining Sr was first eluted from the column using 0.01 M HNO_3 and the ^{88}Y then eluted using 1 M HNO_3. The product was evaporated to dryness and dissolved in 0.1 M HCl.

While the method described above initially showed promise, it was found that using Chelex 100 as a resin to separate the elements was a temperamental process, as some of the strontium target material would not always be washed from the resin effectively and, as a result, be eluted with the ^{88}Y and found as an impurity in the final product. Adjusting the pump speed of the production also did not solve the problem and the results were erratic at best. A more effective separation method for production purposes was necessary.

Another problematic issue in the development of this production was the choice of target material. The obvious (and initial) choice was $SrCl_2$, as it pressed a smooth, compact pellet for bombardment. Initially, the target material, encapsulated in aluminium such that it would not dissolve in the cooling water of the bombardment station, had a tendency to burst when placed in a 66 MeV proton beam, provided by the Separated Sector Cyclotron at iThemba LABS, after a period of time. This work briefly describes how this problem was dealt with.

10.2 Nuclear Data

10.2.1 Experimental Methods and Data Analysis

The excitation function for the production of ^{88}Y via the (p,n) reaction on ^{88}Sr has been reported by several authors. Recently, Kettern *et al.*[2] published new data up to 25 MeV and compared their results with the relevant older (and rather incomplete for this energy region) data[21,22] measured in the fifties and sixties, as well as with a later data set by Levkovskii[23].

At iThemba LABS, trial productions were started using encapsulated $SrCl_2$ and SrF_2 targets. These targets were bombarded behind a Mg target (for ^{22}Na production), thus, they served as the low-energy companion in a tandem target configuration. The yields obtained turned out to be inconsistent and often significantly lower than expectations. Turning to the available nuclear data, it was found that the discrepancies between the relevant data sets were also rather large, almost a factor of 2 between the data of Kettern and Levkovskii. It was, therefore, decided to re-measure the ^{88}Sr(p,n)^{88}Y excitation function up to an energy of nominally 20 MeV.

Similar to the situation described in Chapter 5 for the excitation function measurement of ^{28}Mg, it was, once again, found difficult to prepare thin samples of a compound containing Sr. Sr reacts rapidly with oxygen in the atmosphere in metallic form, while the compounds of Sr available are brittle. As a result, it proved to be difficult to exploit the conventional stacked-foil technique. Although methods exist for preparing thin samples of brittle substances on metallic backing foils, such methods also have their disadvantages. In the case of the well-known sedimentation method[24], for example, the measured data are often plagued by very large scatter, probably due to deterioration of the targets during the course of those experiments. It was, therefore, decided to measure the thick-target production rate curve first, using thick targets, and to deduce the excitation function by means of a differentiation method described in section 5.2.1.

A schematic diagram of the experimental setup, used to measure the thick-target production rate curve for $SrCl_2$ + p, is shown in Fig. 5.2. A brass target holder contained an aluminium degrader, a Cu monitor foil and a $SrCl_2$ target for each of a series of bombardments. All the targets had similar thicknesses of nominally 800 mg/cm^2 and were thick enough to stop the beam. They were prepared by powder compaction of fully anhydrous $SrCl_2$ salt (99.9 %, Alfa Aesar) in a punch-and-die set with a hydraulic press. Activations were performed using degraders of various thicknesses to cover the energy region from threshold up to ~17.5 MeV, the maximum energy which could be obtained from the ATOMKI cyclotron in Debrecen, Hungary. The monitor foils were high purity Cu (99.99 %, Goodfellow, U.K.) with a thickness of 25 µm, for the accurate determination of the incident proton flux. The $^{nat}Cu(p,x)^{65}Zn$ monitor reaction[25] with IAEA recommended cross sections were used for this purpose. The targets were irradiated inside the cyclotron vacuum at an average beam current of 50 nA, each bombardment lasting about 30 minutes.

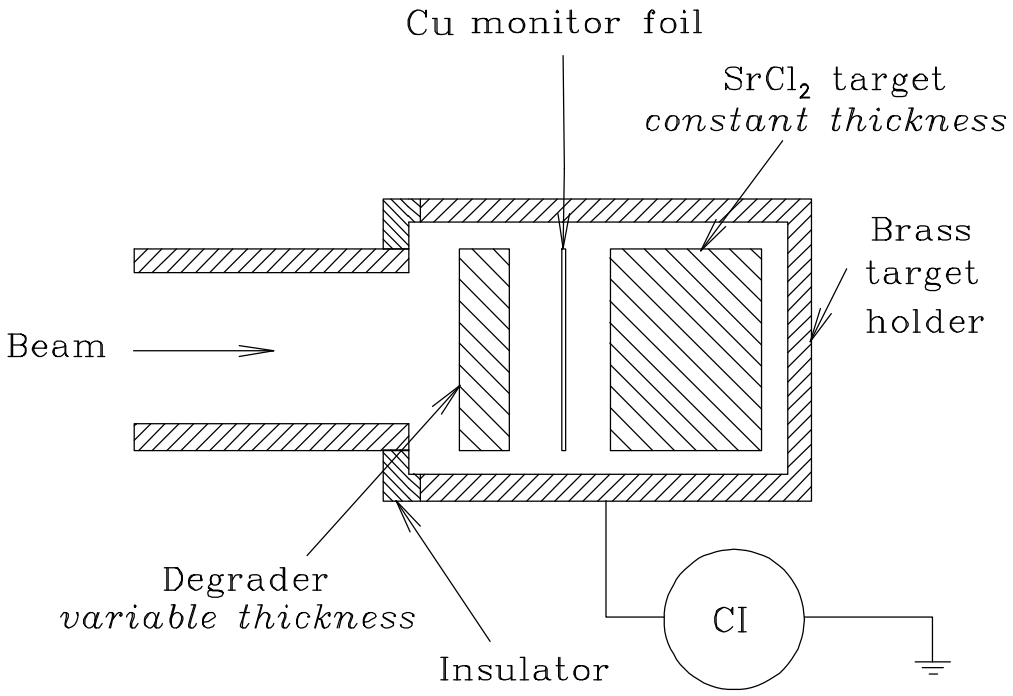

Fig. 10.2: Experimental setup used to activate $SrCl_2$ targets and Cu monitor foils for purposes of measuring the ^{88}Y thick-target production rate curve. Degraders of various thicknesses could be accommodated to adjust the energy, while the targets of constant thickness could stop the beam. CI indicates current integrator.

After bombardment, each $SrCl_2$ target was dissolved in 3 mL of water in a standard serum vial. Once filled and sealed, these vials constituted appropriate counting

sources. The reason why liquid sources were prepared in this way instead of counting the activated $SrCl_2$ discs directly, was because they were considered to be too thick to constitute *bona fide* point sources. Also, the depth of penetration of the beam into these discs differed, depending on the degraded energy. The liquid sources ensured a consistent counting geometry, as well as allowing calibration sources of the same geometry to be easily prepared.

The ^{88}Y activities were determined by off-line γ-ray spectrometry using the 898.0 keV (93.7 %) and 1836.1 keV (99.2 %) γ-lines. The statistical uncertainties were insignificant compared to the systematic uncertainty, except near the reaction threshold, the latter of which was estimated to be about 7 %: beam current integration (4 %), detector efficiency (5 %), counting geometry (1 %) and decay corrections (2 %). The ^{65}Zn cross sections extracted from the Cu monitor foils were also found to be in excellent agreement with the IAEA recommended values, thus, the directly measured current integrator values were independently confirmed.

10.2.2 Results and Discussion

The measured ^{88}Y thick-target production rate curve for $SrCl_2$ + p is shown in Fig. 10.2. The reaction threshold is near 4 MeV and the production rate for the full energy region, *i.e.* from threshold up to the maximum measured energy of 17 MeV, is about 1.6 MBq/μAh. A standard polynomial function was fitted through the measured data using the code TableCurve[26] (the extrapolation beyond 17 MeV will be discussed later).

The polynomial of Fig. 10.3 could be differentiated analytically, allowing the derivation of the excitation function for ^{88}Sr + p, shown in Fig. 10.4. The data of Kettern *et al.*[2] and Levkovskii[23] are also shown. Interestingly, the data of this work are lower than those of Levkovskii but higher than those of Kettern, falling just about half-way between those two data sets. The maximum of the excitation function is at about 12.5 MeV, thus the energy region 4 – 20 MeV is ideal for the routine production of ^{88}Y. The deduced cross-section values of this work as well as production rates for several candidate target materials are presented in Appendix A1.

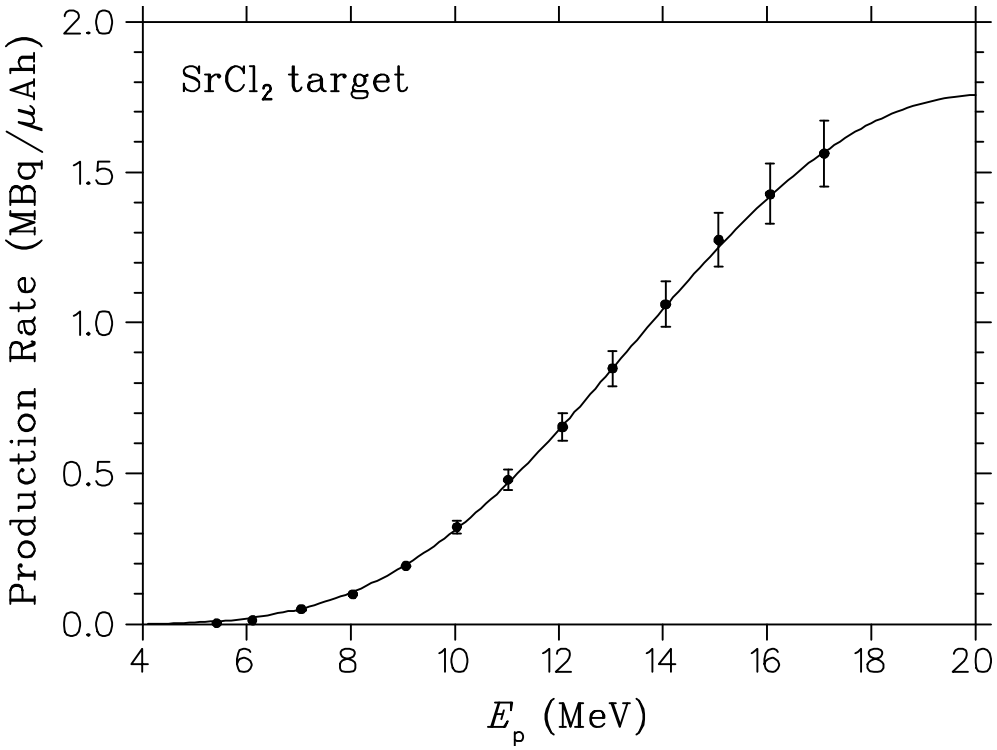

Fig. 10.3: Thick-target production rate curve of ^{88}Y produced in the proton bombardment of $SrCl_2$. The solid symbols are the measured values of this work while the solid curve is a polynomial fit. Error bars are shown when they exceed the symbol size.

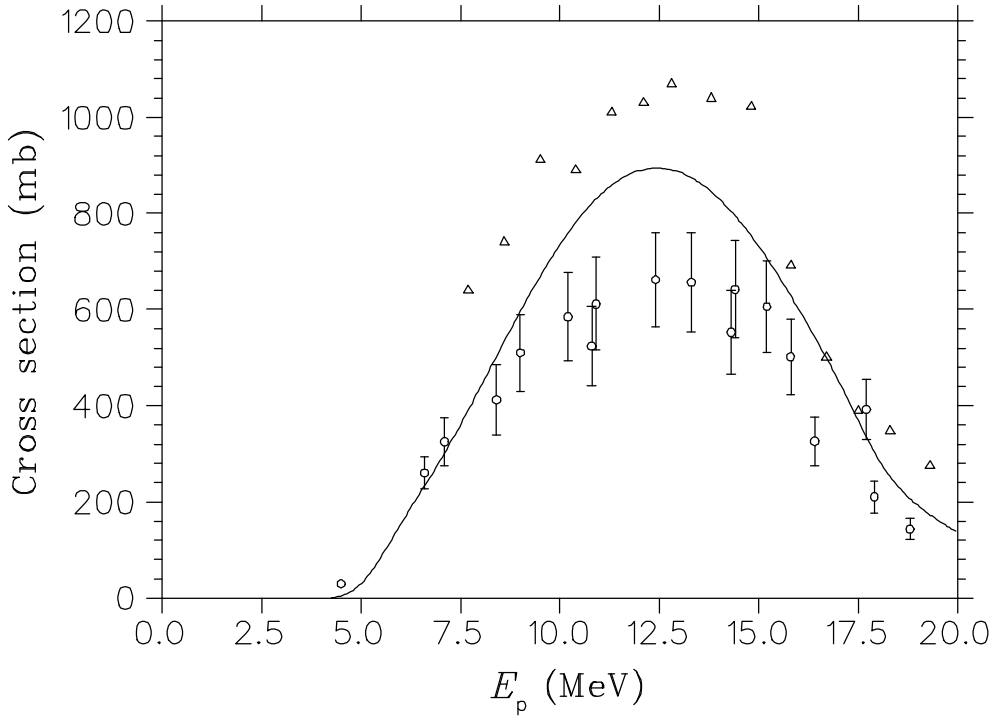

Fig. 10.4: Excitation function of ^{88}Y formed in the reaction of protons with ^{88}Sr. The solid curve was derived from the measured thick-target production rate data of this study (see Fig. 10.3). The open triangles are the data of Levkovskii[23] and the open circles the data of Kettern[2] *et al.*

Theoretical calculations were performed with the code ALICE-IPPE[27] in order to compare with the existing data and, if found to give a reasonable reproduction, to extrapolate the measured curves up to 20 MeV. ALICE-IPPE is a computer implementation of the Geometry Dependent Hybrid (GDH) model, widely used for predicting excitation functions in nucleon-induced nuclear reactions (and also sometimes for reactions induced by heavier projectiles). A standard input prescription was used, the details of which have been summarized elsewhere[28]. The results are shown in Fig. 10.5.

Also shown in Fig. 10.5 is a rescaling of the measured cross-section values of Levkovskii according to a recommended prescription by Takács *et al.*[29]. These authors have accurately re-measured the monitor excitation function used by Levkovskii, namely, that of the ^{nat}Mo(p,x)^{96mg}Tc reaction, by irradiating stacks containing ^{nat}Mo foils inside an electron-suppressed Faraday cage. The entire ^{96mg}Tc excitation function of Levkovskii was found to be about 20 % too high. The renormalized values of Levkovskii are in good agreement with the values of this work. The overall agreement with the ALICE-IPPE prediction is also acceptable, although the shape is somewhat skewed towards a maximum at an energy about 1.5 MeV higher.

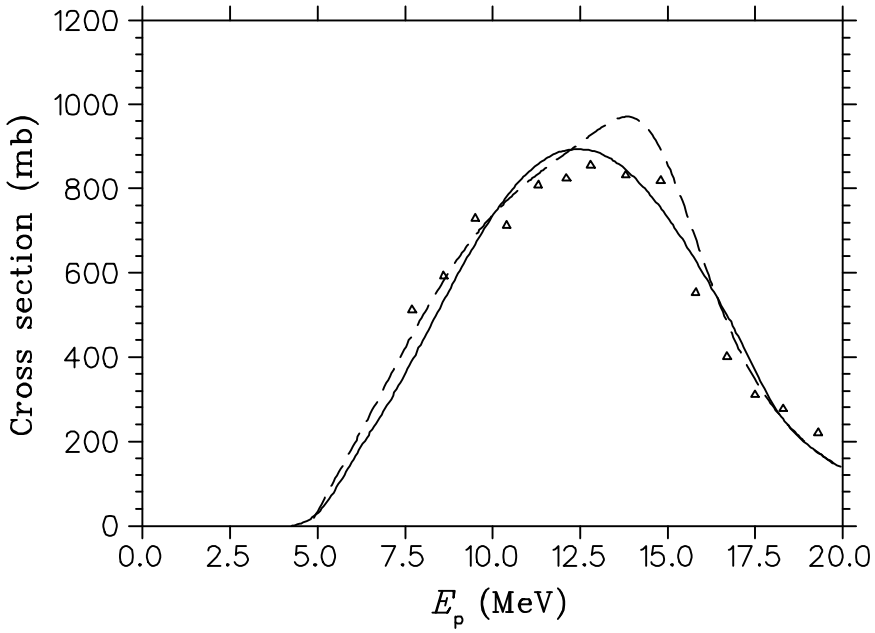

Fig. 10.5: Excitation function of ^{88}Y formed in the reaction of protons with ^{88}Sr. The solid curve was derived from the measured thick-target production rate data of this study (see Figs. 10.3 and 10.4). The open triangles are the re-scaled values of Levkovskii[23] (see text) while the broken curve is a theoretical prediction by means of the computer code ALICE-IPPE[26].

10.3 Radiochemical Investigation

10.3.1 Chemical Separation Methods

Analytical grade reagents were used throughout this work and were obtained from Merck (SA) Pty. Ltd or Sigma Aldrich GmbH, which included Sigma, Aldrich, Fluka and Riedel de Haen products. The AG 50W-X4 cation exchange resin used in this work was obtained from BioRad Laboratories, Richmond, U.S.A. De-ionised water from a Millipore MilliQ Reagent Grade Water System, to a conductivity of greater than 10 megaohm cm^{-1}, was used for all experimental and production work.

Experiment 1

8.0 g $SrCl_2$ was weighed out and dissolved in 20 mL 1.0 M HNO_3, to which ^{85}Sr and ^{88}Y tracer was added. This solution was loaded onto a column, containing 10 mL of AG 50W-X4 cation exchange resin. The Sr was then eluted from the column, using 30 mL 1.0 M HNO_3, with the aim of removing any excess Sr, before the ^{88}Y was finally eluted with 50 mL 4.0 M HNO_3.

Experiment 2

In a parallel investigation, approximately 0.1 g irradiated SrB_6 was dissolved in 10 mL 5.0 M HNO_3 and evaporated to dryness. The activity was then dissolved together with 5.0 g $SrCl_2$ and taken up in 20 mL 1.0 M HNO_3, before being passed through a column containing 10 mL AG 50W-X4 cation exchange resin. The beaker containing the activity was rinsed twice with 10 mL 1.0 M HNO_3 and passed through the column. The ^{85}Sr and ^{7}Be were then eluted from the column with 50 mL 1.0 M HNO_3, and finally eluted with 25 mL 1.7 M HNO_3, before the ^{88}Y was finally removed using 2x 25 mL 3.0 M HNO_3.

Experiment 3

A 10 mL column containing AG MP-1 macroporous anion exchange resin was prepared and treated with 50 mL 25 % NH_3 and the column then rinsed with 100 mL water.

8.0 g of $SrCl_2$ was weighed out and dissolved in 200 mL water. ^{85}Sr and ^{88}Y tracers were added in 10 mL of a solution containing 50 mg ammonium carbonate. The [^{88}Y]yttrium carbonate and a small quantity of strontium carbonate, precipitated by the excess ammonium carbonate, were allowed to settle for an hour. The solution, containing $SrCl_2$ (*ca.* 90 % of the original amount), was gently decanted such that the precipitate was left behind. The precipitate was stirred in 200 mL water and set aside so that the precipitate could settle again. The solution was decanted, the precipitate dissolved in 2 mL 2.0 M HCl and the solution evaporated to dryness. The salts were dissolved in 200 mL water and the resultant solution pumped through the resin column. The beaker was rinsed several times with water, the rinsings passed through the column and the remaining $SrCl_2$ eluted with more water, amounting to *ca.* 100 mL in total. The final product (^{88}Y) was eluted from the resin column with 2x 25 mL 6.0 M HCl.

Experiment 4

The resin to be used in this case, Amberchrom CG161m, was saturated with tributyl phosphate and stirred overnight, before packing a 2.0 mL column with it. Once the column was packed, it was equilibrated by the passage of 30 mL 69 % HNO_3.

5.0 g of $SrCl_2$ was weighed out (to which ^{85}Sr and ^{88}Y tracer was added) and dissolved in 10 mL 69 % HNO_3. This solution was pumped through the column containing the treated Amberchrom CG161m resin and the elements were washed on to the column with a further 20 mL 69 % HNO_3. The Sr was eluted using 50 mL 69 % HNO_3, while the ^{88}Y final product was eluted with 25 mL 0.1 M HCl.

Experiment 5

5.0 g of $SrCl_2$ was dissolved in 50 mL 0.005 M acetic acid (to which ^{85}Sr and ^{88}Y tracer was added). This was loaded on to a column containing 10 mL Purolite S930 chelating resin, equilibrated with 0.005 M acetic acid. The Sr was eluted from the resin using 50 mL 0.005 M acetic acid, followed by 50 mL 0.001 M acetic acid, before the ^{88}Y final product was eluted from the resin using 50 mL 2.0 M HCl.

Experiment 6

A 5 mL column, containing Amberchrom CG71cd, was prepared and treated with 20 mL 25 % NH_3, after which the NH_3 was rinsed from the column using 20 mL water.

An 8 g $SrCl_2$ target, removed from its encapsulated anodized aluminium capsule, was dissolved in 100 mL water and loaded onto the column. The column was rinsed twice using 50 mL of water, to remove any traces of Sr impurities, before the final product (^{88}Y) was eluted from the column using 3x 25 mL 6.0 M HCl.

10.3.2 Results and Discussion

AG50W-X4 resin

The initial experiment (Experiment 1), using ^{85}Sr and ^{88}Y as tracer, produced promising results. Although no ^{85}Sr tracer was eluted with the initial load step, approximately 40 % of the tracer was eluted with the first 30 mL rinse of 1.0 M HNO_3, while all but 1 % of the tracer was removed with the second rinse of the column with 30 mL 1.0 M HNO_3. There was no break-through of ^{88}Y and all of this was eluted from the column when using the 4.0 M HNO_3. The remaining 1 % of the ^{85}Sr tracer, however, was found in the final product.

Attempts at separating Sr from Y using cation exchange resins with higher crosslinkages, such as AG50W-X8 or the macroporous AG MP-50, were not successful. Experiments using AG50W-X8 resin produced “tailing” when eluting the final product, while in the case of AG MP-50 the Sr could not be eluted effectively, resulting in a final product with a great deal of impurity, as well as a mere 65 % yield.

The experiment with the small quantity of SrB_6 (Experiment 2) produced better results, as there was a complete separation of Y from Sr. None of the Sr was eluted with the initial load solution, although 40 % was eluted in the 20 mL rinse step. The remainder of the ^{85}Sr was eluted with the 50 mL 1.0 M HNO_3, but about 29 % of the ^{88}Y tracer was removed from the resin column with the 25 mL 1.7 M HNO_3. The remainder of the tracer was obtained in the final rinse step (50 mL 3.0 M HNO_3).

Owing to the results obtained above, the method was slightly adjusted. Without changing the initial load and rinse steps, 2x 40 mL 1.2 M HNO_3 was used to remove the excess ^{85}Sr. The ^{88}Y was eluted using 50 mL 4.0 M HNO_3.

There was a difference when using the irradiated SrB_6 instead of other target materials, in that the irradiation also produced ^{7}Be, from the boron in the target material. This impurity did not play a significant role in the separation, however, as it was eluted along with the Sr in the 20 mL 1.0 M HNO_3 and the 50 mL 1.0 M HNO_3 elution steps, respectively.

The adjusted procedure used for the subsequent experiment produced excellent results. The results are listed as "Experiment 2a" in Table 10.1 below. All of the impurities were removed with the respective elution steps, while the ^{88}Y yield was 99.1 %. When the experiment was repeated (listed as "Experiment 2b"), the results with regard to the product yield were similar, although the percentage impurities (^{7}Be and ^{85}Sr) removed differed from the previous experiment. They were all effectively removed from the resin column, however.

A full production simulation with 3.9 g SrB_6 was carried out, using a hot cell containing a hot cell panel specifically designed for this purpose. The results obtained (listed in Table 10.1 as "Production 1") were similar to that of Experiment 2, although there was a slight breakthrough of the final product in the final elution step of ^{85}Sr, producing an ^{88}Y yield of 92.97 %.

A second experiment was performed under hot cell conditions, with the same method as previously described applied. The results obtained are listed in Table 10.1 as "Production 2". Once again, there was a slight breakthrough of ^{88}Y in the final ^{85}Sr elution step, although the yield of the final product improved to 96.86 %.

When a production was performed (using $SrCl_2$ as target material), it was decided to decrease the rinse step from 80 mL 1.2 M HNO_3 to 70 mL 1.2 M HNO_3, keeping the rest of the method the same. The results are listed as "Production 3" in Table 10.1. This time, there was no breakthrough of ^{88}Y in the Sr rinse steps and the product yield increased to 97.68 %. The eluate was evaporated to dryness and the product collected

in 5 mL 0.1 M HCl. The product was sent away for evaluation by a client and deemed to be fit for purchasing.

Table 10.1: Percentage impurity removal and percentage product yield using AG 50W-X4 resin.

	Experiment 2a	Experiment 2b	Production 1	Production 2	Production 3
% ^{85}Sr removal in load step	0	0	0	0	0
% ^{7}Be removal in load step	9.42	24.75	11.25	12.22	N/A
% ^{85}Sr removal in intial rinse step	39.46	0	0	0	57.08
% ^{7}Be removal in initial rinse step	85.47	55.76	52.84	53.17	N/A
% ^{85}Sr removal in elution steps	54.54	100	100	100	42.92
% ^{7}Be removal in elution steps	5.11	19.49	35.91	34.61	N/A
% ^{88}Y yield	99.10	100	92.97	96.86	97.68

From the experiments and productions performed, elution curves of ^{7}Be, ^{85}Sr and ^{88}Y were generated and are shown as figures 10.6 and 10.7, respectively.

Figure 10.6 describes the elution of ^{7}Be from the production system, where the first 40 mL of 1.0 M HNO_3 indicates the load and rinse solutions, respectively. The remaining ^{7}Be was eluted from the AG 50W-X4 cation exchange resin with 60 mL 1.2 M HNO_3, which was also used to remove ^{85}Sr from the resin (Fig. 10.7). A further 20 mL 1.2 M HNO_3 was added to ensure that any remaining traces of ^{85}Sr was eluted from the resin column. While there have been experimental results indicating 100 % elution of ^{88}Y in 40 mL 4.0 M HNO_3, the results were not consistent, as many results obtained also indicated that the final traces of the ^{88}Y were removed using a further 10 mL and, thus, Fig. 10.7 describes it as such.

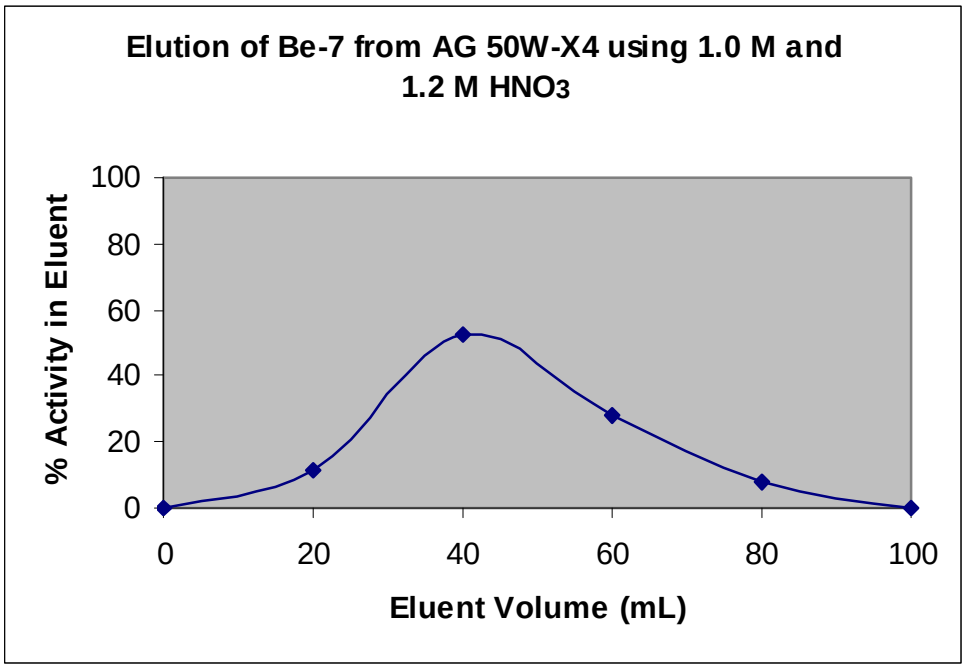

Fig. 10.6: Elution of ^{7}Be from AG 50W-X4 using 1.0 M and 1.2 M HNO_3.

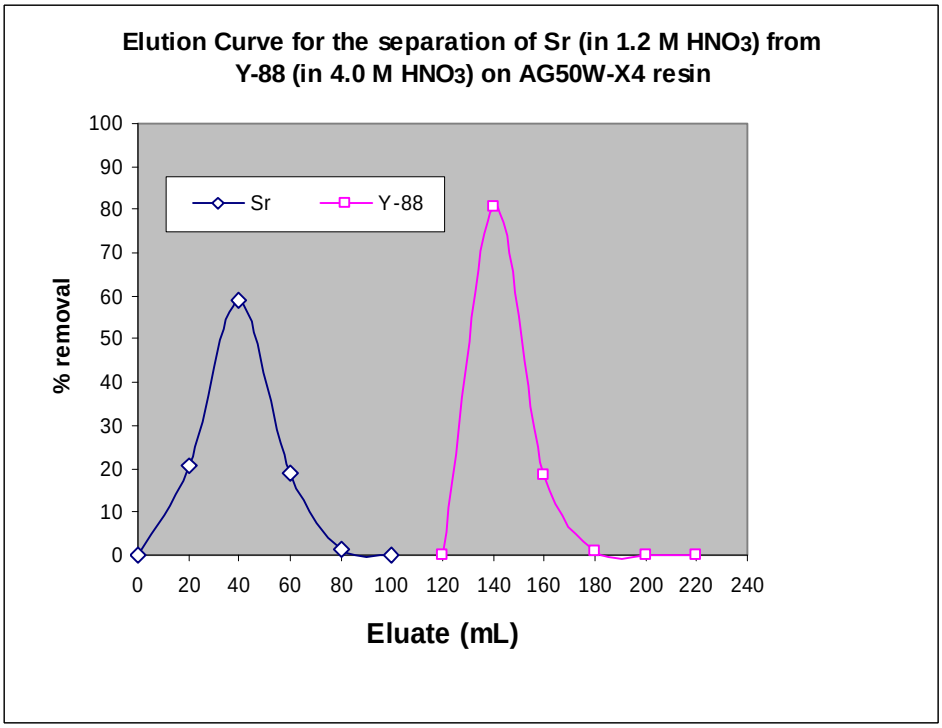

Fig. 10.7: Elution of ^{85}Sr and ^{88}Y from AG 50W-X4 using 1.2 M HNO_3 and 4.0 M HNO_3, respectively.

AG MP-1 resin

The results shown for Experiment 3 (shown as "Experiments 1 and 2" and "Productions 1 and 2") in Table 10.2 indicate the remaining Sr for experimental purposes, as *ca.* 90 % of the total Sr was removed by decanting. The precipitation of ^{88}Y in the carbonate form made it easier to separate the Sr from the final product, while increasing the pH to such a degree that ion exchange in this manner could be achieved with ease. As can be seen from the results, the separation of Sr from Y was obtained successfully and this experiment proved to be reproducible. When eluting the final product it was determined that only 25 mL of 6.0 M HCl would be required, as the entire product was contained in this aliquot. The use of a more concentrated acid for the elution of ^{88}Y was to ensure that any iron in the production process would remain on the resin column. This method was adopted when performing a full production for customer purposes.

An aluminium encapsulated 8.0 g $SrCl_2$ target was bombarded with a 66 MeV proton beam provided by iThemba LABS's separated sector cyclotron. The capsule was cut open and the target material removed. The target was dissolved in 50 mL water and the production carried out in a hot cell according to the method described in Experiment 5. The separation was deemed successful, with a 96.21 % yield of ^{88}Y, the remainder of the product being decanted along with the vast majority of Sr target material when performing the precipitation step with ammonium carbonate. Results from experimental and production runs are listed in Table 10.2.

Table 10.2: Percentage impurity removal and percentage product yield using AG MP-1 resin.

	Experiment 1	**Experiment 2**	**Production 1**	**Production 2**
% Sr decanted	96.97	96.43	98.32	97.03
% Y decanted	3.00	2.96	3.12	3.79
% Sr removal in load step	3.03	3.57	1.68	2.97
% Y removal in load step	0	0	0	0
% Sr removal in rinse step	0	0	0	0
% Y removal in rinse step	0	0	0	0
% Y yield	97.00	97.04	96.88	96.21

There appeared to be a disadvantage to this method, however. 48 % of the ^{88}Y activity migrated to the inside surfaces of the aluminium capsule and could not be removed when dissolving in water. The activity could, however be removed from the capsule when dissolving in 20 mL 1.0 M HNO_3. This solution was then evaporated to dryness, before being taken up in 20 mL of water and, once again, evaporated to dryness. The separation procedure had to be repeated to obtain all of the activity from the bombardment of the target material. For a fully successful production, therefore, the separation procedure had to be performed twice.

An elution curve for this separation can be seen below (Fig. 10.8).

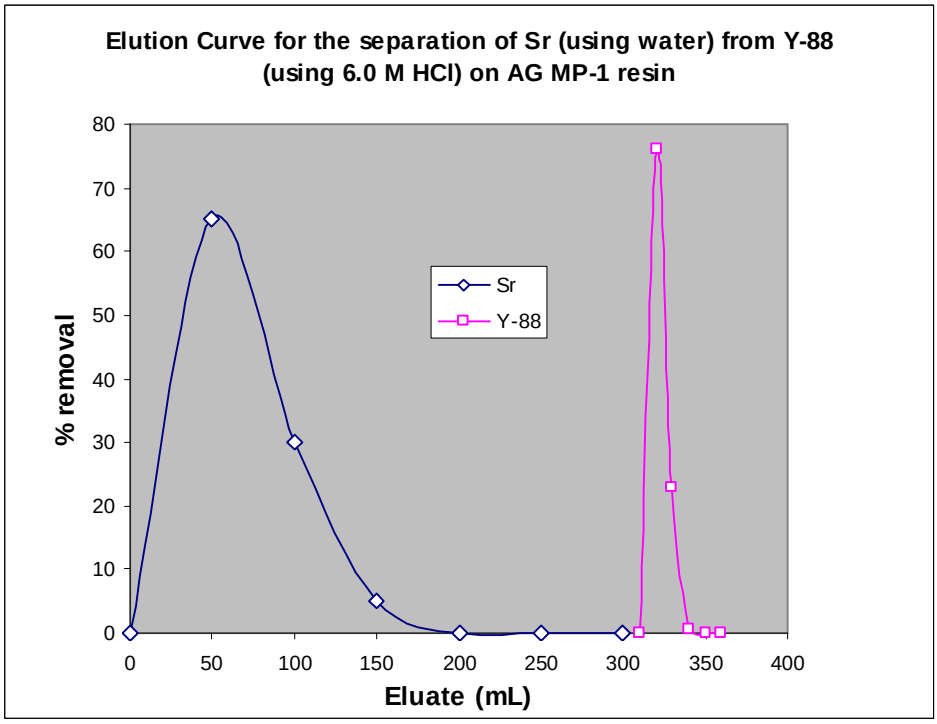

Fig. 10.8: Elution of ^{85}Sr and ^{88}Y from AG MP-1 using water and 6.0 M HCl, respectively.

Amberchrom CG161m

This experiment provided very good results, with 65.074 % Sr being removed in the initial load and rinse steps. The remainder of the Sr was eluted with 50 ml 69 % HNO_3, while 96.991 % of the ^{88}Y final product was eluted with 25 ml 0.1 M HCl. The remainder of the activity was found in the initial load waste.

This method, while showing a great deal of promise, was rejected, however, due to the fact that the final product appeared oily in nature, due to the tributyl phosphate from the column. Numerous attempts were made to rid the final product of its oily nature (by evaporation and by ion exchange), without success. As it is known that customers use the product for the making of point sources and the like, providing a product produced by this method would clearly not be appropriate. The constant use of concentrated nitric acid when using a production panel would also not be desirable, as the pump tubing and catheters will get damaged, creating a possibility of production failure.

Purolite S930

While the retention of the ^{88}Y using this resin appeared to be promising, the same could not be said for the Sr target material: 44.78 % of the material was removed in the load and rinse steps, while the remaining 65.22 % was found with the final product, containing 97.38 % of the measured ^{88}Y. Changing the concentration of the acetic acid did not improve matters and this method was rejected.

Amberchrom CG71cd

The method followed for this experiment (Experiment 6) was virtually identical to that followed for that used when using AG MP-1 as resin (Experiment 3). The results obtained were virtually identical, in that the ^{88}Y was well retained by the resin, while the Sr contaminants passed through the resin column. The iron from the aluminium capsule was also retained, however, but this was not eluted with the final product when using 6.0 M HCl. Greater tailing was obtained when eluting the ^{88}Y final product, resulting in 75 mL of HCl being required, instead of the 25 mL required when using AG MP-1.

The result of this experiment is significant, as this indicates that the Fe and Y is *co-precipitated* on the resins (Amberchrom and AG MP-1) and not retained as an anion on the AG MP-1 macroporous anion exchange resin. This could be exploited in future experiments for other radionuclides.

Choice of target material

When dissolving the irradiated SrB_6 target, using 50 mL 5.0 M HNO_3, the dissolution offered a vicious exothermic reaction and, thus, the solution was added drop-wise to ensure that all of the activity would be contained within the reaction vessel.

The dissolution of the target material proved to be problematic. When the aluminium capsule was cut open, the target did not appear as a whole, compressed disc. Instead, it crumbled into the reaction vessel, along with some aluminium shavings. While no problems previously occurred when dissolving a small piece of target material, the dissolution of the full target was messy, creating a scum on the surface and pieces of what was thought to be aluminium at the bottom of the vessel. As a result, the resultant solution had to be filtered using a glass column containing a porous G2 glass frit at the bottom. Furthermore, a 5 micron filter had to be placed on the production panel, so that the finer material from the dissolution step was retained. While this target material showed resilience when placed in the proton beam for bombardment, it was decided that this would not be the target material of choice from a chemical and production point-of-view.

As mentioned previously, problems were encountered when using $SrCl_2$ as target material in high-intensity proton bombardments (*i.e.* target capsules bursting and aberrant yields). To overcome this, several other types of target material were investigated in an attempt to prevent activity losses. Unsuccessful attempts were made using SrF_2 instead of $SrCl_2$. More successful irradiations were obtained with repeated attempts using SrS and SrB_6, but both targets proved problematic to dissolve as it was almost impossible to remove all traces of aluminium (as a result of the targets reacting with the Al capsule) from the target material.

It is well known that $SrCl_2$ can be successfully used as target material, but it was not known why the target had a tendency of bursting when placed in the proton beam for an extended period. Upon perusing the literature[30], it was noticed that the hexahydrate only lost its last water molecule at temperatures greater than 170 ºC.

Previous experience with the preparation of other chloride targets showed that freeze-drying chloride salts would suffice to ensure they are anhydrous. Prepared targets

were also heated once pressed. It transpired that the sixth water molecule remaining might have been the source of the bursting targets, because once the method of target preparation was changed, by drying the $SrCl_2$ salt in a vacuum oven at a temperature higher than 170 ºC, subsequent bombardments of the target material were performed successfully.

The theory developed was that the sixth water molecule was the cause of the burst target capsules (as the salts melt under bombardment conditions and the water vapour released creates pressure within the aluminium target capsule). As a result, extreme care will have to be taken to prevent any exposure of the target material to the atmosphere after the baking process.

Target encapsulation

From experience gained when performing ^{88}Y productions, it became apparent that bench experiments and routine productions differed greatly. Initially, target capsules were cut open and the target provided for processing. When SrB_6 was used, unsuccessfully, as target material, the capsule had to be included and it was discovered that approximately 48 % of the ^{88}Y product had migrated to the inside surfaces of the aluminium capsule.

When performing production processes using $SrCl_2$ as target material, it was discovered that, once again, about 48 – 50 % of the ^{88}Y activity had migrated to the aluminium capsule walls. Ideally, it would be better to encapsulate the target material in a more inert capsule, such as niobium, but this would be costly to iThemba LABS as it would require the acquisition of an electron-beam welding apparatus (for capsule sealing under vacuum).

It is clear that the use of aluminium capsules is a limiting factor in the production of ^{88}Y. Making matters worse during the experimental phase was the fact that the aluminium capsule material was not pure and contained impurities, such as iron and silica. The activated target material could be dissolved in 1.0 M HNO_3, but with the risk of the Y forming silicates as a result of the impurities, resulting in it not being quantitatively retained by the resin.

An attempt to overcome the issue of the reaction between the $SrCl_2$ and the aluminium was to anodize the aluminium capsule. Once the target material was placed inside the capsule, it was bombarded and processed as usual. It was discovered that *ca.* 10 % of the ^{88}Y migrated to the Al and *ca.* 90 % of the ^{88}Y activity could be recovered successfully without having to treat the capsule further, implying that one can use the production method involving AG MP-1 macroporous anion exchange resin successfully with minimal losses of final product.

Should one wish to obtain all of the activity for production purposes, it would be necessary to perform the production successfully using two columns.

Adopted production method

The target material was dissolved in 100 mL water. To it was added a 10 mL solution containing 50 mg of ammonium carbonate and stirred. The solution was then left to stand for 30 minutes. The ^{88}Y was precipitated and the Sr solution was gently decanted, leaving the precipitate behind. The precipitate was dissolved in 2 mL 2.0 M HCl, evaporated to dryness and the salts dissolved in 200 mL water. The solution was loaded on to a 10 mL column containing AG MP-1 resin (treated with 50 ml 25 % NH_3 and the column rinsed with 100 mL water prior to use). While the bulk of the Sr was expected to be removed with the decanting and load steps, the remaining contaminant was removed from the column by eluting it with 100 mL water. The final product (^{88}Y) was eluted from the resin column with 25 mL 6.0 M HCl and evaporated to dryness, before finally being picked up in 5 mL 0.1M HCl.

The anodized target capsule was treated separately and the activity attached to it dissolved in 1.0 M HNO_3. The capsule was removed and the solution evaporated to dryness. 50 mL of water was added to the beaker and this was, once again, evaporated to dryness, before the activity was taken up in 200 mL water. The solution was treated with 10 mL water containing 50 mg ammonium carbonate. The Y was co-precipitated as carbonate with *ca.* 80 mg $SrCO_3$ and was allowed to settle. The container was decanted to get rid of the water (and the Sr activity) and the process repeated. Once the solution had been decanted a second time, the precipitate was dissolved in 50 mL 0.5 M HCl and loaded on to a 10 mL column containing AG50W-X4 cation exchange resin (equilibrated with 50 mL 0.5 M HCl). Any excess ^{85}Sr was

removed from the resin column using 70 mL 1.2 M HNO_3. The ^{88}Y was eluted using 50 mL 4.0 M HNO_3 and evaporated to dryness, before finally being picked up in 5 mL 0.1 M HCl.

10.4 Conclusion

A thick-target production rate curve was measured for ^{88}Y produced in the proton bombard-ment of $SrCl_2$, from which the $^{88}Sr(p,n)^{88}Y$ excitation function was derived using a differentiation method. Good agreement was found with one set of literature data once those values were renormalized according to more recent monitor reaction data.

An effective separation between ^{88}Y from the Sr target material could be successfully obtained when using AG MP-1 macroporous anion exchange resin at a pH > 7 or when performing a production using AG50W-X4 cation exchange resin. As it was discovered that the Al was attacked by the $SrCl_2$ during bombardment and that much of the ^{88}Y activity was found to have migrated to the aluminium target capsule, it was deemed preferable to anodize the capsule. The production is performed using both resin columns, namely, the AG MP-1 resin for the target dissolution and separation (obtaining 90 % of the total ^{88}Y activity) and the AG50W-X4 resin for the removal of the remaining activity from the aluminium capsule in acidic media. The use of a co-precipitation step, using ammonium carbonate, proved to be very effective in the removal of the bulk of strontium from yttrium using both chromatographic methods.

The use of aluminium encapsulation is not recommended, however, as better materials for this purpose have been demonstrated and successfully implemented at other laboratories. Unfortunately, the technology to encapsulate target materials in Nb (or anything other than aluminium) does not yet exist at iThemba LABS. During the course of this study, it became abundantly clear that electron-beam welding technology is absolutely essential for the manufacturing of high-current radionuclide production targets at an intermediate energy accelerator facility such as iThemba LABS. It is unlikely that any significant further progress on ^{88}Y production will be made until such a system has been acquired.

10.5 References

1. Firestone R. B., Eckström, 2004. WWW Table of Radioactive Isotopes, Version 2.1. URL: <http://i.e.lbl.gov/toi>.
2. Kettern K., Linse K.-H., Spellerberg S., Coenen H. H., Qaim S. M., 2002. *Radiochim. Acta*, **90**, 845.
3. Sachdev D. R., Porile N. T., Yaffe L., 1967. *Can. J. Chem.*, **45**, 1149.
4. Homma Y., Ishii M., Murase Y., 1980. *Int. J. Appl. Radiation Isotopes*, **31**, 399.
5. Grahek Z., Eskinja I., Kosutic K., Lulic S., Kvastek K., 1999. *Analytica Chim. Acta*, **379**, 107.
6. Grahek Z., Kosutic K., Lulic S., 1999. *J. Radioanal. Nuclear Chem.*, **242** (1), 33.
7. Grahek Z., Eskinja I., Kosutic K., Cerjan-Stefanovic S., 2000. *Croatica Chemica Acta*, **73** (3), 795.
8. Aardaneh K., Perrang C., Dolley S., van der Meulen N., van der Walt T.N., 2006. *J. Radioanal. Nuclear Chem.*, **270** (3), 641.
9. Saito N., 1984. *Pure & Appl. Chem.*, **56** (4), 523.
10. Shikano K., Katoh M., Shigematsu T., Yonezawa H., 1987. *J. Radioanal. Nuclear Chem.*, **119** (6), 433.
11. Reischl G., Rösch F., Machulla H.-J., 2002. *Radiochim. Acta*, **90**, 225.
12. Lange G., Hermann G., Strassmann F., 1957. *J. Inorg. Nucl. Chem.*, **4**, 146.
13. Fassbender M., Nortier F. M., Phillips D. R., Hamilton V. T., Heaton R. C., Jamriska D. J., Kitten J. J., Pitt L. R., Salazar L. L., Valdez F. O., Peterson E. J., 2004. *Radiochim. Acta*, **92**, 237.
14. Lone M. A., Edwards W. J., Collins R., 1993. *Nucl. Instr. Meth A*, **332**, 232.
15. Katoh M., Shigematsu T., Shikano K., Yonezawa H., 1987. *J. Radioanal. Nuclear Chem.*, **119** (6), 237.
16. Rösch F., Qaim S. M., Stöcklin G., 1993. *Appl. Radiat. Isot.*, **44** (4), 677.
17. Behr T. M., Béhé M., Stabin M. G., Wehrmann E., Apostolidis C., Molinet R., Strutz F., Fayyazi A., Wieland E., Gratz S., Koch L., Goldenberg D. M., Becker W., 1999. *Cancer Research*, **59**, 2635.

18. Goodwin D. A., Meares C. F., Watanabe N. McTigue M., Chaovapong W., Ransone C. McK., Renn O., Greiner D. P., Kukis D. L., Kronenberger S. I., 1994. *Cancer Research*, **54**, 5937.

19. Griffiths G. L., Govindan S. V., Sharkey R. M., Fischer D. R., Goldenberg D. M., 2003. *J. Nucl. Med.*, **44** (1), 77.

20. Arzumanov A., Batischev, Berdinova N., Borissenko A., Chumikov G., Lukashenko S., Lysukhin S., Popov Yu., Sychikov G., 2001. In: *Cyclotrons and Their Applications, Sixteenth International Conference, East Lansing, Michigan* (Marti F.: Ed.), 34.

21. Blaser J. P., Boehm F., Marmier P., Scherrer P., 1951. *Helv. Phys. Acta* **24**, 441.

22. Sachdev D. R., Porile N. T., Yaffe L., 1967. *Can. J. Chem*. **45**, 1149.

23. Levkovskii V. N., 1991. *Cross-section of Medium Mass Nuclide Activation (A=40-100) by Medium Energy Protons and Alpha Particles (E=10-50) (Experiment and Systematics),* Inter-Vesi, Moscow, p. 147.

24. Rösch F., Qaim S. M., Stöcklin G., 1993. *Radiochim. Acta* **61**, 1.

25. Gul K., Hermanne A., Mustafa M. G., Nortier F. M., Obložinský P., Qaim S. M., Scholten B., Shubin Y., Takács S., Tárkányi F. T. and Zhuang Z., 2005. IAEA-TECDOC-1211, IAEA, Vienna, May 2001. Available from URL: http://www-nds.iaea.org/medical/.

26. TABLECURVE 2D, 1996. Automated Curve Fitting and Equation Discovery, Jandel Scientific, San Rafael, California.

27. Ignatyuk A. V., Weil J. L., Raman S., Kahane S, 1993. *Phys. Rev. C*, **47**, 1504.

28. Vermeulen C., Steyn G. F., Nortier F. M., Szelecsényi F., Kováks Z., Qaim S. M., 2007. *Nucl. Instrum. Meth. B,* **255**, 331.

29. Takács S., Tárkányi F., Sonck M., Hermanne A., 2002. *Nucl. Instrum. Meth. B,* **198**, 183.

30. Merck Index, 12th Ed, Whitehouse Station, NJ, 1996.

CHAPTER 11 THE PRODUCTION OF 133Ba IN THE PROTON BOMBARDMENT OF Cs

11.1 Introduction

^{133}Ba is a long-lived radionuclide, with a half-life of 10.54 years[1]. It is mainly used as a calibration source for γ-rays in the energy region 81 to 356 keV as it has several strong γ-emitting transitions in this region[2], although the 81 keV photo-peak is often difficult to resolve from the 79 keV transition[3]. It is generally obtained from the bombardment of Cs-based materials via the ^{133}Cs(p,n)^{133}Ba reaction (see Fig. 11.1). It is also sometimes used for biomedical applications, predominantly bone studies[4,5], although investigations have also been performed to determine whether there is a long-term retention of the element elsewhere in the body[6,7], by means of testing on rats. It has also been used in studies of perturbed angular correlation[8,9], as well as in the study of the attachment of cryptates containing radioactive metal ions to proteins[10].

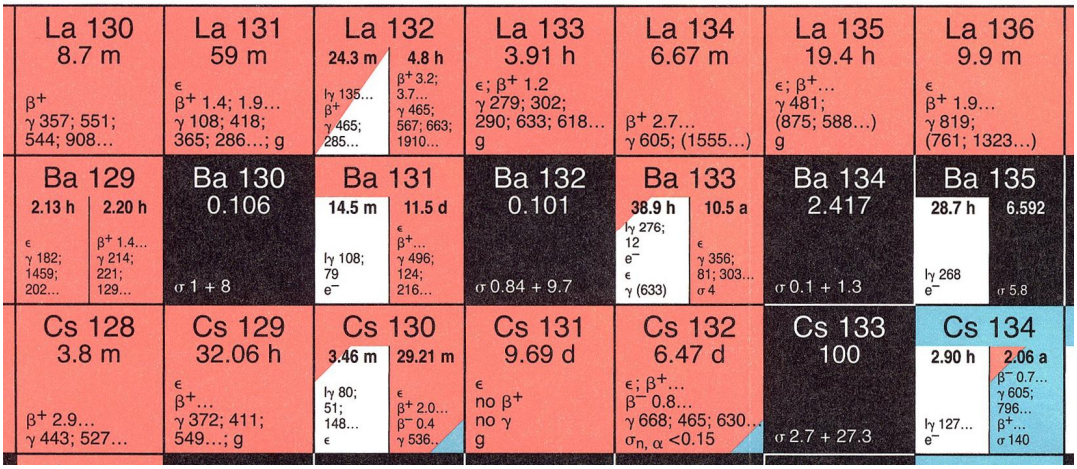

Fig. 11.1: Relevant part of the "Karsruher Nuklidkarte" of 2006 for the production of ^{133}Ba.

^{133}Ba can also be used as tracer for predicting ^{226}Ra in soil-plant transfer studies[11], as it is a good analogue of the environmental behaviour of ^{226}Ra[12]. As a result, it has also been used for the study of estuarine sediments[12,13]. The radionuclide has also been used as a surrogate for HEU[14], to determine the probability of K-electron capture

to the two excited states of ^{133}Cs[15] and for the determination of non-ionic surfactants of ethylene dioxide type[16].

^{133}Ba is an expensive radionuclide to make and, as a result, very few accelerator facilities consider it financially viable to produce routinely. There have been reports on producing the radionuclide using reactor facilities[17], however, that product is not carrier free. ^{133}Ba is usually produced at accelerator facilities by bombarding caesium metal-based target material using high-energy proton beams. Due to its long half-life, it can take an excruciatingly long time to manufacture a reasonable quantity of the product.

Ion exchange methods have been reported to separate Ba from Cs[18,19], although lately these methods have largely been based on inorganic ion exchangers[20,21]. In this work, however, organic ion exchange resins were investigated to separate ^{133}Ba from a number of proton-bombarded Cs compounds. The production of ^{133}Ba may be attractive to iThemba LABS as it can, in principle, be done as the lower-energy companion of ^{22}Na or ^{82}Sr productions in a tandem target geometry. Even though its production rate may be quite low, the price per unit activity that the market offers is relatively high, making it worthwhile to produce it as a "by-product" of the regular ^{22}Na and ^{82}Sr productions.

11.2 Nuclear Data

11.2.1 Experimental Methods and Data Analysis

No excitation function data for the reaction $^{133}Cs(p,n)^{133}Ba$ could be found in the literature. It was, therefore, decided to measure some data for this reaction, however, the long half-life made it impossible to measure an extensive new data set. In fact, these measurements were performed at the same time that data for ^{88}Y were measured at ATOMKI, Debrecen, Hungary (see Chapter 10). The experimental method of section 10.2.1 is, therefore, applicable, thus, only the salient features of these particular measurements will be described here.

Referring to Fig. 10.2, the targets were prepared by powder compaction of fully anhydrous CsF salt (99.9 %, Alfa Aesar) in a punch-and-die set with a hydraulic press. All the targets irradiated had a nominal thickness of 1000 mg/cm^2, thus, thick enough to stop the beam. Activations were performed using degraders of various thicknesses to cover the energy region from threshold up to ~17.5 MeV, the maximum energy which could be obtained from the ATOMKI cyclotron. The monitor foils were high purity Cu (99.99 %, Goodfellow, U.K.) with a thickness of 25 µm, for the accurate determination of the incident proton flux. As before, the ^{nat}Cu(p,x)^{65}Zn monitor reaction with IAEA recommended cross sections were used for this purpose. The targets were irradiated inside the cyclotron vacuum at an average beam current of 50 nA, each bombardment lasting two hours. The longer bombardment time was necessary in order to induce sufficient ^{133}Ba activity to complete the off-line γ-ray analysis in a reasonable time. During the allocated time on the ATOMKI cyclotron, only four such activations could be performed, after which the beam had to be handed over to other users.

After bombardment, each CsF target was dissolved in 3 mL of water in a standard serum vial. Once filled and sealed, these vials constituted appropriate counting sources. The reason why liquid sources were prepared in this way instead of counting the activated CsF discs directly, was because they were considered to be too thick to constitute *bona fide* point sources. (See section 10.2.1 for further details on the sources for counting).

The ^{133}Ba activities were determined by off-line γ-ray spectrometry using the 302.85 keV (18.33 %) and 356.02 keV (62.05 %) γ-lines[1]. The statistical uncertainties were insignificant compared to the systematic uncertainty, the latter of which was estimated to be about 7 %: beam current integration (4 %), detector efficiency (5 %), counting geometry (1 %) and decay corrections (2 %). The ^{65}Zn cross sections extracted from the Cu monitor foils were also found to be in excellent agreement with the IAEA recommended values, thus, the directly measured current integrator values were independently confirmed.

11.2.2 Results and Discussion

The measured ^{133}Ba thick-target production rate curve for CsF + p is shown in Fig. 11.2. Since only four data points were measured, not enough information was available to uniquely fit a polynomial function. It was, therefore, necessary to fit a model-generated function to the measured values. For this purpose, the Geometry Dependent Hybrid (GDH) model as implemented in the ALICE-IPPE code was used (see also section 10.2.2). The solid curve shown in Fig. 11.2 was calculated from the ALICE-IPPE predicted excitation function for the ^{133}Cs(p,n)^{133}Ba reaction. The dashed curve is the same information but renormalized to the data. Note that whereas the corresponding curve in the case of ^{88}Y was found in a model-independent way (*i.e.* by a least-squares fitting of a polynomial function), in the case of ^{133}Ba the shape of the curve is model-dependent, thus, the four measured data points served to constrain the theoretical prediction. It can, therefore, be thought of as an integral test of the predicted model-generated data. The expected production rate for the proton energy window 4 – 20 MeV is about 25.6 kBq/µAh.

The corresponding excitation functions are shown in Fig. 11.3. It has the typical shape for a (p,n) reaction and reaches a maximum of about 550 mb at a proton energy of 10.2 MeV. An energy window of 4 – 20 MeV should, therefore, be ideal for ^{133}Ba production.

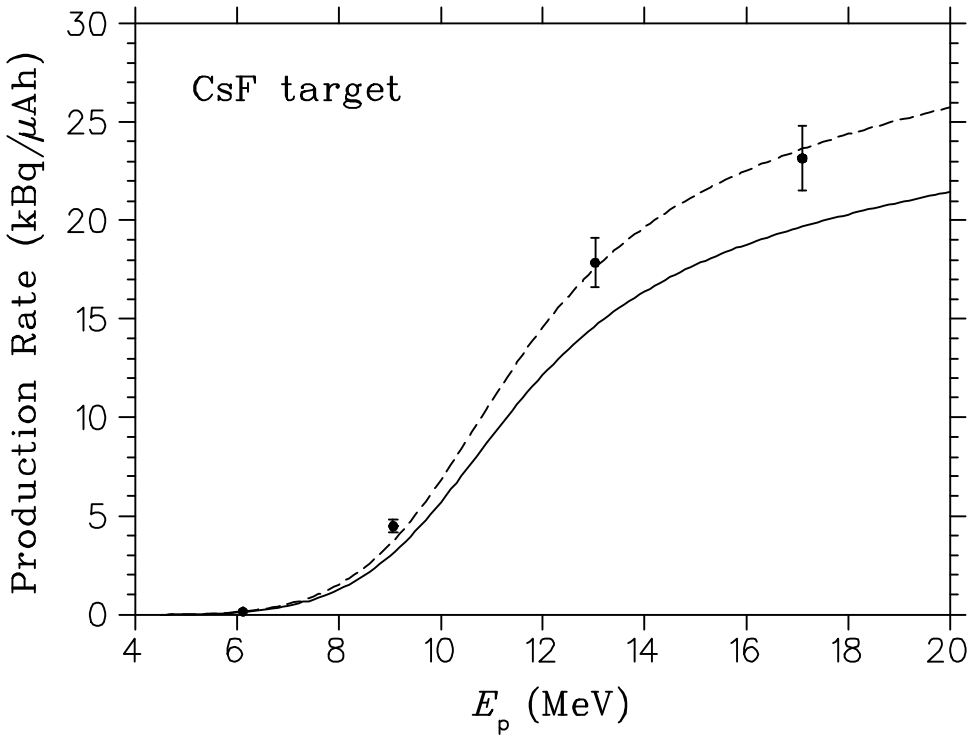

Fig. 11.2: Thick-target production rate curve of ^{133}Ba produced in the proton bombardment of CsF. The solid symbols are the measured values of this work while the solid curve is a prediction based on the Geometry Dependent Hybrid (GDH) model. The dashed curve presents the same information as the solid curve but renormalized to the measured data. Error bars are shown when they exceed the symbol size.

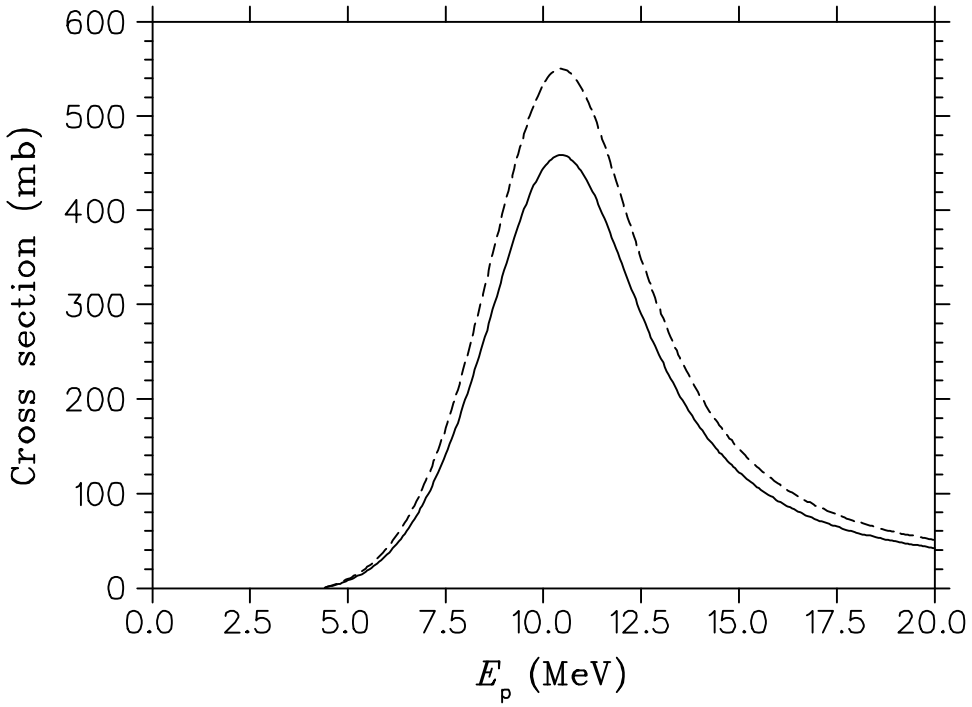

Fig. 11.3: Excitation function of ^{133}Ba formed in the reaction of protons with ^{133}Cs. The solid curve was derived from the ALICE-IPPE prediction (see text) while the dashed curve represents the renormalized excitation function according to the integral yield measurements of this study.

11.3 Radiochemical Investigation

11.3.1 Chemical Separation Methods

Analytical grade reagents were used throughout this work and were obtained from Merck (SA) Pty. Ltd or Sigma Aldrich GmbH, which included Fluka and Riedel de Haen products. The AG MP-50 and AG 50W-X4 cation exchange resins used in this work was obtained from BioRad Laboratories, Richmond, U.S.A. De-ionised water from a Millipore MilliQ Reagent Grade Water System, to a conductivity of greater than 10 megaohm cm^{-1}, was used for all experimental and production work.

All radioactive determinations were performed using a standard calibrated HPGe detector, with a relative efficiency of 13 % (relative to three inch NaI), connected to a multichannel analyser.

Experiment 1

3.0 g CsCl and 0.015 g $BaCl_2$ were dissolved in 50 ml 0.1 M HCl. The solution was passed through a 5 mL column containing AG 50W-X4 cation exchange resin, which had been equilibrated by the passage of 50 mL 0.1 M HCl through the resin column. The column was rinsed with 20 mL 0.1 M HCl, to remove impurities, before the remainder of the Cs was eluted from the column using 150 mL 0.5 M HCl. It was planned to elute the Ba from the resin column using 80 mL 2.0 M HNO_3.

Experiment 2

3.0 g CsCl and 0.015 g $BaCl_2$ were dissolved in 50 ml 0.1 M HCl. The solution was passed through a 5 mL column containing AG 50W-X4 cation exchange resin, which had been equilibrated with 0.1 M HCl. The column was rinsed with a further 30 mL 0.1 M HCl (both of these two steps performed at a pump speed of 8 mL per minute), followed by 200 mL 0.4 M HCl. The Ba product was eluted using 50 mL 2.0 M HNO_3. The final two steps of the experiment were performed at a pump speed of 4 mL per minute.

Experiment 3

3.0 g CsCl and 0.015 g $BaCl_2$ were dissolved in 50 ml 0.1 M HCl. The solution was passed through a 5 mL column containing AG 50W-X4 cation exchange resin, which had been equilibrated with 0.1 M HCl. The column was rinsed with a further 30 mL 0.1 M HCl (both of these two steps performed at a pump speed of 8 mL per minute), and the Cs eluted with 200 mL 0.3 M HCl. The Ba product was eluted using 100 mL 1.5 M HNO_3. The final two steps of the experiment were performed at a pump speed of 4 mL per minute.

Experiment 4

3.0 g CsCl and 0.015 g $BaCl_2$ were dissolved in 50 ml 0.1 M HCl. To this was added ^{132}Cs and ^{131}Ba tracer. The solution was passed through a 5 mL column containing AG 50W-X4 cation exchange resin, which had been equilibrated with 0.1 M HCl. The load solution vessel was washed with 50 mL 0.1 M HCl and passed through the resin column. The Cs was eluted from the column using 3x 50 mL 0.3 M HCl, after which the Ba was eluted from the resin using 25 mL 2.0 M HNO_3.

Experiment 5

A bombarded CsCl target (~ 4.0 g) was dissolved in 50 mL 0.1 M HCl and the method followed as with Experiment 4. After eluting the ^{133}Ba with HNO_3, 160 mL methanol was added to the eluate. This solution was pumped through a second column (5 mL AG 50W-X4, equilibrated with 0.1 M HCl) at a pump speed of 10 mL per minute. The column was then rinsed with 75 mL 0.1 M HCl, before it was rinsed further using 100 mL 0.3 M HCl and the ^{133}Ba eluted with 50 mL 2.0 M HNO_3. The eluate was evaporated to dryness and picked up in 10 mL 0.1 M HCl.

Experiment 6

3.0 g CsCl and 0.015 g $BaCl_2$ were dissolved in 40 ml 0.5 M HCl. To this was added ^{132}Cs and ^{131}Ba tracer. The solution was passed through a 10 mL column containing AG MP-50 macroporous cation exchange resin, which had been equilibrated with 0.5 M HCl. The elements were washed on to the resin column using another 3x 10 mL 0.5 M HCl, before the Cs was eluted from the resin using 3x 30 mL 3.0 M HCl. The Ba final product was eluted from the resin column using 2x 30 mL 6.0 M HNO_3, followed by a further 40 mL 6.0 M HNO_3.

Experiment 7

A bombarded CsCl target (~ 4.0 g) was dissolved in 50 mL water and left to stir for 10 minutes while the solution was heated at 70 ºC. The solution was decanted to separate the solution from any aluminium pieces and the beaker washed four times with 10 mL water and added to the original decanted solution. 5 mL concentrated HCl, followed by 5 mL water was added to the solution and mixed well. The resultant solution was loaded on to a column containing 10 mL AG MP-50 macroporous cation exchange resin, equilibrated with 0.5 M HCl. The resin was rinsed with 30 mL 0.5 M HCl, before the Cs was eluted using 90 mL 3.0 M HCl. The ^{133}Ba final product was eluted from the resin using 3x 50 mL 6.0 M HNO_3.

11.3.2 Results and discussion

Experiment 1

The Ba was well retained by the resin, with a neglible quantity eluted in the initial load step and the first rinse step. 1.1 % of the product was eluted with the 150 mL 0.5 M HCl, the last 50 mL showing signs of breakthrough, while the remaining 98.9 % was eluted with the HNO_3. Cs started breaking through the column from the initial load step and continued to do so with 20 mL 0.1 M HCl, with 95.5 % of the Cs being eluted via the two steps. The remainder of the Cs was eluted from the column with 90 mL of the 150 mL 0.5 M HCl. A good separation can be obtained should 100 mL 0.5 M HCl be used in the second rinse step, thereby, preventing Ba breakthrough.

Experiment 2

Once again, no Ba was found in the initial load and rinse waste. While initially, there was no Ba in the 0.4 M HCl waste, Ba started breaking through after 130 mL had passed through the resin, eventually releasing 34.5 %. The remaining 65.5 % of the product was eluted from the resin column with the 2.0 M HNO_3, although it only required 20 mL to do so. As found with Experiment 1, Cs was eluted from the column in the initial load waste, as well as the 30 mL 0.1 M HCl rinse step, producing 96.3 % in the waste. The remaining Cs was eluted in the first 70 mL 0.4 M HCl. As with the previous experiment, a decent separation separation can be obtained should

one decrease the 0.4 M HCl rinse step (to, maybe, 90 mL), thereby, preventing Ba breakthrough from the resin column.

Experiment 3

As with the previous two experiments, the Ba was well retained by the resin when loading the solution on to the column and rinsing the resin with 30 mL 0.1 M HCl. When rinsing with 0.3 M HCl, the remainder of the Cs was eluted with the first 90 mL. There was, however, once again breakthrough of Ba in the last 10 mL of the 200 mL 0.3 M HCl passed through the resin column (2.1 %). The remaining 97.9 % of the ^{133}Ba product was eluted using 40 mL of the 100 mL 1.5 M HNO_3.

Experiment 4

This experiment proved to be far more successful than the previous three, in that there was no breakthrough of Ba at all and it was eluted from the column when using the 2.0 M HNO_3. The Cs behaved as expected, with 46.5 % being eluted from the column in the initial 50 mL 0.1 M HCl load solution. A further 34.9 % was eluted with the 50 mL 0.1 M HCl rinse step, while the remainder of the Cs was eluted with the first two 50 mL fractions of 0.3 M HCl (18.2 % of the total Cs in the first 50 mL fraction and the remaining 0.3 % in the second fraction). All of the ^{133}Ba was eluted with the HNO_3.

Experiment 5

While Experiment 4 worked perfectly well, with no Cs in the final product, it was feared that there may be "cold" Cs in the final product, which is the reason for the extra steps added to the previous method. The ^{133}Ba behaved impeccably in the steps as for Experiment 4 and was loaded on to the second column successfully. It was hoped that any remaining Cs would be removed with the extra 75 mL 0.1 M HCl, before the ^{133}Ba was eluted from the resin column. Analysis of the final product using atomic absorption indicated a negligible quantity of Cs carrier.

Experiment 6

Interestingly, no Cs or Ba was found in the initial load waste, or the 30 mL 0.5 M HCl used to wash the elements onto the column. The Cs was eluted with the 3.0 M HCl rinse step, 93.2 % of the element in the first 30 mL fraction and the remaining 6.8 %

in the second fraction. The ^{131}Ba took some time to elute, requiring the full 100 mL of 6.0 M HNO_3 to remove the element. 40.4 % of the product was removed from the column in the first 30 mL fraction, 49.5 % was removed with the second 30 mL fraction and the remaining 10.1 % was removed with the last 40 mL fraction, indicating a bit of a "tailing" effect.

Experiment 7

The results obtained were very similar to that of Experiment 6, in that all of the Cs was eluted in the 3.0 M HCl rinse, while the ^{133}Ba final product was eluted from the column using a large quantity of 6.0 M HNO_3. It transpired that 100 mL was enough to remove the final product.

Choice of target material

CsCl and CsF were tested for use as target material. Both materials made decent target pellets, with the CsF behaving slightly better than the CsCl under bombardment conditions. Both targets required encapsulation in aluminium. The CsCl required more pre-treatment, in that it had to be placed in a vacuum oven for a period to ensure that it was truly anhydrous, thereby, preventing the encapsulation from bursting under bombardment conditions.

The CsCl target behaved better than the CsF target, as it was considerably easier to dissolve the CsCl pellet. Furthermore, when using ion exchange, the product could be easily eluted when using the CsCl target material, while the same could not be said when using the CsF target. No sufficient explanation could be found for this.

Ideal separation method

A separation of ^{133}Ba from its target material can be effectively performed when using a 5 mL AG 50W-X4 resin column, equilibrated with 0.1 M HCl. Once the target is dissolved in 50 mL 0.1 M HCl, the column can be rinsed with a further 30 mL 0.1 M HCl, to continue to rid the system of Cs impurities, before removing the last of the Cs with 100 mL 0.3 M HCl. The ^{133}Ba can be eluted from the resin column with 30 mL 2.0 M HNO_3. As the product is generally requested in the chloride form, the product can be evaporated to dryness before being picked up in 10 mL 0.1 M HCl. An elution curve for this separation can be seen in Fig. 11.4 below.

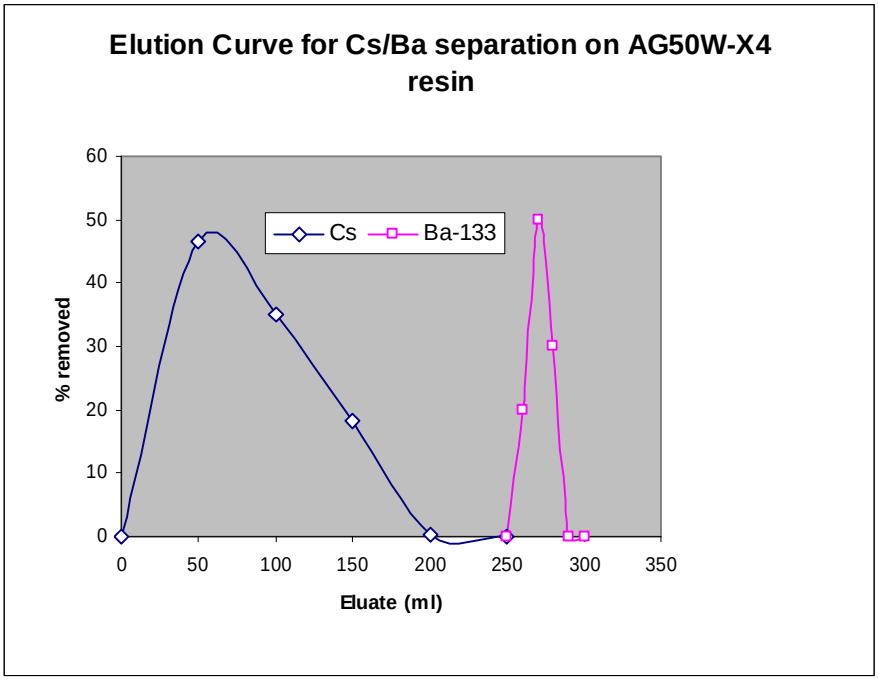

Fig. 11.4: **The separation of ^{133}Ba from Cs target material using HCl and HNO_3 as eluents.**

Should a residue be discovered at the base of the evaporator once dry, the residue can be dissolved in 2.0 M HNO_3 (20 mL) and 160 mL methanol then added. The resultant solution can be loaded on to a 5 mL AG 50W-X4 resin column, the column rinsed with 75 mL 0.1 M HCl, followed by 75 mL 0.3 M HCl, before the ^{133}Ba can be eluted with 30 mL 2.0 M HNO_3. This solution can be evaporated to dryness, before being picked up with 10 mL 0.1 M HCl for dispatch.

11.4 Conclusion

A number of integral yield measurements performed in the proton bombardment of CsF targets with protons provided enough information to constrain a model calculation of the excitation function for the ^{133}Cs(p,n)^{133}Ba reaction. Within the experimental uncertainties, the measured points confirm the shape of the theoretical thick-target production rate curve.

An effective method was developed to separate ^{133}Ba from Cs target material, provided the Cs target material is in the chloride form, using AG 50W-X4 cation exchange resin, and applying various concentrations of HCl before eluting the final product with HNO_3. Almost a 100 % yield was obtained and the product was radionuclidically pure.

The use of aluminium as encapsulation material is again considered to be far from ideal (see also section 10.4). It was found that after extended bombardment (*i.e.* several thousand μAh) these capsules in a few cases developed leaks, indicating that the CsCl (which is largely in a molten state during bombardment) may be slowly reacting with the aluminium. It is, therefore, recommended that a more inert capsule material be used, such as Nb.

11.5 References

1. Firestone R. B. and Eckström L. P., 2004. WWW Table of Radioactive Isotopes, Version 2.1. URL: <http://ie.lbl.gov/toi>.
2. Tuli J. K., 2004. Nuclear Wallet Cards for Radioactive Nuclides. Brookhaven National Laboratory, Upton, New York, U.S.A.
3. Nichols A. L., 2005. In *IAEA Workshop on Nuclear Structure and Decay Data: Theory and Evaluation* (Ed: Nichols A. L. and McLaughlin P. K.). IAEA Nuclear Data Section, Vienna. 294.
4. Newton D., Ancill A. K., Naylor K. E., Eastell R., 2001. *Radiat. Prot. Dosimetry*, **97** (3), 231.
5. Ellsasser J. C., Farnham J. E., Marshall J. H., 1969. *Journal of Bone and Joint Surgery*, **51**, 1397.
6. Takahashi S., Patrick G., 1987. *Radiat. Res.*, **110** (3), 321.
7. Patrick G., Stirling C., 1977. *Proc. R. Soc. Land. B.*, **198**, 455.
8. Rimbert J. N., Kellershohn C., Dumas F., Hubert C., 1981. *Phys. Med. Biol.*, **26**, 221.
9. Singh H., Binarh H. S., Ghumman S. S., Sahota H. S., 1990. *Int. J. Rad. Appl. Instrum. [A]*, **41** (9), 797.
10. Pettit W. A., Swailes B. K., 1993. *J. Label Compd. Radiopharm.*, **33**, 305.

11. Vandenhove H., Eyckmans T., Van Hees M., 2005. *J. Environ. Radioact.*, **81** (2-3), 255.
12. Barros H., Laissaoui A., Abril J. M., 2004. *Sci. Total Environ.*, **319** (1-3), 253.
13. Barros H., Abril J. M., 2004. *Water Res.*, **38** (3), 749.
14. Pohl B. A., Archer D. E., 2004. URL: <http://www.llnl.gov/tid/Library.html>
15. Mahapatra B. K. D., Mukherjee P., 1974. *Phys. A: Math. Nucl. Gen.*, **7**, 388.
16. Krtil J. Selucky P., Rais J., Kuvik V., 1985. *J. Radioanal. Nucl. Chem.*, **94**, 251.
17. Karelin Y. A., Gordeev Y. N., Filimonov V. T., Toporov Y. G., Yadovin A. A., Karasev V. I., Lebedev V. M., Radchenko V. M., Kuznetsov R. A., 1997. *Appl. Radiat. Isot.*, **48** (10-12), 1585.
18. Ferraris M. M., 1964. *Health Phys.*, **10**, 833.
19. Groll P., Gran F., Buchtella K., 1969. *Radiochim. Acta*, **12**, 152.
20. Roy K., Pal D. K., Basu S., Nayak D., Lahiri S., 2002. *Appl. Radiat. Isot.*, **57** (4), 471.
21. Dhara S., Dey S., Basu S., Drew M. G. B., Chattopadhyay P., 2007. *Radiochim. Acta*, **95**, 297.

CHAPTER 12 EPILOGUE

Radiochemical research has been performed at iThemba LABS for the last 18 years, in the form of radiolabelling, extraction or ion exchange towards the radionuclide production of radiopharmaceuticals. Ion exchange chromatography has proven to be most effective in this type of research, resulting in products for radiolabelling purposes or radionuclides for dispatch of radiopharmaceuticals to local clinics and hospitals.

Radiochemical research using ion exchange chromatography at iThemba LABS has also borne fruit with regard to the production of longer-lived radionuclides for export. Indeed, research from this work has resulted in productions (and sales) of ^{88}Y, ^{82}Sr and ^{68}Ge in 2007 alone. Furthermore, radiochemical experiments have been carried out in conjunction with physicists for experiments of a more physical nature. Four papers based on this work have been published, namely, for the production of ultrapure ^{67}Ga, the cross-sectional measurements towards the production of ^{28}Mg, the separation of Th from ^{227}Pa and the exotic decay of ^{223}Ac. Further submissions for publication are planned.

It is hoped that this work will again underline the importance of ion exchange chromatography in radiochemistry research and radionuclide production.

APPENDIX A1 EXPERIMENTAL CROSS SECTIONS AND THICK-TARGET PRODUCTION RATES

In the tables below, the cross sections were derived from fitted curves through experimental thick-target production rate data, by differentiating these curves. Once the excitation functions were determined in this way, thick-target production rates for alternative target materials were derived by folding with appropriate stopping powers and integrating, which is the more usual procedure. See also Appendix A2.

Table A1.1: Selected ^{28}Mg cross sections from the fitted excitation function and the derived thick-target production rates for various target materials, as indicated.

Proton Energy (MeV)	Cross section (μb)	Production Rate (MBq/μAh)		
		NaCl	LiCl	Solid Cl_2
50	0.41 ± 0.07	3×10^{-6}	4×10^{-6}	5×10^{-6}
55	5.9 ± 0.5	3.48×10^{-3}	4.79×10^{-3}	5.82×10^{-3}
60	13.2 ± 0.9	0.0153	0.0210	0.0255
65	21.1 ± 1.5	0.0381	0.0524	0.0636
70	28.4 ± 2.0	0.0731	0.101	0.122
75	34.6 ± 2.4	0.120	0.165	0.200
80	39.6 ± 2.8	0.178	0.245	0.298
85	43.8 ± 3.1	0.247	0.339	0.412
90	47.4 ± 3.3	0.325	0.447	0.542
95	51.1 ± 3.6	0.413	0.568	0.689
100	55.3 ± 3.9	0.511	0.704	0.853
105	60.0 ± 4.2	0.622	0.857	1.038
110	65.4 ± 4.6	0.747	1.029	1.246
115	71.3 ± 5.0	0.888	1.223	1.481
120	77.5 ± 5.4	1.046	1.440	1.744
125	83.7 ± 5.9	1.222	1.683	2.039
130	89.7 ± 6.3	1.417	1.952	2.363
135	95.3 ± 6.7	1.631	2.247	2.720
140	100.4 ± 7.0	1.863	2.567	3.107
145	105.2 ± 7.4	2.113	2.911	3.524
150	109.9 ± 7.7	2.381	3.280	3.971
155	114.5 ± 8.0	2.667	3.674	4.447
160	119.4 ± 8.4	2.971	4.094	4.955
165	124.4 ± 8.7	3.295	4.540	5.495
170	129.7 ± 9.1	3.639	5.015	6.069
175	134.7 ± 9.4	4.005	5.519	6.678
180	139.2 ± 9.7	4.391	6.051	7.322
185	142.8 ± 10.0	4.795	6.610	7.996
190	145.3 ± 10.2	5.216	7.189	8.697
195	147.6 ± 10.3	5.651	7.789	9.421
200	152.3 ± 10.7	6.102	8.412	10.173

Table A1.2: Selected ^{88}Y cross sections from the fitted excitation function and the derived thick-target production rates for various target materials, as indicated.

Proton Energy (MeV)	Cross section (mb)	Production Rate (MBq/μAh)			
		$SrCl_2$	SrF_2	SrS	Sr metal
4.5	15.3	0.001	0.000	0.001	0.001
5.0	45.09	0.005	0.004	0.005	0.008
5.5	112.72	0.012	0.009	0.013	0.019
6.0	161.52	0.022	0.018	0.024	0.037
6.5	220.05	0.039	0.030	0.042	0.064
7.0	287.09	0.061	0.048	0.066	0.101
7.5	360.76	0.092	0.072	0.099	0.151
8.0	438.63	0.131	0.103	0.142	0.215
8.5	517.92	0.181	0.142	0.195	0.296
9.0	595.70	0.241	0.189	0.260	0.394
9.5	669.09	0.312	0.245	0.337	0.510
10.0	735.38	0.394	0.310	0.426	0.644
10.5	792.22	0.487	0.383	0.526	0.794
11.0	837.71	0.590	0.463	0.637	0.961
11.5	870.46	0.701	0.551	0.756	1.141
12.0	889.59	0.820	0.644	0.884	1.332
12.5	894.78	0.944	0.741	1.017	1.532
13.0	886.18	1.071	0.841	1.154	1.738
13.5	864.40	1.200	0.943	1.293	1.946
14.0	830.42	1.328	1.043	1.431	2.152
14.5	785.51	1.454	1.142	1.566	2.355
15.0	731.17	1.575	1.237	1.696	2.549
15.5	669.05	1.690	1.327	1.819	2.733
16.0	600.85	1.796	1.411	1.933	2.904
16.5	528.30	1.893	1.487	2.037	3.060
17.0	453.06	1.979	1.554	2.129	3.198
17.5	376.71	2.054	1.613	2.209	3.317
18.0	300.68	2.116	1.662	2.276	3.417
18.5	226.27	2.165	1.700	2.329	3.496
19.0	154.59	2.201	1.729	2.368	3.554
19.5	86.57	2.225	1.747	2.393	3.592
20.0	67.96	2.236	1.756	2.405	3.609

Table A1.3: Selected ^{133}Ba cross sections from the fitted excitation function and the derived thick-target production rates for various target materials, as indicated.

Proton Energy (MeV)	Cross section (mb)	Production Rate (kBq/μAh)	
		CsF	Cs metal
4.5	1.55	—	0.001
5.0	9.03	0.011	0.016
5.5	21.82	0.045	0.064
6.0	41.99	0.120	0.171
6.5	71.85	0.263	0.375
7.0	113.61	0.509	0.724
7.5	168.88	0.906	1.285
8.0	237.84	1.506	2.131
8.5	318.00	2.365	3.339
9.0	402.53	3.531	4.974
9.5	479.10	5.019	7.057
10.0	531.69	6.796	9.537
10.5	547.39	8.764	12.280
11.0	524.55	10.786	15.093
11.5	473.72	12.729	17.790
12.0	410.29	14.501	20.246
12.5	346.69	16.062	22.407
13.0	289.75	17.412	24.273
13.5	241.81	18.572	25.873
14.0	202.70	19.568	27.247
14.5	171.27	20.429	28.431
15.0	146.13	21.178	29.462
15.5	125.99	21.837	30.367
16.0	109.78	22.422	31.169
16.5	96.65	22.947	31.888
17.0	85.94	23.421	32.538
17.5	77.12	23.854	33.130
18.0	69.81	24.254	33.675
18.5	63.71	24.624	34.181
19.0	58.56	24.970	34.653
19.5	54.20	25.296	35.097
20.0	50.48	25.604	35.516

APPENDIX A2 CROSS SECTIONS AND PRODUCTION RATES

A2.1 The Thin-Target Approximation

It is appropriate to consider a thick solid target as consisting of a series of *thin targets* or, alternatively, to think of a thick target in the same way one would view a typical stacked-foil experiment, by which most of the excitation functions for the production of radionuclides are determined. Next, it is convenient to consider an arbitrary "slice" of the target (or foil in the foil stack) in isolation and to formulate three important equations in the so-called *thin-target approximation.* It will be shown below that by solving these three equations simultaneously, the well-known *activation equation* can be derived. Two more approximations, however, have to be introduced: Firstly, the beam current (or intensity) will be considered to be constant during the entire bombardment. Secondly, that the beam loses energy according to the *continuous slowing-down approximation* as it traverses the target. According to this latter approximation, the average beam energy is a unique function of penetration depth, which can be represented by a continuous equation, thus neglecting the fact that beam particles lose their energy in discrete collisions. The continuous slowing-down approximation is extremely successful because, by and large, beam particles lose very small increments of energy in an extremely large number of collisions, mainly by Coulomb interactions.

The beam penetration through an arbitrary slice (or foil) is shown schematically in Fig. A2.1.

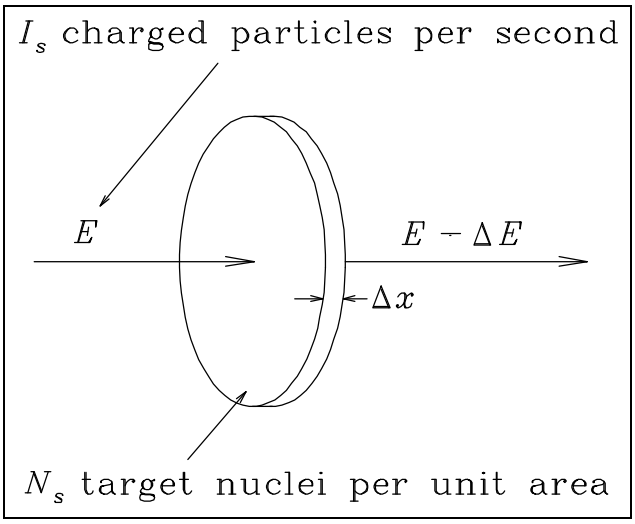

Fig. A2.1: Beam penetration through a thin target.

The average energy of beam particles incident on the thin target is E and the average energy after traversing it is $E - \Delta E$. The thin target approximation is fulfilled if $\Delta E << E$, *i.e.* if the energy loss is small compared to the energy. This can be achieved by making the slice thickness, Δx, sufficiently small compared to the total thickness of the target or stack. The incremental thickness, Δx, and the incremental energy loss, ΔE, is related by the stopping power S: $\Delta E = S\Delta x$. This will be further discussed later.

Let N_s be the number of target nuclei per unit area and I_s the number of beam particles per second hitting the target. Let Y_{PR} be the number of residual nuclei of the desired type produced per second (the production rate). It is clear that Y_{PR} will be directly proportional to both N_s and I_s. To first order, no other quantities will affect the production rate in the thin target approximation, therefore

$$Y_{PR} = s\, N_s I_s, \tag{A2.1}$$

where σ is a proportionality constant. As often found in the derivation of physical expressions, a proportionality constant may have a definite physical meaning. In this case, σ can be associated with the probability of formation of the radionuclide in question and it is called the *cross section*, with dimensions of area. Note that the production rate (Y_{PR}) and the cross section (σ) are both, in general, functions of energy. It is appropriate to identify the cross section and production rate of the thin

target depicted in Fig. A2.1 with a unique energy midway between the incident and exit energies, thus $\sigma(E - \Delta E/2)$ and $Y_{PR}(E - \Delta E/2)$.

The production rate of equation (A2.1) is often called the thin-target production rate. A plot of either Y_{PR} versus E or σ versus E is called an excitation function.

A2.2 Activity at EOB

If the thin target of Fig. A2.1 is a foil, its activity can be measured, most probably by means of standard off-line γ-ray spectrometry. The activity of a radionuclide, related back to the end of bombardment (EOB), is given by

$$Y_{EOB} = \frac{A_p}{t e_b e_e \, \mathrm{e}^{-l T_m}}, \tag{A2.2}$$

where A_p is the peak area of an appropriate γ-line of the radionuclide in question, τ is the live counting time set on the multi-channel analyzer system, ε_b is the branching ratio of the γ-line, ε_e is the detector efficiency for that photon energy, λ is the decay constant of the radionuclide (related to the half-life by $\lambda = \ln(2)/T_{1/2}$), and T_m is the time period from EOB to the mean time within the counting interval of the measurement performed.

A2.3 Relation Between Yield and Production Rate

The yield at EOB and the production rate are related by the following equation:

$$Y_{EOB} = Y_{PR} \left\{ \frac{1 - \mathrm{e}^{-l T_b}}{l T_b} \right\} [1 - P], \tag{A2.3}$$

where T_b is the duration of the bombardment and P is the probability for non-elastic nuclear interactions[1] to occur during the passage of the beam through the preceding target material, before it reaches the thin target in question. Note that the expression in curly brackets takes care of the decay of the radionuclide during bombardment, while the expression in square brackets is the *survival probability* of a beam particle

at that particular depth in the target or foil stack (also called the beam attenuation factor).

It is worthwhile to note that P may be small and the $[1 - P]$ expression neglected in an experiment with a low beam energy, *e.g.* with a primary proton beam of 20 MeV. With a 66 MeV proton beam, however, P can have values up to 5 % deep inside the stack or target, thus no longer negligible. At 200 MeV, P can reach values of up to 30 %, depending on the target material and depth of penetration. Thus, at higher energies, it becomes crucial to take beam attenuation effects into account.

A2.4 The Activation Equation

From equations (A2.1) to (A2.3), an expression for the cross section in terms of experimentally determined and other available properties can be derived by substitution:

$$s = \frac{A_p}{te_b e_e \, \mathrm{e}^{-lT_m} \, N_s I_s \left\{ \frac{1-\mathrm{e}^{-lT_b}}{lT_b} \right\} [1-P]}, \qquad \text{(A2.4)}$$

where the quantity P can be calculated according to a prescription by Janni[1].

This is one form of the so-called activation equation and the one used in this work. All cross sections in this work have been expressed in units of millibarn (mb); 1 mb ≡ 10^{-27} cm^2.

A2.5 The Thick-Target Production Rate Curve

In this work, thick-target production rate curves have been presented, as they are very useful for determining optimum target thicknesses and yield predictions. As already mentioned, the quantities σ, Y_{PR}, S and P are functions of the bombarding particle energy. The average energy at a particular penetration depth can be calculated using standard stopping power expressions. The energy versus penetration depth have been calculated using the code ELOSS, which is an implementation of the stopping power formulae of Anderson and Ziegler[2]. The thick-target production rate is given by

$$Y_{PR}^{T}(E') = \int_{E_{Threshold}}^{E'} Y_{PR}(E)dE, \qquad \text{for all} \qquad E_{Threshold} \le E' \le E_0, \tag{A2.5}$$

where E' is any energy value between the threshold energy for the production of the particular radionuclide ($E_{Threshold}$) and the primary incident beam energy (E_0): The curve defined by equation (A2.5) is a monotonically increasing function with energy and is characteristic of a particular production route, independent of the actual bombardment conditions and radioactive decay. For any given energy window (E_{in}, E_{out}) the thick-target production rate is given by

$$Y_{PR}^{T}(E_{in}, E_{out}) = Y_{PR}^{T}(E_{in}) - Y_{PR}^{T}(E_{out}). \tag{A2.6}$$

If no E_{out} is specified, $E_{Threshold}$ is automatically assumed.

A2.6 Actual Thick-Target Yield at EOB

Expressions (A2.5) and (A2.6) do not give the actual yield of a thick target because radioactive decay and beam attenuation losses have not yet been taken into account. A similar form to equation (A2.3) is usually appropriate, albeit an approximation:

$$Y_{EOB}^{T} = Y_{PR}^{T}\left\{\frac{1-e^{-lT_b}}{lT_b}\right\}\overline{[1-P]}, \tag{A2.7}$$

where $\overline{[1-P]}$ is the mean beam attenuation factor. For a very large energy window, one can divide it first into a number of smaller intervals and apply equation (A2.7) successively, finally summing all the individual contributions, in order to increase the accuracy.

All the above expressions for production rates and yields give values in terms of *number of nuclei per second*. Throughout this work, yields and production rates were converted to units of kBq/µAh, MBq/µAh or GBq/µAh, simply because these are more convenient. The accumulated charge (*i.e.* the integrated beam current) is given by the instrumentation used in units of µAh. The units Ci (Curie) or mCi (milli-

Curie) are still popular today. In order to convert to those units, note that 37 MBq ≡ 1 mCi.

A2.7 Other considerations

When the half-life of the radionuclide to be investigated is long compared to the bombardment time, the assumption of the constancy of the beam intensity is appropriate even if the beam was not constant at all. This is not the case if the half-life is short or comparable to the bombardment time. In those cases, an alternative formalism, summarized by Buthelezi[3], should be used instead. The above expressions are also not appropriate in cases where contributions from relatively long-lived precursor decay are significant, in which case the growth-and-decay curves should be calculated, as summarized by Vermeulen[4].

A2.8 References

1. Janni J. F., 1982. At. Data Nucl. Data Tables, **27**, 150.
2. Anderson H. H., Ziegler J. F., 1977. In *Stopping of Ions in Matter*, Vol. 3 (Ziegler J. F., Ed), Pergamon, New York, p. 1.
3. Buthelezi E. Z., 2004. *Ph.D. Thesis*, University of Stellenbosch, Stellenbosch, South Africa.
4. Vermeulen C., 2007. *M.Sc. Thesis*, University of Stellenbosch, Stellenbosch, South Africa.